João Miguel Monteiro

Localization studies of the FemXAB protein family in *Staphylococcus aureus*

LISBOA

2009

UNIVERSIDADE NOVA DE LISBOA

FACULDADE DE CIÊNCIAS E TECNOLOGIA

DEPARTAMENTO DE CIÊNCIAS DA VIDA

João Miguel Monteiro

Localization studies of the FemXAB protein family in *Staphylococcus aureus*

Dissertação apresentada para a obtenção do Grau de Mestre em Genética Molecular e Biomedicina, pela Universidade Nova de Lisboa, Faculdade de Ciências e Tecnologia

Orientador:
Doutora Mariana Gomes de Pinho (ITQB/UNL)
Co-orientadora:
Profª. Doutora Ana Madalena Ludovice (FCT/UNL)

LISBOA

2009

Acknowledgements

I would like to thank my family, first and foremost, for always supporting me in every single way and for their unquestionable faith in my abilities. I would also like to thank my supervisor, Mariana Pinho, for sharing her vision with me and guiding my work throughout this year, stimulating my development as a scientist. Sérgio Filipe, for opening up new paths and offering useful ideas to test our hypotheses. Professor Ana Madalena Ludovice for being my link between the university and ITQB, for her utmost care and concern about my professional performance. My laboratory group at ITQB, for teaching a chemist how to work in a microbiology setting, and for always providing a friendly and trusting environment, which I found delightful to be a part of. It is impossible to overstate the way that our sessions of brainstorming contributed to this thesis. A special thanks to Margarida Santos, for her preliminary work and Pedro Pereira, for validating or discarding my conjectures, for his insights and for being ever intrinsically involved with my research. Last but not least, to my closest friends who eased my mind and carried me through the more doubtful times.

Abstract

The public health burden of methicillin-resistant *Staphylococcus aureus* (MRSA) strains and the emergence of vancomycin resistance in *S. aureus* call for alternative strategies in chemotherapy. The FemXAB family of proteins is responsible for the assembly of the characteristic pentaglycine cross-bridge in the peptidoglycan of *S. aureus*, which is essential both for cell viability and for the expression of high level methicillin resistance. Fem proteins are, therefore, good candidate targets for the development of pathogen specific antimicrobial compounds, acting alone or synergistically with β-lactams. In this work, we characterized the localization of the FemX, FemA and FemB proteins (which add the 1^{st}; 2^{nd} and 3^{rd}; 4^{th} and 5^{th} glycines of the crossbridge, respectively) during the bacterial cell cycle, using fluorescence microscopy. These proteins localized preferably at the membrane, including the septum, and de-localized in the absence of the peptidoglycan precursor. FemA and FemB proteins co-localized in all cells observed during the different stages of the cell cycle, whilst FemX and FemA proteins co-localized in 64% of the cells. To determine if the FemB protein was dependent on FemA for proper localization, different approaches were used to attempt inactivation of the *femA* gene, but all were unsuccessful, suggesting that *femA* may be a lethal target.

Sumário

Estirpes da bactéria *Staphylococcus aureus* que são resistentes à meticilina (MRSA) têm um profundo impacto na saúde pública. O aparecimento de estirpes resistentes à vancomicina, antibiótico de recurso para o tratamento de infecções por MRSA, urge o desenvolvimento de estratégias alternativas de quimioterapia. A família de proteínas FemXAB é responsável pela síntese da ponte lateral de pentaglicinas, característica do peptidoglicano de *S. aureus*, que é essencial tanto para a viabilidade da bactéria, como para a expressão de resistência elevada à meticilina. As proteínas Fem são alvos promissores para o desenvolvimento de compostos antimicrobianos específicos, que poderão actuar sozinhos ou em sinergia com o tratamento convencional. Neste trabalho, caracterizámos a localização das proteínas FemX, FemA e FemB (que adicionam a 1ª, 2ª e 3ª, 4ª e 5ª glicinas, respectivamente) durante o ciclo celular de *S. aureus*, por meio de microscopia de fluorescência. Demonstrou-se que estas proteínas localizam-se preferencialmente na membrana bacteriana, incluindo o septo, e que deslocalizam-se na ausência do muropéptido percursor do peptidoglicano. As proteínas FemA e FemB co-localizaram durante o ciclo celular em todas as células observadas, enquanto que FemX e FemA co-localizaram em 64% das células observadas. Para determinar se a localização de FemB é dependente de FemA, foram utilizadas diversas estratégias que promovessem a inactivação de *femA*, porém nenhuma teve sucesso. Estes resultados permitem levantar a hipótese que FemA é uma proteína essencial para a célula.

Contents

Introduction

Methicillin resistant *Staphylococcus aureus*

Staphylococcus aureus is a Gram-positive coccus that is usually part of the human flora, mostly inhabiting the skin and the nasopharynx. However, it can also cause a wide range of infections, from skin and soft tissue infections to pneumonia, septicemia, infective endocarditis and osteomyelitis (Wenzel and Perl, 1995). Asymptomatic nasal carriers account for one third of the population (Gorwitz *et al.*, 2008; Kluytmans *et al.*, 1997) and are believed to be an important source of the strains that spread among individuals (Casewell and Hill, 1986; Noble *et al.*, 1967). *S. aureus* is transmitted usually by skin-to-skin contact between individuals or by contact with contaminated objects or surfaces (Kazakova *et al.*, 2005; Lowy, 1998; Miller and Diep, 2008; Muto *et al.*, 2003).

Penicillin, a β-lactam antibiotic discovered accidentally in a mouldy *S. aureus* culture by Alexander Fleming in 1929, was one of the first antibiotics developed and its applicability in treating Gram-positive bacterial infections was deemed miraculous. However, a few years after the beginning of widespread use of penicillin in clinical practice, resistant strains were encountered in hospitals (Barber and Rozwadowska-Dowzenko, 1948). The situation has since escalated and, despite the development of successive generations of new antibiotics, infection by antibiotic-resistant strains of *S. aureus* has reached epidemic proportions globally (Chambers and Deleo, 2009; Grundmann *et al.*, 2006). Particularly, methicillin-resistant *S. aureus* (MRSA) strains have become serious pathogens. Nowadays, MRSA represents >60% of nosocomial *S. aureus* isolates in many countries (Klevens MR, 2007) and carriage of hospital-acquired MRSA (HA-MRSA) is now endemic among hospitalized patients in many countries (Boyce *et al.*, 1994), with reported proportions of MRSA in staphylococcal bloodstream infections as high as 44% in the UK (European Antimicrobial Resistance Surveillance System in http://www.rivm.nl/earss) and 50% in the US (National Nosocomial Infections Surveillance System in http://www.cdc.gov_ncidod_). Community-associated MRSA (CA-MRSA) emerged worldwide, having been reported in the US, Canada, Asia, South America and Europe (Laupland *et al.*, 2008; Li *et al.*, 2009; Moran *et al.*, 2006; Vandenesch *et al.*, 2003). CA-MRSA is now a major public health concern in the United States, where the vast majority of infections are caused by a clone known as pulsed-field type

USA300, responsible for particularly rapidly progressing fatal diseases and known for easy spreadability. Unlike HA-MRSA, CA-MRSA strains infect healthy individuals without predisposing risk factors and outside the hospital setting (Chambers, 2005; Kennedy *et al.*, 2008; Moran *et al.*, 2006).

Methicillin resistance has a broad spectrum, covering the entire β-lactam class of antibiotics, including penicillins, cephalosporins and carbapenems. Of particular note is the strain COL which was isolated from a patient in Colindale, UK, in 1961 and became probably the most studied MRSA strain (Jevons *et al.*, 1963). MRSA strains used to be reliably susceptible to the glycopeptide vancomycin, which is usually only employed as a last resort drug; however, the ever increasing spread of MRSA infections in hospital settings prompted a significant increase in its use. This intensive selective pressure resulted in the emergence of vancomycin-intermediate (VISA) (Hiramatsu *et al.*, 1997) and vancomycin resistant (VRSA) (CDC, 2002) *S. aureus* strains, further confirming the extraordinary ability of this bacterium to adapt and develop resistance. As of now, there have been reports of *S. aureus* isolates resistant to the most recent antibiotics introduced in clinal practice for the treatment of staphylococcal infections, namely potent protein synthesis inhibitors such as minocycline and linezolid (Bishburg and Bishburg, 2009) or the membrane depolarization effect of daptomycin (Gales *et al.*, 2006; Hirschwerk *et al.*, 2006; Howden *et al.*, 2004; Llarrull *et al.*, 2009). The development of compounds that do not inhibit bacterial growth on their own but either act synergistically with a primary antibiotic, by impairing expression of resistance, or decrease the virulence of bacterial cells, facilitating their elimination by the host immune system, seems to be an attractive alternative.

Genetic mechanisms underlying bacterial resistance to β-lactams

β-lactam antibiotics target penicillin binding proteins (PBPs), a family of proteins involved in bacterial cell wall biosynthesis. The first wave of resistant strains that emerged in the 1940s produced a plasmid-encoded β-lactamase (penicillinase) (Barber and Rozwadowska-Dowzenko, 1948; Kirby, 1944), which prompted the development of methicillin in 1959. Methicillin is a penicillin derivative that can still bind PBPs but is insensitive to β-lactamases. Unlike the first penicillin resistant strains, the major determinant of high-level β-lactam resistance in MRSA is the *mecA* gene (Ubukata *et al.*, 1989), which is

carried by an exogenous DNA element designated SCC*mec* (staphylococcal cassette chromosome *mec*) inserted in the chromosome of *S. aureus*. SCC*mec* integrates at a locus known as *attBscc* near the origin of replication (Holden *et al.*, 2004; Katayama *et al.*, 2003; Kuroda *et al.*, 2001; Luong *et al.*, 2002), a region that appears to be a common insertion point for acquired, foreign, DNA (Mongkolrattanothai *et al.*, 2004; Noto *et al.*, 2008). Integration and excision of the SCC*mec* mobile element is, in part, mediated by recombinases of the invertase/resolvase family, encoded by the included *ccr* gene complex. SCC*mec* seems to be a staphylococcal site-specific genomic island that serves as a vehicle of transfer for various genetic markers between staphylococcal species (Ito *et al.*, 2001), as suggested by the existence of a structurally similar genetic element lacking *mecA* present in the chromosome of *Staphylococcus hominis* strain GIFU12263 (Katayama *et al.*, 2003). *mecA* is a highly conserved gene among MRSA isolates (Oliveira *et al.*, 2000) and it is proposed to have been originated from *Staphylococcus sciuri* (Wu *et al.*, 2001) due to the finding of a *mecA* putative evolutionary ancestor in all isolates of this species. It seems unlikely though, that *S. aureus* acquired *mecA* directly from *S. sciuri*, as the two sequences lack the necessary identity level (Couto *et al.*, 2003). *mecA* encodes for a 76 kDa penicillin-binding protein, PBP2a (also referred to as PBP2'), which was found in MRSA but not MSSA strains. PBP2a has lower affinity for β-lactam antibiotics than the other four PBPs native to *S. aureus*, and thus maintains its activity at therapeutic levels of methicillin, allowing the survival and growth of the bacteria (Hartman and Tomasz, 1984). Adjacent to *mecA* in the staphylococcal chromosome are *mecR1*, that encodes a membrane bound signal transdution protein, and *mecI*, encoding a tight transcriptional regulator (Sharma *et al.*, 1998). The transcription of *mecA* can also be regulated by the plasmid-encoded *bla* system and it has been shown that the *bla* regulator is more effective at inducing *mecA* than the *mec* regulator. Most β-lactam antibiotics do not efficiently activate *mecR1*, explaining the occurrence of *mecA* positive pre-MRSA isolates that are methicillin sensitive (Kobayashi *et al.*, 1998). Again, selective pressure through antibiotic usage has resulted in isolates that either contain both regulation systems, in which β-lactam induced upregulation of *mecA* by the *bla* system allows for the transcription of PBP2a, or that display mutations/deletions in the *mecI* or *mecA* promoter region, with the same effect (McKinney *et al.*, 2001).

Blanket high level β-lactam resistance is, by no means, a simple matter of whether the strain carries the *mecA* gene or not. Additional native genes of *S. aureus*, also present in MSSA strains, were identified as essential for the full expression of methicillin resistance. By

constructing a large library of *Tn551* insertional mutants in COL, it was possible to isolate mutants where the high and homogeneous level of methicillin resistance was reduced, although an intact *mecA* gene was still present (Berger-Bächi, 1983; de Lencastre and Tomasz, 1994). Each of these determinants was termed *fem* (factor essential for methicillin resistance) or *aux* (auxiliary) gene and approximately 30 *fem* genes have been identified (De Lencastre *et al.*, 1999). Even if a strain carries *mecA*, the inactivation of *fem* genes usually leads to a heterogeneous profile of oxacillin resistance and lower minimum inhibitory concentrations of this antibiotic, despite the fact that the *fem* gene in question may not be essential for bacterial viability. Most of these factors are housekeeping genes that are probably present in all *S. aureus* strains and cover a wide array of functions, encoding proteins that have a direct or indirect role in peptidoglycan biosynthesis and turnover (ex. PBP2, FemA, MurF), proteins with putative sensory/regulatory activities (kinases or ABC transporters), alternate transcription factors (SigB) and proteins of unknown function (Berger-Bächi and Rohrer, 2002; Berger-Bächi *et al.*, 1992; De Lencastre *et al.*, 1999). Although the exact relatedness of most of the *fem* factors to oxacillin resistance is still unresolved, their identification led to formidable insights into the structure of bacterial peptidoglycan.

Peptidoglycan synthesis

The key structural component in bacteria is the cell wall, composing the outermost layer of the cell in Gram-positive bacteria (except in capsulated ones) or lying underneath the outer membrane of Gram-negative bacteria. Its stability and integrity are critical for cell viability, shape and stress bearing. The scaffold of the cell wall consists, in both Gram-negative and Gram-positive bacteria, of the cross-linked polymer peptidoglycan (PG), a mesh-like structure also called murein. In Gram-positives this structure can be 20-40 nm thick (Vollmer *et al.*, 2008). The cell wall envelope in *S. aureus,* as in most Gram-positive bacteria, is also comprised of polysaccharides, teichoic acids and proteins that are covalently or non-covalently immobilized to the PG (Navarre and Schneewind, 1999). The cell is constantly under high internal osmotic pressure that is sustained by the long linear glycan strands of peptidoglycan, linked to each other via flexible peptide bridges. This bonding is referred to as crosslinking, and generates a strong but elastic structure that prevents the protoplast from lysing. The crosslinking organizes linear peptidoglycan strands into a single, large molecule, referred to as the murein sacculus (Glauner *et al.*, 1988).

All cell wall-containing Eubacteria share the same basic PG architecture, with the glycan strands being composed of alternating 1,4-linked *N*-acetylglucosamine (GlcNAc, NAG) and *N*-acetylmuramic acid (MurNAc, NAM) disaccharide subunits. Attached to the carboxyl group of each MurNAc residue is a peptide chain commonly referred to as stem peptide whose amino acid composition is of considerable variation between species (Schleifer and Kandler, 1972). Also variable is the size and composition of the bridge crosslinking two stem peptides. In *S. aureus*, the very high crosslinking degree (up to 90%) has been attributed to the presence of long flexible pentaglycine bridges, supposedly able to connect glycan strands from different PG layers (Lapidot and Irving, 1977, 1979). The spatial structure of peptidoglycan is one of the most important unsolved structural problems in biochemistry, because of its inherent complexity and lack of pure and discrete segments for analysis. NMR studies using synthetic fragments of NAG-NAM(pentapeptide)-NAG-NAM(pentapeptide) tetrasaccharide suggested that peptidoglycan would have a structural aspect of a right-handed helical saccharide conformation corresponding to three NAG-NAM pairs per turn of the helix (Meroueh *et al.*, 2006). This representation is better accommodated in the "scaffold model" (also called the hedgehog model) of peptidoglycan growth, which states that glycan strands grow outward of the cytoplasmic membrane and orthogonal to it (Dmitriev *et al.*, 2004; Dmitriev *et al.*, 2003), as opposed to the classical parallel mode that depicts layers of peptidoglycan parallel to the membrane. Furthermore, it implies that each glycan strand can crosslink to a maximum of three neighboring strands and the resulting honeycomb-like structure, as seen in Figure 1, is able to accommodate both syntethic machinery proteins (shown by small arrow) and large membrane bound proteins (shown by large arrow), which is in agreement with the atomic force microscopy images depicting *S. aureus*' dot-filled surface described by Touhami and colleagues (Touhami *et al.*, 2004). However, the scaffold model has its shortcomings, mainly because the amount of PG in the cell may not be enough to cover its surface entirely, at least when this model is applied to Gram-negative bacteria as it was demonstrated for *Escherichia coli* (Vollmer and Höltje, 2004). The "scaffold model" is also not compatible with recent electroncryotomography studies on Gram-negative sacculi that revealed a single layer of glycan strands parallel to the bacterial membrane (Gan *et al.*, 2008).

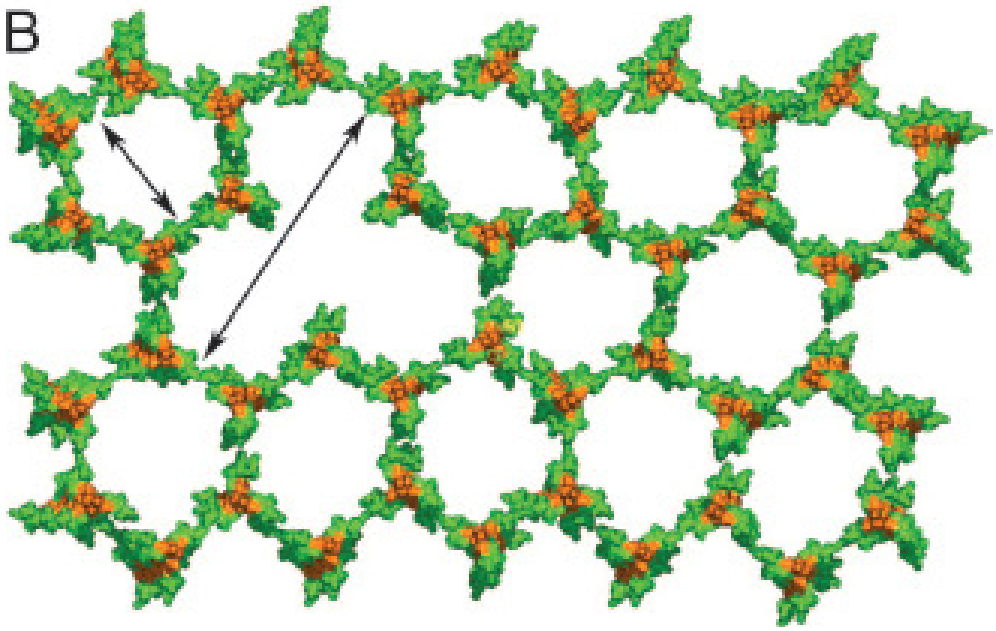

Figure 1 – Top view of the structure of the polymeric peptidoglycan segment showing the glycan strands in orange and the stem peptides in green, in agreement with the "scaffold model". Adapted from Meroueh *et al.*, 2006.

Peptidoglycan synthesis in *S. aureus* can be divided in three stages (van Heijenoort, 1998): it starts in the cytoplasm, where the reaction between nucleotide sugar-linked precursor UDP-*N*-acetylglucosamine (UDP-GlcNAc) and phosphoenolpyruvate, catalysed by MurA and MurB enzymes, is its first committed step (Rogers *et al.*, 1980). The products of the reaction are inorganic phosphate and UDP-*N*-Acteylmuramic acid (UDP-MurNAc) (Eschenburg *et al.*, 2003; Skarzynski *et al.*, 1996). Stem peptide synthesis begins at the carboxyl group of UDP-MurNAc, with moieties L-Ala, D-Glu, L-Lys and D-Ala-D-Ala being sequentially added by MurC, MurD, Mur E and MurF enzymes, respectively, at the expense of ATP, thus originating the basic cytoplasmic precursor UDP-MurNAc-pentapeptide (Munoz *et al.*, 1967; Tipper *et al.*, 1967a; Tipper *et al.*, 1967b). In the second stage (Figure 2), that takes place at the inner side of the membrane, the phospho-MurNAc-pentapeptide of the UDP-MurNAc-pentapeptide is transferred to the membrane acceptor bactoprenol (also known as C55), yielding an intermediate known as lipid I. This reaction is catalyzed by the MraY translocase. Bactoprenol is a lipophillic molecule which allows the transport of hydrophilic molecules through the cell's hydrophobic membrane (Ikeda *et al.*, 1991). UDP-GlcNAc is then added by MurG to lipid I via a β-1,4 linkage, yielding lipid intermediate II (Mengin-Lecreulx *et al.*, 1991). The assembly of the amino acid bridge in *S. aureus*, for the subsequent crosslinking

reaction, is made by the FemXAB family of transferases, adding directly and sequentially five glycines to the L-Lys residue of the stem peptide on lipid II (Kopp *et al.*, 1996). It is postulated that the lipid II intermediate is then translocated from the inner side to the outer side of the membrane via a translocase/flippase specific activity of a yet uncharacterized protein. A homologue of the MurJ (MviN) protein identified in *E. coli* (Ruiz, 2008) could be a likely candidate for this function. However, it was very recently demonstrated that deletion of four homologues of *murJ* in *Bacillus subtillis* caused no defects in bacterial growth, indicating that the corresponding proteins most likely do not function as flippases in this organism (Fay and Dworkin, 2009).

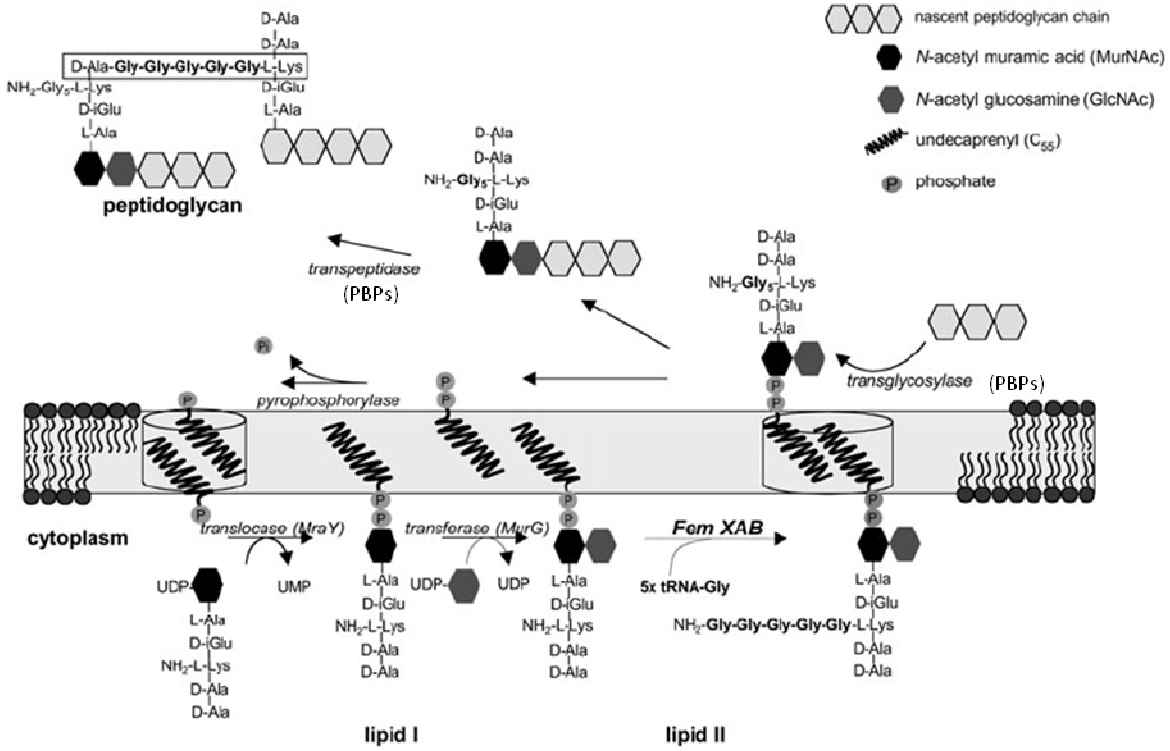

Figure 2 – Membrane-bound stages of peptidoglycan biosynthesis in *S. aureus*. The formation of the pentaglycine interbridge, catalyzed by FemXAB proteins, precedes the translocation of the monomeric peptidoglycan unit across the cytoplasmic membrane, with subsequent polymerization via transglycosilation and transpeptidation reactions catalyzed by PBPs. UMP, uridine monophosphate; UDP, uridine diphosphate. Adapted from Schneider *et al.*, 2004.

The final stage of peptidoglycan synthesis consists in the incorporation of the new subunit (henceforth referred to as muropeptide) into the growing glycan chain and occurs mainly, if not only, at the bacteria's division septum in *S. aureus* (Pinho and Errington, 2003).

This event is mediated by the membrane anchored PBPs, localized at the extracellular surface of the cytoplasmic membrane. PBPs can catalyze both a transglycosylase activity (TGase)– elongation of the glycan strands, and a transpeptidase activity (TPase) – peptide crosslinking between glycan strands. While all *S. aureus* native PBPs have a TPase domain, only PBP2 is bifunctional, capable of both transpeptidation and transglycosylation reactions (Goffin and Ghuysen, 2002; Massova and Mobashery, 1998; van Heijenoort 2001). In PBP2, the TGase and TPase domains are spatially well separated (Fuda *et al.*, 2005). The transglycosilation reaction probably occurs between the reducing end of the MurNAc present in the nascent lipid-linked PG strand, and the C-4 carbon of the glucosamine residue in the lipid-linked precursor, thus attaching the new subunit to the growing glycan chain. Transpeptidation and crosslinking are accomplished by cleavage of the D-Ala-D-Ala bond at the terminus of one stem peptide in the glycan chain, which drives energetically the subsequent reaction between the peptidyl moiety and an acceptor present on the subunit being incorporated. In *S. aureus*, the acceptor is the last glycine of the synthesized bridge, whereas in bacteria with direct crosslinking, transpeptidation occurs between D-Ala and the dibasic amino acid of the stem peptide being incorporated (van Heijenoort, 1998). Cell growth and division require not only the synthesis of new PG but also its breakage, remodeling and reinsertion. This is accomplished by specific hydrolases that cleave PG bonds and can be classified as muramidases, glucosaminidases, amidases, endopeptidases and carboxypeptidases. It has been proposed that the role of hydrolases in processes of cell wall turnover, cell separation and muropeptide recycling is of critical importance (Höltje and Heidrich, 2001; Shockman *et al.*, 1996; Smith *et al.*, 2000).

The mechanism of inhibition of peptide crosslinking by β-lactams, which leads to cell death, is based on the irreversible acylation of the PBPs catalytic serine in the TPase active site by the antibiotic molecules, acting as suicide substrate homologues (Fuda *et al.*, 2005; Waxman and Strominger, 1983). Acquired protein PBP2a is virtually non-susceptible to β-lactam acylation but lacks a functional TGase domain. In MRSA strains that are challenged by a β-lactam, PBP2a's TPase domain and PBP2's TGase domain cooperate in building the staphylococcal cell wall, perhaps by means of a multi-enzymatic complex (Pinho *et al.*, 2001). As PBP2 seems to be dependent on its transpeptidation substrates to localize to the division septum where PG is being synthesized, PBP2a could recognize the substrate, localize to the septum and recruit acylated PBP2 by direct or indirect protein interaction (Pinho and Errington, 2005). Glycopeptide antibiotics, of which vancomycin is an example, inhibit PG

biosynthesis by forming a non-covalent but stable complex with D-Ala-D-Ala residues at the terminus of the stem peptides, thus blocking the access of PBPs to their substrates (Pootoolal *et al.*, 2002).

Fem family of proteins

Two closely linked *fem* factors, required for the full expression of methicillin resistance, that were identified after *Tn551* insertions in the COL genome were termed *femA* and *femB*. *femA* and *femB* were mapped in an operon in the chromosome of MSSA strain NCTC 8325 and their inactivation in MRSA backgrounds was shown to have no effect on the production of PBP2a, therefore suggesting a direct role in cell wall synthesis (Berger-Bächi *et al.*, 1992). These genes encode for the proteins FemA and FemB, which were the first described members of the class of non-ribosomal peptidyl transferases (Berger-Bächi *et al.*, 1989). These proteins are responsible for the assembly of the characteristic pentaglycine side-chain that connects muropeptide subunits of peptidoglycan in *S. aureus* (Berger-Bächi and Tschierske, 1998; Kamiryo and Matsuhashi, 1972). It was found that FemA attaches only the second and third glycines of the peptide interbridge, whereas FemB adds exclusively the fourth and the fifth. Thus, it was also postulated that the addition of the first glycine would be catalyzed by a putative FemX protein (Figure 3) (Ehlert *et al.*, 1997). Three *femAB*-like sequences were identified in the *S. aureus* genome: *fmhA*, *fmhB* and *fmhC*. Whereas inactivation of *fmhA* and *fmhC* sequences had no effect on growth and physiology, *fmhB* was shown to be an essential gene (Tschierske *et al.*, 1999). *fmhB* was put under the control of a xylose regulon and a clear correlation between repression of the gene and accumulation of unsubstituted monomeric peptidoglycan precursors was observed. These results identified the protein encoded by the gene as FemX, the enzyme responsible for initiating the synthesis of the interchain peptide in the peptidoglycan. Precursor analysis of *S. aureus* cytoplasmic fractions revealed that only UDP-MurNAc-pentapeptide with no glycine substitutions was present, leading to the conclusion that FemX's substrate would be either membrane bound lipid intermediate I or lipid intermediate II (Rohrer *et al.*, 1999). The FemXAB family of proteins adds glycine residues directly as glycyl-$tRNA^{gly}$ (Matsuhashi *et al.*, 1976). There are three different cell wall specific and two proteinogenic glycil-tRNAs in *S. aureus*, which

points to the hypothesis that each Fem factor may use dedicated gly-tRNAs (Kopp *et al.*, 1996).

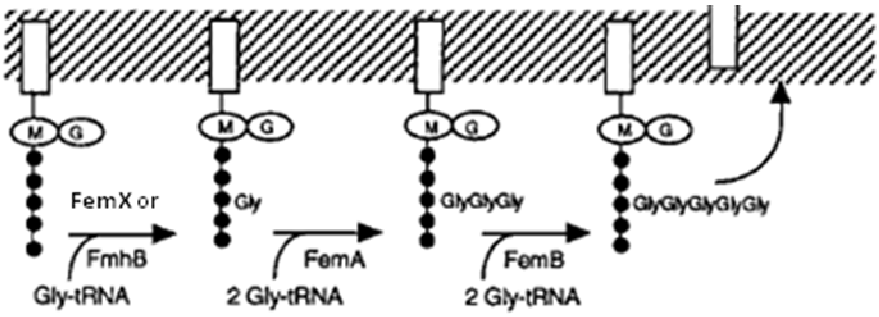

Figure 3– Pentaglycine side-chain formation of PG muropeptides in *S. aureus*. Glycines are added in a sequential fashion to L-Lysine, the third amino acid in the stem peptide. Each Fem protein has substrate specificity: FemX adds the first glycine; FemA adds the second and the third; FemB adds the fourth and fifth glycines. M, *N*-acetyl-muramic acid; G, *N*-acetyl-glucosamine. Adapted from Rohrer *et al.*, 1999.

The expression of *femAB* is regulated and was found to be increased in MRSA strains, relatively to MSSA strains, either by the binding of a putative protein to the upstream sequence, or by antibiotic induction (Li *et al.*, 2008). Amino acid analysis of the peptidoglycan of *S. aureus* strains carrying a transposon inactivated *femA* locus showed a lower glycine to glutamic acid or lysine ratio, when compared to wild-type strains, decreased cell wall turnover and autolysis and also decreased susceptibilities to lysostaphin (Maidhof *et al.*, 1991). Lysostaphin is a glycil-glycine endopeptidase, secreted by *Staphylococcus simulans* serovar Staphyloliticus, that preferably cuts between the third and fourth glycines of the crossbridge (Schneewind *et al.*, 1995). The structural and physical effects of lysostaphin on the cell can be viewed in Figure 4. *S. simulans* protects itself from lysostaphin via a lysostaphin immunity factor (Lif), a FemAB-like protein that incorporates serines into the crossbridge (Tschierske *et al.*, 1997).

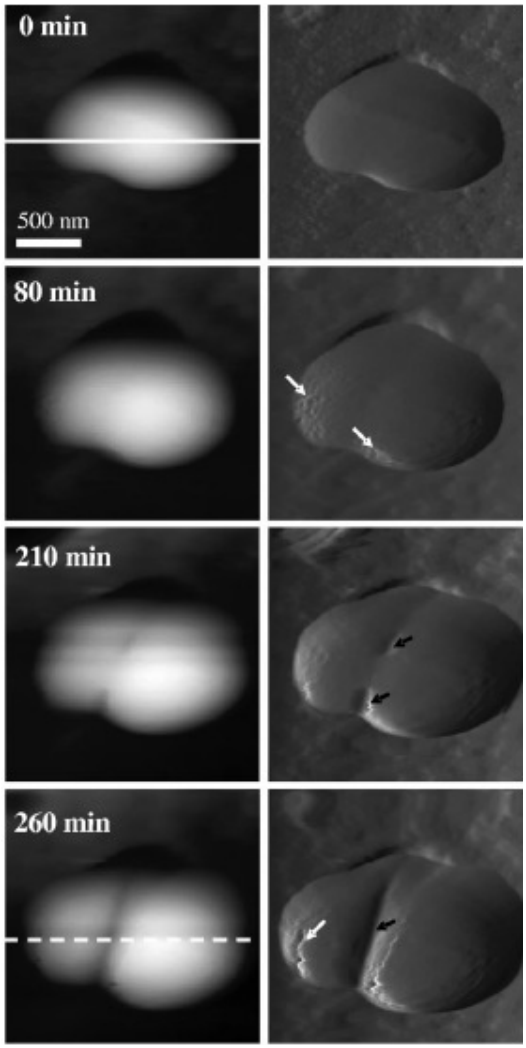

Figure 4 – Time-lapse imaging by atomic force microscopy of a single *S. aureus* cell prior to and after incubation with 16 µg/ml lysostaphin. Major structural changes occur, including cell swelling, splitting of the septum (black arrows) and nanoscale perforations (white arrows). Adapted from Francius *et al.*, 2008.

Muropeptide analysis of *femA* mutants by HPLC techniques revealed an increase in the proportion of muropeptides with low crosslinking degree (monomers, dimers, trimers), relative to larger oligomers. Also, all pentaglycil substituted muropeptides were absent from the profile with concomitant accumulation of monomeric pentapeptides substituted with a single glycine residue and alternative muropeptides containing serine residues in the second position of the cross-bridge. Oligomers of single glycine substituted muropeptides may have been present in the muropeptide profile as well, although this was never verified. Overall, these conformational changes caused a reduction in the net degree of crosslinking by 10% in *femA* mutants. This data suggested a role for the *femA* gene product either in a cytoplasmic

phase of di-glycine biosynthesis or addition of glycine to the stem peptide at the inner membrane (de Jonge *et al.*, 1993). Studies on *femB* inactivation revealed very similar consequences on peptidoglycan composition, with shortening of the peptide interbridges to three glycines. In both cases, pleiotropic consequences were observed as, besides altered cell wall composition, cells were shown to have aberrant septum formation and retarded cell separation, the so called *femA*-like phenotype (Figure 5). This led to the assumption that *femB* could be as important as *femA*, especially considering that *femA* and *femB* are transcribed in a polycistronic mRNA under the control of the same promoter (Henze *et al.*, 1993).

Figure 5 – Thin section of *S. aureus femA* mutant, displaying cells with irregular septa and defects in cell separation. Adapted from Henze *et al.*, 1993.

It is interesting to note that the *Tn551* insertion on the *femA* gene occurred in the control region of the operon. This insertion led to a 90% decrease in *femAB* transcription, thus the *femA* inactivation mutant essentially behaved as a leaky *femAB* mutant. Insertional mutants of *femB* analyzed by Henze and colleagues (Henze *et al.*, 1993), on the other hand, presumably led to complete knockout of the gene. These findings still raised the question of whether *femA* knockout mutations, which would abolish any residual transcription, would be incompatible with cell viability. Recent studies on the UK17 strain (which contains a nonsense mutation near the 3' end of *femA)* peptidoglycan composition by solid-state NMR estimated a 57% reduction in the degree of crosslinking, relative to wild-type *S. aureus*. It was

postulated that, in order to achieve crosslinking with monoglycil bridges, a rearrangement of the whole cell wall structure seemed likely (Ling and Berger-Bächi, 1998; Sharif *et al.*, 2009).

FemA and FemB have 39% identity and 70% similarity to each other, however, FemB cannot substitute for FemA. It is unusual for two nearly identical proteins to have such high substrate specificities and it is likely that the active sites lie near the C-terminus of the proteins, as that is the region where FemA and FemB differ the most (Ehlert *et al.*, 1997). *femAB*-like sequences have been identified not only in *S. aureus* but in other staphylococcal species as well (Alborn *et al.*, 1996). Besides the aforementioned Lif factor in *S. simulans*, which was shown to complement a *femB* mutant (Tschierske *et al.*, 1997), the *epr* gene in *Staphylococcus capitis* also catalyses the addition of serines into the crossbridge, protecting its producer from End, a lysostaphin-like glycil-glycine endopeptidase. Crossbridges containing serine in *S. aureus* have been shown to be incompatible with high methicillin resistance, contrary to pentaglycil ones, so it seems that either PBP2a has strict substrate requirements or that a putative interaction of this protein with Fem-like factors is altered in the presence of serine (Sugai *et al.*, 1997). The low frequencies of serine and alanine containing crossbridges observed in all the FemA, FemB and FemAB mutants hint at residual activities of FemAB-like proteins, with specificities to amino acids other than glycines. It seems that during *S. aureus*' evolution, cells that would synthesize pentaglycil bridges could crosslink glycan strands more efficiently and, therefore, bear the osmotic pressure inside better (Berger-Bächi and Tschierske, 1998). The event that triggered this leap was probably sequence duplication of a putative ancestral fem sequence (Berger-Bächi *et al.*, 1989).

Structural studies of Fem proteins

Crystallography studies into the structure of *S. aureus* FemA provided priceless insights into the mechanism of this protein's activity. FemA folds into a globular domain with two helical arms extending into the solvent (Figure 6) (Benson *et al.*, 2002). Analysis of this globular domain revealed a three dimensional fold similar to the histone acetiltransferase (HAT) domain of *Tetrahymena thermophila* protein GCN5, which is known for its ability to bind peptide and peptide-like substrates. GCN5 is involved in acetylation of peptides in the core histones, by means of coenzyme-A (Dutnall *et al.*, 1998). It was reasonable to assume, therefore, that FemA's HAT domain could accommodate both the monoglycine substituted

stem peptide of lipid II and coenzyme A, the latter serving as an intermediate acceptor between the glycil-tRNA and the peptidoglycan precursor. Further data didn't support the binding of coenzyme A to FemA, indicating direct transfer from the charged tRNA to the peptide.

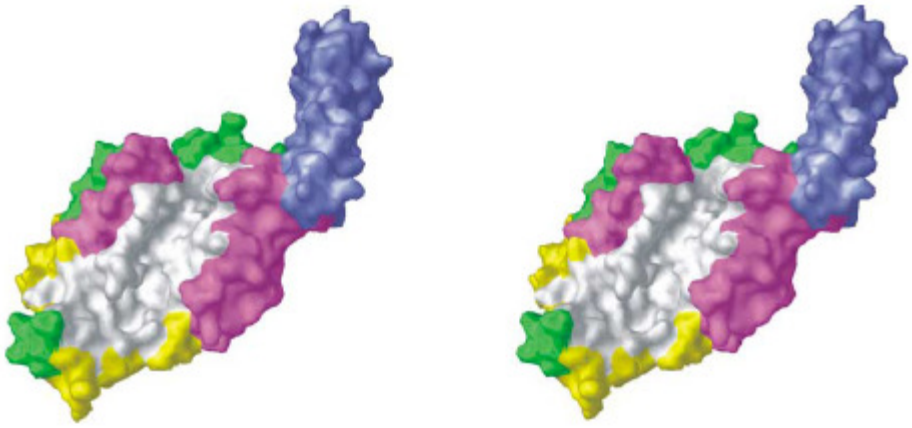

Figure 6 – Stereo view of the proposed structure of *S. aureus* FemA, depicting both the globular domain and the helical arms. White – deep L-shaped channel that can hold the stem peptide in an extended conformation; blue – antiparallel coiled-coil helical arms that could serve to hold an amino acid charged tRNA. Adapted from Benson *et al.*, 2002.

A deep L-shaped channel (Fig. 6 – in white) transversing FemA is a binding cavity suitable for an extended conformation of the stem peptide. The antiparallel coiled-coil helical arms (Fig. 6- in blue) could serve to hold an amino acid-charged tRNA molecule near the junction between the channel and the arms, during addition of the glycine residues to the growing peptide bridge (Benson *et al.*, 2002) This type of mechanism has also been shown for the seryl-tRNA synthetase protein in *Tetrahymena termophila* (Biou *et al.*, 1994; Cusack *et al.*, 1996). After tRNA binding, structural changes would enable the enzyme to orient and position the acceptor end of the tRNA near the L-channel, for transfer of the glycine to the precursor. It was also postulated that addition of the two glycines would occur in a sequential fashion, with only one glycil-tRNA binding in the junction at a time. The substrate could probably be held in place between the two helixes located at the top of the channel. It can be argued that, after two rounds of transfer, the triglycil substituted stem peptide would not fit into the cavity anymore, preventing FemA from adding more glycines. An alternative mechanism states that the addition of the two glycines could be accomplished by two separate

FemA proteins interacting with each other near the substrate (Benson *et al.*, 2002). Bacterial two hybrid studies showed homodimerization of FemA. Homodimerization was also found on FemB as well as heterodimerization between FemA and FemB, therefore it seems possible that both proteins function in a large complex attached to its substrate near the membrane. This data does not necessarily imply, however, that interaction contributes to the mechanism of glycine attachment. No interactions were found between FemX and the other Fem proteins nor between FemX monomers, suggesting that FemX is very likely a monomer *in vivo*, although physical interactions mediated by an auxiliary molecule cannot be ruled out (Rohrer and Berger-Bächi, 2003).

In contrast to *S. aureus,* Gram-negative *Weissella viridescens* (basionym *Lactobacillus viridescens*) contains monoglycil substituted UDP-MurNAc-pentapeptide in the cytoplasm, suggesting that in these bacteria, FemX adds the glycine before the translocation to bactoprenol occurs (Hegde and Shrader, 2001). Structural analysis of the FemX protein from *Weissella viridescens* (hereafter referred to as $FemX_{wv}$*)* provided new insights into FemXAB protein family folding. $FemX_{wv}$, unlike *S. aureus* FemX, is active in the cytoplasm, recognizing UDP-MurNAc-pentapeptide as a substrate and adding an alanyne. This enzyme contains one domain for UDP-MurNAc-pentapeptide binding and one for alanyl-tRNA binding (Biarrotte-Sorin *et al.*, 2004). The overall structure of $FemX_{wv}$ is similar to *S. aureus* FemA (Benson *et al.*, 2002). However, the former lacks the coiled-coil arms described in the latter. This structural characteristic was proposed to divide the FemXAB family in two groups: group 1 proteins contain the helical arms and comprise FemA and most FemXAB-related sequences, including those from staphylococci, enterococci and streptococci; group 2 proteins lack the structural motif and, along with $FemX_{wv}$, comprise Fem-like sequences from *Streptomyces coelicolor, Deinococcus radiodurans, Treponema pallidum* and *Borrelia burgdorferi* (Biarrotte-Sorin *et al.*, 2004). *Streptococcus pneumoniae* Fem subgroup I protein MurM incorporates either alanines or serines to the growing peptide chain. This was shown to be a consequence of allelic variability in a 35 amino acid sequence contained in the coiled-coil domain of the protein. This supports the notion that the species of aminoacyl-tRNA that is added to the peptide chain is dependent on specific interactions at the junction between the helical arms and the globular domain of Fem proteins (Filipe and Tomasz, 2000). $FemX_{wv}$ contains a cleft in domain I, similar to the one in FemA, that can accommodate the UDP-MurNAc substrate, which was shown to make polar interactions with the protein. Structural

differences observed between the complexed and the non-complexed versions of $FemX_{wv}$ are minor, with noteworthy exceptions. For example, amino acid Lys36, equivalent to Lys33 of FemA, was reported to undergo a notable change in conformation, thus suggesting that it could be a critical residue for substrate binding. Domain II comprises a long channel with a global positive electrostatic surface potential that could complement the negatively charged phosphate backbone of tRNA. Interestingly, residue Tyr254 (equivalent to Tyr327 in FemA), strictly conserved across the FemXAB family, points inside the channel, presenting its side group to the entering tRNA. This orientation suggests a role in tRNA binding and recognition (Biarrotte-Sorin *et al.*, 2004). Subsequent studies on $FemX_{wv}$'s structure identified nine residues located in the binding cavity for UDP-MurNAc-pentapeptide as possible essential factors for protein activity, six of which are depicted in Figure 7 (Maillard *et al.*, 2005).

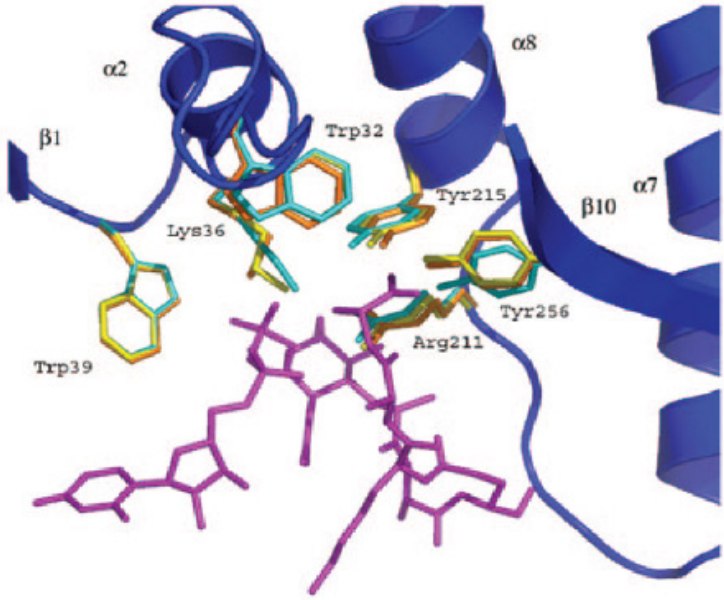

Figure 7 – Structure of the binding cavity of $FemX_{wv}$ superimposed with the UDP-MurNAc-pentapetide substrate (in magenta). Secondary structure of the protein is colored in dark blue. The $FemX_{wv}$ side chains of relevant residues are colored in yellow/orange for the apo wild type enzyme and in cyan for the complex. Adapted from Maillard *et al.*, 2005.

Site-directed mutagenesis of these residues showed that two of them, Lys36 and Arg211, when substituted by methionines, decreased transferase activity below detectable levels without affecting protein folding. Furthermore, analogues of UDP-MurNAc-pentapeptide lacking the phosphate groups or the C-terminal D-Ala-D-Ala residues were not substrates of $FemX_{wv}$. It seems that Lys36 and Arg211 participate in a complex hydrogen

bond network that connects the C-terminal D-Ala residues to the phosphate groups of UDP-MurNAc-pentapeptide and constrains the substrate in a conformation essential for transferase activity. By analogy, the corresponding residues Lys33 and Arg220 in *S. aureus* FemA should also be critical for the enzyme's function, albeit in this case, the phosphate groups recognized in the lipid II are linked to bactoprenol (Maillard *et al.*, 2005).

Biochemical studies of the Fem proteins *in vitro* activity

In vitro reconstitution of the inner-membrane bound steps of peptidoglycan synthesis, leading to the production of the lipid II-Gly_5 precursor was achieved from purified lipid I, lipid II, FemXAB proteins and glycil-tRNA synthetase. Lipid II was identified as the only substrate of the *S. aureus* peptidyltransferases and it was shown that these proteins were active individually and were highly substrate specific. As neither the soluble UDP-MurNAc-pentapetide nor lipid I were converted to glycine-labeled precursors, it is assumed that FemX protein and, by analogy, FemA and FemB, should recognize lipid II via the sugar moiety MurNAc-GlcNAc, which is in agreement with the aforementioned placement of the substrate in the L-shaped groove. Interestingly, when lipid II was incubated with FemXA, only lipid II-Gly_3 was found. A scenario where both FemA and FemB function as homodimers, in a way that each subunit is loaded with a Gly-tRNA to ensure sequential addition of both Gly to the growing interpeptide bridge seems likely. It is reasonable to assume that this is a tightly coordinated process interlinked with the other membrane associated steps of cell wall synthesis. Moreover, it is possible that Fem proteins are transiently associated with each other, as well as with other cell wall biosynthesis enzymes (Schneider *et al.*, 2004).

In this thesis, our goal was to characterize the localization of the FemXAB family of proteins in live *S. aureus* cells, during the cell cycle and in the presence or absence of different antibiotics, by means of fluorescence microscopy techniques.

Materials and Methods

Bacterial strains and plasmids

The bacterial strains and plasmids used in this study are described in Table 1.

Table 1- Strains and plasmids used in this work.

Strain/Plasmid	Genotype/Description	Origin/Reference
Strain		
S. aureus RN4220	MSSA strain, restriction negative	Rockefeller University collection
S. aureus UK17	*mecA*$^{+}$, *femA*$^{-}$	(Ehlert *et al.*, 1997)
S. aureus COL	Homogeneous MRSA (MIC 800 ug/ml)	Rockefeller University collection
E.coli DH5α	Cloning strain, *recA endA1 gyrA96 thi-1 hsdR17 supE44 relA1* ϕ80 Δ*lacZ*ΔM15	Gibco-BRL
RNpFemX-N	RN4220 expressing FemX with an N-terminal GFP fusion, Erm^{r}	This work
RNpFemX-C	RN4220 expressing FemX with a C-terminal GFP fusion, Erm^{r}	This work
RNFemA-C	RN4220 expressing FemA with a C-terminal mCherry fusion	This work
RNpFemB-C	RN4220 expressing FemB with a C-terminal GFP fusion, Erm^{r}	This work
RN-FemXA	RN4220 expressing FemX with an N-terminal GFP fusion and FemA with a C-terminal mCherry, Erm^{r}	This work
RN-FemAB	RN4220 expressing FemB with a C-terminal GFP fusion and FemA with a C-terminal mCherry fusion, Erm^{r}	This work
COLpFemX-N	COL expressing FemX with an N-terminal GFP fusion, Erm^{r}	This work
COLpFemX-C	COL expressing FemX with a C-terminal GFP fusion, Erm^{r}	This work
COLFemA-C	COL expressing FemA with a C-terminal mCherry fusion	This work
COLpFemB-C	COL expressing FemB with a C-terminal GFP fusion, Erm^{r}	This work
COL-FemXA	COL expressing FemX with an N-terminal GFP fusion and FemA with a C-terminal mCherry fusion, Erm^{r}	This work
COL-FemAB	COL expressing FemB with a C-terminal GFP fusion and FemA with a C-terminal mCherry fusion, Erm^{r}	This work

Table 1 (cont.)

Strain/plasmid	Genotype/description	Origin/Reference
COLpPBP2-31	COL expressing PBP2 with anN-terminal GFP fusion, Erm^r	(Pinho and Errington, 2005)
Plasmid		
pMAD	*E. coli-S. aureus* shuttle vector with the *bgaB* gene encoding a ß-galactosidase. Amp^r/Erm^r	(Arnaud *et al.*, 2004)
pSG5082	Plasmid for C-terminal GFP fusions of proteins, Amp^r/Erm^r	(Pinho and Errington, 2004)
pSG5086	Plasmid for N-terminal GFP fusions of proteins, Amp^r/Erm^r	(Pinho and Errington, 2005)
pBCB4-CHERRY	Plasmid for C-terminal mCherry fusions of proteins, Amp^r/Erm^r	P. Pereira (unpublished)
pFemA-C	Derivative of pMAD containing *femA*-mCherry-*femB*	This work
pFemB-C	Derivative of pSG5082 containing *femB* upstream of *gfpmut*	M. Santos (unpublished)
pFemX-C	Derivative of pSG5082 containing *femX* upstream of *gfpmut*	M. Santos (unpublished)
pFemX-N	Derivative of pSG5086 containing *femX* downstream of *gfpmut*	This work
pFemA-UK	Derivative of pMAD containing a *femA* with a nonsense mutation	This work
pFemA-Lys33	Derivative of pFemA-C containing a *femA* with a K33→A substitution	This work
pFemA-Arg220	Derivative of pFemA-C containing a *femA* with an R220→A substitution	This work
pFemA-Tyr327	Derivative of pFemA-C containing a *femA* with a Y327→Ala substitution	This work

S. aureus strains were grown on tryptic soy broth (TSB, Difco), supplemented with erythromycin at 10 µg/ml, when needed, with aeration at 37°C, except where indicated. *E. coli* strains were grown in Luria–Bertani broth (Difco), supplemented with ampicillin at 100 µg/ml when needed, with aeration at 37°C. Growth was followed by monitoring the optical density at 600 nm.

Molecular cloning methods

The oligonucleotide primers used in this study are described in Table 2, restriction sequences are underlined.

Table 2 – Oligonucleotide primers used in this study

Primer Name	Nucleotide Sequence (5' – 3')
FEMAKP1	TTGGCCACTATGAGTTAGCGCTTGCTGAAGGTTATG
FEMAKP2	CATAACCTTCAGCAAGCGCTAACTCATAGTGGCCAAC
FEMAKP3	TTGGCCACTATGAGTTAG
FEMAP1eco	CCGGGAATTCGCAAATACGGAAATGAAATTAATTAACGAG
FEMAP2	AGAACCAGCAGCGGAGCCAGCCGACTTAAAAATTCTGTCTTTAAC
FEMAP3	TCCGCTGCTGGTTCTGGCGAGTTCATGATTGTGAGCAAGG
FEMAP4	TTTGATAATTCCCTTCCTAGTACAGCTCGTCCATGCCACC
FEMAP5	AAGGGAATTATCAAAACATGAAATTTACAGAGTTAACTGTTACCG
FEMAP6bam	GGCGCGCGGGATCCCTATTTCTTTAATTTTTTACGTAATTTATC
FEMARP1	AAAAGCTTTTGCTGATGCCGATGACAAAGCCTACTAC
FEMARP2	TAGTAGGCTTTGTCATCGGCATCAGCAAAAGCTTTTG
FEMARP3	CAAAAGCTTTTGCTGATG
FEMAUP1bam	GCTGCGGATCCGAGTTTGGTGCCTTTACAGATAG
FEMAUP2eco	GCAGCGAATTCGGCTCGATGTATCATACTC
FEMAUP3	ACAACTTGATGCAAATGAGT
FEMAUP4	GCTCGATGTATCATACTC
FEMAuutr	CTATAAAAGTATACGCAATTAAAGCG
FEMAYP1	CAATCCATTTGAAGTTGTTGCCTATGCTGGTGGTACATC
FEMAYP2	GATGTACCACCAGCATAGGCAACAACTTCAAATGGATTG
FEMAYP3	ATCCATTTGAAGTTGTTG
FEMBP1kpn	GTTGGTACCGATTCCTTGAACGTGATGAG
FEMBP2xho	CCGTCTCGAGTTTCTTTAATTTTTTACGTAATTTATCC
FEMXP1kpn	GCAGGTACCTTCTTAACGCGTGATATTAG
FEMXP2xho	CCGACTCGAGTTTTCGTTTTAATTTACGAG
FEMXP3xho	AAAGGGCTCGAGATGGAAAAGATGCATATCAC
FEMXP4eco	CCCTTTGAATTCGATTTCAGTCGTTAATCTATTTTCG
gfpmutP1	TTTGTATAGTTCATCCATGCCATGTGTAATCC
gfpmutP2	AGTAAAGGAGAAGAACTTTTCACTGGAGTTGTC
pMADII	CGTCATCTACCTGCCTGGAC

DNA purification

For chromosomal DNA purification, cell cultures were grown to exponential phase. A 30 ml sample was collected at OD_{620nm} of 1, pelleted and resuspended in 50mM EDTA. Cells were then incubated at 37ºC with 5µl of lysostaphin (10 mg/ml, Sigma) and 10µl of RNAse (10mg/ml, Sigma) for 30min and, subsequently, incubated at 80ºC with Nuclei lysis solution (Promega) for 5min. Protein precipitation solution (Promega) was added and cells were incubated 10min on ice. DNA was then precipitated with isopropanol, washed with ethanol 70% and resuspended in sterile water.

For the screening of *S. aureus* mutants by PCR, genomic DNA was isolated from 1-ml cultures grown overnight using a modified alkaline wash protocol (Hall *et al.*, 2003). Briefly, cells were pelleted, resuspended in 500 µl of alkaline wash solution (0.05 M sodium citrate, 0.5 M NaOH), and incubated at room temperature for 20 min. Tubes were spun at 14.000 x *g* for 1 min, pellets were washed with 500 µl of 0.5 M Tris-HCl, pH 8.0, and subsequently resuspended in 100 µl of sterile water. Tubes were placed in boiling water for 10 min and spun at 14.000 x *g* for 5 min. Five microliters of supernatant were used in each 50 µl PCR reaction.

Plasmid DNA from *E. coli* strain was extracted using Wizard SV Plus Miniprep kit (Promega). Ethanol precipitation was used for the concentration of DNA. Quantification of DNA was carried out by comparing the fluorescent intensities of the samples and DNA markers on 0.8% agarose gels stained with ethidium bromide

DNA manipulations

Restriction enzymes were purchased from New England Biolabs. DNA fragments were digested with restriction enzymes of interest (0.5-1µg DNA, 1X restriction buffer, and 1X BSA if required, 20U restriction endonuclease and water to 50µl for 16 hours), purified using Wizard SV Plus Cleanup kit (Promega) and ligated together. A typical ligation reaction contains vector and insert DNAs (0.1–5 µg), 1X Ligase buffer, 20–100 U T4 DNA ligase (Fermentas) for 1h at room temperature or overnight at 4ºC. PCR reactions were done with either the GoTaq Polymerase (Promega) for colony screenings or Phusion polymerase (Finnzymes) for subsequent cloning into plasmids, both following manufacturer's instructions, except where noted.

Transformation of *E.coli*

Competent cells were prepared according to the Rubidium chloride method (Sambrook *et al.*, 1989). Briefly, early exponential cells (O.D.600nm = 0.3-0.4) were incubated on ice for 15min, centrifuged and resuspended in 1/3 of culture volume of RF1 buffer (RbCl 100mM; $MnCl_2$ tetrahydrate 50mM; Potassium acetate pH 7,5 35mM; Calcium chloride bihydrate 10mM; Glycerol 15%). Cells were incubated on ice for 15 minutes and pelleted. The pellet was resuspended in 1/2 volume of RF2 buffer (MOPS 10mM; RbCl 10mM; Calcium chloride bihydrate 75mM; Glycerol 15%) and stored at -80°C in 300 µl aliquots. For the transformation, either plasmid or ligation mixtures were added to the competent cells and kept on ice for 10 min. Foreign DNA was introduced using a heat shock method (45 sec at 40°C). Cells were mixed with 1 ml LB medium and incubated at 37°C for 1h. Appropriate aliquots were spread on antibiotic selection plates.

S. aureus transformation and transduction

Transformation of *S. aureus*

S. aureus competent cells were prepared essentially as previously described (Kraemer, 1990). Briefly, bacteria were grown to $O.D._{600nm}$ = 0.4 and centrifuged. Cells were washed once with equal culture volume of ice cold filter sterilized 0.5M sucrose (Sigma), and once with half the volume of 0.5M sucrose. Cells were then incubated on ice for 20min and resuspended in 1/100 of the initial volume of 0.5M sucrose with 10% glycerol (Fluka), and stored at -80°C. 45µl of competent cells were mixed with 5 - 8 µl DNA purified using the Wizard SV Plus clean-up kit (Promega) and electroporated. The standard electroporation conditions were: 2.5 kV, 100 Ω, 25 µF in a 0.2cm BioRad Gene Pulser cuvette. After electroporation, cells were mixed with 1 ml TSB and incubated for 1 h at 37°C. Appropriate dilutions were spread on antibiotic selection plates.

Transduction with phage 80α

Transduction was done as previously described (Oshida and Tomasz, 1992). For the preparation of transduction lysates, donor strains were grown in Tryptic Soy Agar (TSA, Difco) overnight at 37ºC. Cells were collected with 1ml of TSB and calcium chloride was added to a final concentration of 5 mM. Phage 80α lysate was diluted (10^{-2}, 10^{-3} and 10^{-4}) in phage buffer (1mM $MgSO_4$, 4mM $CaCl_2$, 50mM Tris-HCl pH 7.8, 5,9g/l NaCl and 1g/l gelatin). The cell suspension (10µl) was mixed with 10µl of each of the phage dilutions and 3ml of phage top agar (casamino acids 3g/l, Difco; yeast extract 3g/l, Difco; sodium chloride 5,9g/l, Sigma; and agar 5g/l, Difco, pH 7.8), supplemented with 5mM of $CaCl_2$, pre-warmed for one hour at 45ºC. The mixture was poured onto phage bottom agar (identical to the top but with 15g/l of agar) with 5mM of $CaCl_2$ and incubated over night at 30ºC. On the following day, phage buffer (3ml) was added to plates showing confluent lysis. Plates were kept at 4ºC for one hour. The phage top agar and the phage buffer were then collected into a centrifuge tube and vigorously vortexed in order to disrupt the phage bottom agar. The tubes were kept for one hour inverted at 4ºC. The agar was centrifuged at 3500 rpm for 30min at 4ºC. The supernatant was collected and filtered through a 0.45 µm sterile filter. For the transduction, recipient strains were grown overnight in TSA at 37ºC. Cells were collected with 1ml TSB with $CaCl_2$ 5mM. Cell suspension (100µl) was added to the phage lysate (1µl and 10µl) and phage buffer was added to a final volume of 300µl. A control tube without phage lysate was also prepared. The mixtures were incubated for 20min at 37ºC and 3ml of 0.3GL top agar (casamino acids 3g/l, Difco; yeast extract 3g/l, Difco; NaCl, 5,9g/l Sigma; sodium lactate 60% syrup, 3,3ml/l, sigma; glycerol 50%, 2ml/l, Sigma; Tri-sodium citrate, 0,5g/l, Sigma; and agar 7,5g/l, Difco; pH 7,8) at 45ºC (pre-warmed for one hour) were added. The mixture was then poured onto plates made with 10ml of 0.3GL bottom agar (identical to 0.3GL top but with 15g/l agar) with 30mg/l of Erythromycin (Sigma) and 20ml of 0.3GL bottom agar without antibiotic. Plates were used within one hour after preparation.

Construction of derivatives of the FemXAB proteins

Construction of FemX-GFP fusions

A 650 bp fragment of the 3' end of the *femX* gene was amplified from COL using primers FEMXP1kpn/FEMXP2xho, digested and cloned into Kpn/XhoI restriction sites of pSG5082, upstream and in frame with *gfpmut* resulting in pFemX-C. The entire *femX* gene was amplified from COL using primers FEMXP3xho/FEMXP4eco, digested and cloned into the XhoI/EcoRI restriction sites of pSG5086, downstream and in frame with *gfpmut*, resulting in pFemX-N**.** Both plasmids were electroporated into RN4220 competent cells and transduced to COL. Transformants were selected on Ery 10 µg/ml plates at 37ºC and successful integration of the plasmids into the chromosome was validated by PCR, with primer pairs FEMXP1kpn/GFPMUTP1 for the C-terminal fusion and GFPMUTP2/FEMXP4eco for the N-terminal fusion. C-terminal GFP mutants of FemX were termed RNpFemX-C and COLpFemX-C. N-terminal GFP mutants of FemX were termed RNpFemX-N and COLpFemX-N

Construction of a FemB-GFP fusion

A 660 bp fragment of the 3' end of the *femB* gene was amplified from COL using primers FEMBP1kpn and FEMBP2xho, digested and cloned into KpnI/XhoI restriction sites of pSG5082, upstream and in frame with *gfpmut*, resulting in pFemB-C**.** The plasmid was then electroporated into RN4220 competent cells and transduced to COL. Transformants were selected on Ery 10 µg/ml plates at 37ºC and successful integration of the plasmid into the chromosome was validated by PCR with primer pair FEMBP1kpn/GFPMUTP1. In this way, mutants RNpFemB-C and COLpFemB-C were obtained.

Construction of FemA-mCherry fusions

In order to introduce a *femA-mcherry* fusion into the chromosome of *S. aureus* without disrupting the *femAB* operon, the thermosensitive pMAD vector (Arnaud *et al.*, 2004) was used to clone a *femA-mcherry-femB* PCR fragment (Figure 8).

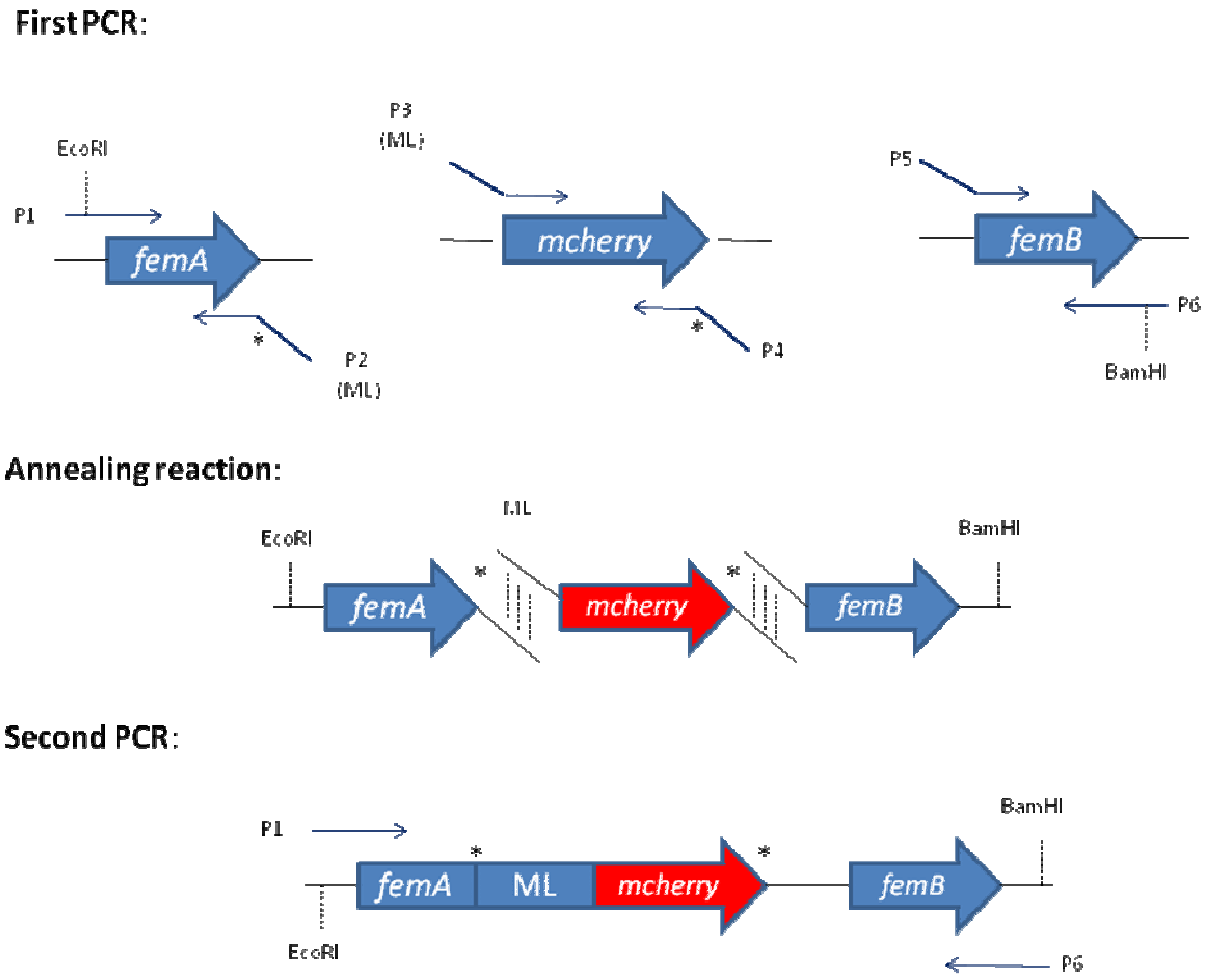

Figure 8 – Strategy for the construction of the fusion *femA-mcherry-femB*. ML = protein linker. P1-P6: primers FEMAP1eco, FEMAP2, FEMAP3, FEMAP4, FEMAP5 and FEMAP6bam, respectively.

Construction of the fusion gene was made as previously described (Wurch *et al.*, 1998). In the first PCR, *femA* and *femB* genes were amplified from COL genomic DNA with primer pairs FEMAP1eco/FEMAP2 and FEMAP5/FEMAP6, respectively. *mcherry* was amplified from pBCB4-Cherry with primers FEMAP3 and FEMAP4. These PCRs were done using Phusion polymerase (Finnzymes) in 20 cycles of: denaturation at 98ºC for 10s, annealing at 74ºC for 20s, extension at 72ºC for 90s. Primer FEMAP2 contains a point mutation to remove the *femA* stop codon and primer FEMAP4 contains a point mutation to insert a stop codon at the end of *mCherry*, both depicted by an asterisk in Figure 8. Both primers FEMAP2 and FEMAP3 include an overlapping sequence of nucleotides encoding a peptide linker. In the annealing reaction, the overlapping sequences from primer pairs allowed the fusion of the construct. Equimolar amounts of each PCR product were mixed together and subjected to 1 cycle in the conditions described above. In the second PCR, primers

FEMAP1eco and FEMAP6bam were used to amplify the fusion gene with the Phusion polymerase for 20 cycles of: denaturation at 98ºC for 10s, annealing at 74ºC for 20s, extension at 72ºC for 4m. The final PCR fragment was cut with EcoRI and BamHI and cloned into pMAD vector, generating plasmid pFemA-C. After extraction of the plasmid from *E. coli* DH5α, restriction digest confirmation was performed with the same enzymes used for cloning and the plasmid insert was sequenced. pFemA-C was electroporated into RN4220 competent cells at 30ºC to keep the plasmid from integrating. Transformants were selected on an erythromycin 10 µg/ml plate. The plasmid was transduced from RN4220 background to COL and transductants were selected on erythromycin 10 µg/ml plates at 30ºC.

Both for COL and RN4220, one erythromycin resistant colony was inoculated in fresh TSB containing Ery 10 µg/ml, at 30ºC for 16 hours. The overnight culture was diluted 1:1000 to the same medium and incubated for 7 hours, then diluted 1:1000 again and incubated in the same medium at 43ºC overnight. The overnight culture was serially diluted to 10^{-4}, 10^{-5} and 10^{-6} and plated on TSA containing Ery 10 µg/ml and bromo-chloro-indolyl-galactopyranoside (X-GAL) 100 µg/ml and incubated overnight at 43ºC. Several light blue colonies were picked and restreaked in the same conditions. Genomic DNA of selected clones was purified and PCR was done to confirm integration (Figure 9 –step 2) using one primer complementary to the upstream region of *femA* (FEMAuutr) and an internal pMAD primer (PMADII). One positive clone for integration was inoculated in TSB medium with no antibiotic at 30ºC overnight. The overnight culture was diluted 1:500 into TSB, in the same conditions. After 7 hours, the culture was serially diluted to 10^{-3}, 10^{-4} and 10^{-5} and plated to TSA + X-Gal 100 µg/ml at 43ºC overnight**.** White colonies, representing candidates for the double crossover event and loss of the plasmid (Figure 9, step 3), were restreaked on TSA. Colonies which retained the *mcherry* fusion to *femA* in the chromosome were first selected by susceptibility to erythromycin and then by PCR screening using PFEMAP1eco and PFEMAP2xho. These mutants were named COLFemA-C and RNFemA-C.

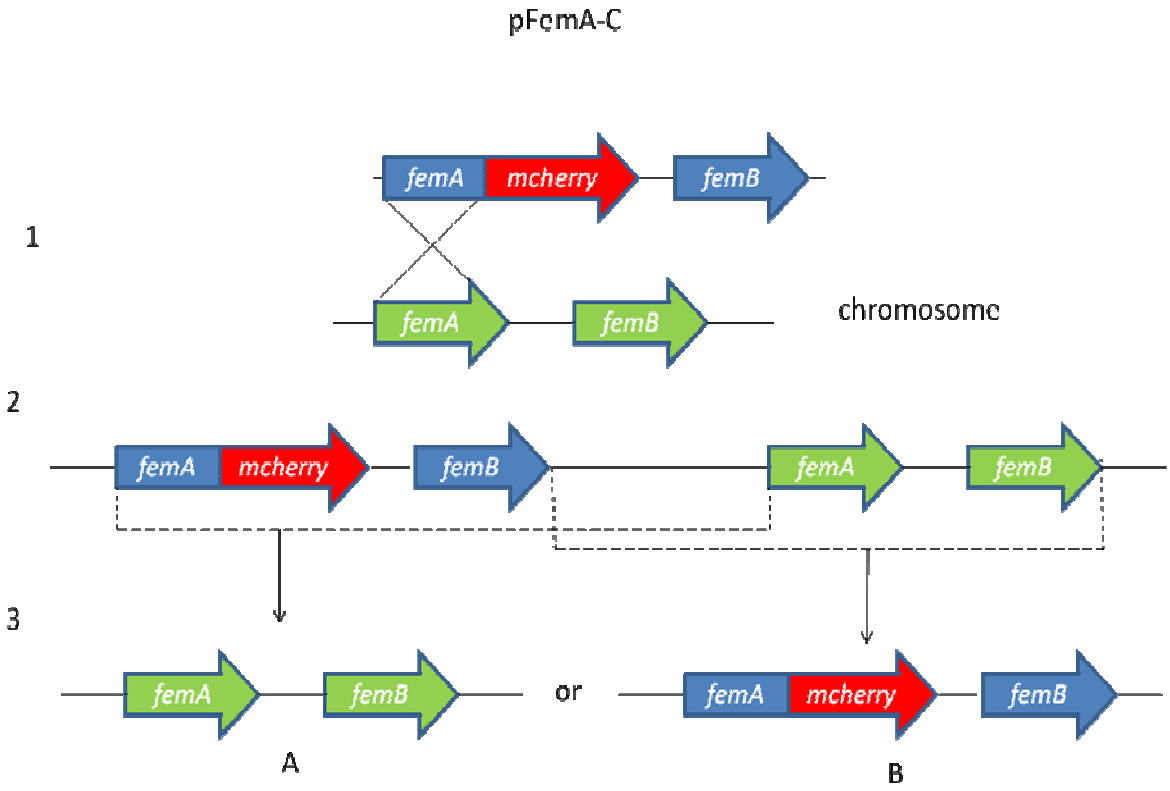

Figure 9 – Allelic replacement strategy using pMAD derived plasmid pFemA-C. Integration through *femA* is shown but homologous recombination in the first step can also occur through the *femB* region. In the third step, the second recombination event and loss of the plasmid can yield a wild type strain (A) or a strain containing a *femA-mcherry* fusion in the *femA* native locus (B). Step 1 – homologous recombination between pFemA-C and the bacterial chromosome; Step 2 – integration; Step 3 – excision and loss of the plasmid.

Construction of strains encoding fluorescent derivatives of two Fem proteins

In order to generate a strain expressing simultaneously FemA-mCherry and FemB-GFP, plasmid pFemB-C was electroporated into RNFemA-C competent cells. Transformants were selected on Ery 10 µg/ml plates at 37ºC and named RN-FemAB. The fragment containing the *femAB* operon was transduced to COL, with selection on Ery 10 µg/ml plates at 37ºC. The resulting strain was named COL-FemAB. The presence of both fusion genes was confirmed by PCR with primers PFEMAP1eco and GFPMUTP1.

In order to generate a strain expressing simultaneously GFP-FemX and FemA-mCherry, plasmid pFemX-N was transduced from RNpFemX-N into COLFemA-C.

Transductants were selected on Ery10 µg/ml plates at 37ºC and named COL-FemXA. Integration of the plasmid was confirmed with primers GFPMUTP2 and FEMXP4eco.

Mutagenesis of the *femA* gene

A 1900 bp DNA fragment encompassing *femA* was amplified from strain UK17 using primers FEMAUP1 and FEMAUP2. This strain contains a nonsense mutation at position 985 of the *femA* gene. The PCR fragment was digested and cloned into the EcoRI/BamHI restriction sites of pMAD, generating plasmid pFemA-UK.

In order to construct mCherry-tagged *femA* defective mutants, the following residue replacements were performed in the *femA* region of the pFemA-C plasmid: Lys33 to Ala (resulting in plasmid pFemA-K33), Arg220 to Ala (resulting in plasmid pFemA-R220) and Tyr327 to Ala (resulting in plasmid pFemA-Y327). Site-directed mutagenesis was done using primer pairs FEMAKP1/FEMAKP2, FEMARP1/FEMARP2, FEMAYP1/FEMAYP2 for the Lys, Arg and Tyr mutations, respectively. Primers of each pair are complementary to each other and contain the desired mutations in the middle, to replace residues K33, R220 and Y327 with alanines. PCR reactions were done with Phusion polymerase following manufacturer's instructions but using a template/primer concentration ratio of 2. PCR products were incubated at 37ºC for 1 hour with DpnI restriction enzyme, to digest the methylated pFemA-C template. The amplicons were ligated and transformed to DH5α competent cells. Following plasmid extraction, restriction confirmation was performed, using EcoRI and BamHI. Plasmids were sequenced to confirm the presence of the desired mutations.

Plasmids pFemA-UK, pFemA-Lys33, pFemA-Arg220 and pFemA-Tyr327 were electroporated into RN4220 competent cells and transformants were selected on Ery 10 µg/ml plates at 30ºC. Integration of the plasmids into the chromosome was performed as described above. Excision and allelic exchange of the *femA* wt gene by the mutant copy was attempted by three separate methods (see below). In all cases, white colonies were streaked to TSA Ery 10 µg/ml plates to confirm excision, to lysostaphin 5 ug/ml plates to confirm resistance and to TSA plates at 42ºC to confirm thermosensitivity, as *femA* defective mutants are lysostaphin resistant and thermosensitive (Kusuma *et al.*, 2007). Allelic replacement was also checked by PCR with primer pairs PFEMAUP3/PFEMAUP4, PFEMAKP3/PFEMAUP4,

PFEMARP3/PFEMAUP4, PFEMAYP3/PFEMAUP4 for the UK17, Lys33, Arg220 and Tyr327 mutations, respectively. Screening PCRs were done with GoTaq polymerase, following manufacturer's instructions, but with annealing temperatures 2 ºC below the melting temperature of the primer pair, using wild-type RN4220 and the *femA* mutant UK17 strains as controls.

Method I – Regular methodology for excision of pMAD plasmid as described above, except that mutants were plated at 37ºC instead of 43ºC.

Method II – Integrates were allowed to grow for 10, 15, 20 and 25 generations at 30ºC without erythromycin, before being plated on TSA at 30ºC or 37ºC. As *femA* defective mutants are reported to have a fitness defect (Kusuma *et al.*, 2007), this method aimed to isolate them before they were outcompeted by wild-type excisates in the culture.

Method III –. Integrates were allowed to grow for 10, 15, 20 and 25 generations at 30ºC without erythromycin, before being plated on TSA supplemented with 5 µg/ml lysostaphin at 30ºC or 37ºC This method aimed at introducing selective pressure during excision, to isolate the desired mutants as soon as the second recombination event took place.

Cell wall analysis

Cell wall extract preparation

Cell wall was purified essentially as previously described (de Jonge and Tomasz, 1993). *S. aureus* cells were grown for 16 h in TSB. Cultures were diluted to an OD600 of 0.001 and allowed to grow for approximately nine generations in fresh TSB. Cultures were chilled in an ice-ethanol bath and then centrifuged (15,000 x *g*) for 10 min at 4ºC. The cells were resuspended in 40 ml of cold water and added to 40 ml of boiling 8% sodium dodecyl sulphate (SDS, Sigma). This solution was boiled for 30 min and then allowed to cool to room temperature (RT). The SDS-insoluble material was collected by centrifugation (17,000 x *g*) for 15 min at 20ºC. The pellet was washed five times with warm water until no more SDS could be detected by the Hayashi method, to check SDS presence. Hayashi method: 0.5 mL of the supernatant (water as control), 0.25 mL methylene blue solution (1 volume of chloroform per 20 volumes of 0.5% methylene blue solution, diluted 1:100 with 0.7 mM phosphate buffer

pH 7.2.) and 1.5 mL chloroform, were added and samples were vortexed at maximum speed for 60 s and were let to settle for 1 minute. If the sample is SDS free, the lower phase presents as clear as the control. SDS free cells were resuspended in 1 to 2 ml of water and broken with glass beads (Sigma-Aldrich) in a Bio101 Savant Apparatus (Thermo Electro Corporation). Non-broken cells and glass beads were removed by low speed centrifugation (500 x *g*) for 15 min. The collected broken cells were centrifuged (17.000 x *g*) for 15 min at 4ºC. The pellet was resuspended in 2 ml of 50 mM Tris-HCl (pH= 7) with 0.05% sodium azide and MgSO4 at final concentration of 20mM. DNase and RNase (Sigma) were added at a concentration of 10 µg/ml and 50 µg/ml, respectively, and the mixture was incubated for 2 h at 37ºC with agitation. The peptidoglycan associated proteins were removed by overnight incubation at 37ºC with 50 µg/ml of trypsin (Whorthington) in the presence of 20 mM $CaCl_2$. The insoluble material was boiled again in 1% of SDS for 15 min, collected and washed with water, as described above, three times. The cell wall pellet was then treated with 8 mM LiCl for 15 min at 37ºC, collected by centrifugation (17.000 x *g*) for 15 min, resuspended in 100 mM EDTA (pH= 7) and again incubated for 15 min at 37ºC. The pellet was washed two times with water, resuspended in 10 ml of acetone, sonicated for 5 min and then washed again in water, lyophilized, and stored at 4ºC.

Preparation of highly purified peptidoglycan

Peptidoglycan was obtained from purified cell wall by degradation of teichoic acids with hydrofluoric acid. Lyophilized cell walls were resuspended in 2 ml of ice-cold hydrofluoric acid for 48 h at 4ºC. Peptidoglycan was recovered by centrifugation (48.000 x *g*) for 45 min at 4ºC. The pellet was washed twice with water, twice with 50mM Tris-HCl (pH=7) and finally again twice with water, after which samples were lyophilized.

Preparation of the muropeptides.

Lyophilized peptidoglycan was resuspended in 25 mM sodium phosphate buffer with 0.05% sodium azide (pH=5.5) to a concentration of 10 mg/ml and digested with mutanolysin (0,135 U/µg peptidoglycan) overnight at 37ºC. The enzyme reaction was stopped by boiling the sample for 5 min, and insoluble materials were removed by centrifugation (15.000 x *g*) for 5 min.

HPLC analysis of muropeptides profiles

The muropepetides profile was obtained by HPLC system analysis. The digested peptidoglycan was injected in a Chromolith column using a 3ml linear gradient from 0.05% of trifluoroacetic acid (TFA) to a 0.05 % TFA buffer with 10% acetonitrile for 26 min.

Electrophoretic analysis of proteins by SDS-PAGE

Cells were grown to exponential phase (20mL) and harvested by centrifugation (3000 x g, 4ºC). The pellet was then washed once with equal volume of PBS and resuspended in 1/20 of the original volume in PBS with 1 mM of PMSF (Sigma). The cells were disrupted with approximately 800µl of glass beads in a Bio101 Savant apparatus. Glass beads were removed by centrifugation at 500 × g for 5 min. 10µl of supernatant were mixed with an equal volume of SDS-PAGE sample buffer. Samples were applied to a 10% polyacrylamide (30% acrylamide/bis solution, 37.5:1) protein gel. The molecular weight marker used was the SDS-PAGE Molecular Weight Standards, low range (Biorad). The samples were run at 20mA for approximately 30 minutes.

Minimum inhibitory concentration assays

MICs of relevant antimicrobial compounds were determined by broth microdilution in sterile 96-well plates. The medium used was TSB, containing a series of two-fold dilutions of each compound. Cultures of *S. aureus* strains and mutants were added at a final density of $5x10^{-5}$ CFU/ml to each well. Wells were reserved in each plate for sterility control (no inocula added) and inocula viability (no compound added). Plates were aerobically incubated at 37 C. Endpoints were recorded visually after 24 and 48 h. All assays were done in duplicate.

Fluorescence microscopy

S. aureus strains were grown for 16 hours on TSB, supplemented with erythromycin when needed, diluted 1:1000 in the same medium without erythromycin and allowed to grow to mid-exponential phase (O.D = 0.7). 1 ml of culture was centrifuged for 1 min at 13500 rpm at RT and resuspended in 50 µl of fresh TSB. 2 µl of culture were then placed on microscope slides with a thin film of 1% agarose prepared in PBS. When it was relevant to inspect bacterial membranes, cells were incubated with either Nile Red (Invitrogen) or FM1-43 (Invitrogen) fluorescent lipophillic dyes at 0.5-5 µg/ml for 5 minutes at room temperature with shaking, before being placed on the microscope slides. When it was relevant to inspect nucleoid shape, cells were incubated with DAPI (Invitrogen) fluorescent DNA-binding dye at 2 µg/ml for 10 minutes at room temperature with shaking, before being placed on microscope slides. Fluorescence microscopy visualizations were conducted in a Zeiss Axio Observer microscope equipped with a Photometrics CoolSNAP HQ2 camera (Roper Scientific), using Metamorph software. Analysis of fluorescent images was performed using ImageJ software.

Substrate depletion experiments

To visualize protein localization after substrate depletion, *S. aureus* strains and mutants were grown to O.D 600 nm = 0.7 and incubated for 30 minutes with either tunicamycin or fosfomycin at 10X the corresponding MIC values. Cells were then washed 2 times with fresh TSB and visualized on the microscope as described above.

Results

Construction of fluorescent derivatives of FemXAB

In order to study the localization of the FemX, FemA and FemB proteins during the cell cycle, we constructed fluorescent derivatives of each protein and expressed them from their native chromosome loci in *S. aureus.* The FemX protein was fused either at its C-terminal (FemX-GFP) or N-terminal (GFP-FemX) to Green Fluorescent Protein (GFP). The FemA and FemB proteins were fused at their C-terminus to fluorescent protein mCherry (FemA-mCherry) or GFP (FemB-GFP), respectively. All fusions corresponded to the only copy of the specific *fem* gene present in the genome and were placed under the control of the native promoter of the respective *fem* genes, except *gfp-femX*, which was put under the control of the xylose promoter from *B. subtilis* (Pinho and Errington, 2005), that is contitutively expressed in *S. aureus*. Although each protein fusion was constructed both in RN4220 and COL backgrounds, the characterization of the mutant derivatives of the former were mostly excluded from this thesis, as RN4220 is a highly mutagenized strain and only suitable as a cloning intermediate.

Mutants in the Fem proteins usually display growth defects (Henze *et al.*, 1993; Kusuma *et al.*, 2007; Rohrer *et al.*, 1999), therefore we determined the growth rates of the strains expressing fluorescent derivatives of the Fem proteins as a measure of the functionality of the fusions. Figure 10 shows the growth rates of parental MSSA strain RN4220 and of the strains expressing fluorescent FemX derivatives constructed in this background. Strain UK17 has a stop codon in the *femA* gene, therefore expressing a truncated form of FemA, which has no activity (Ehlert *et al.*, 1997). This strain was included as a control to show the effect of lack of a Fem protein in the cell's division rate. We could not use a *femX*-inactivated mutant as a control because FemX is an essential protein to the cell (Rohrer *et al.*, 1999). It is however important to notice that UK17 has a different genetic background from COL and RN4220 strains and therefore the *femA* mutation may eventually show different phenotypes. RN4220 expressing a GFP-FemX fusion was shown to have a growth rate close to the parental RN4220 strain, with doubling times of 24 minutes for RNpFemX-N and 19 minutes for RN4220. The FemX-GFP fusion mutant, on the other hand, displayed slower growth than

the wt strain during the exponential phase (doubling time 50 minutes) than the wild-type strain. This suggests a growth defect of RNpFemX-C, probably because the FemX-GFP protein is only partially functional.

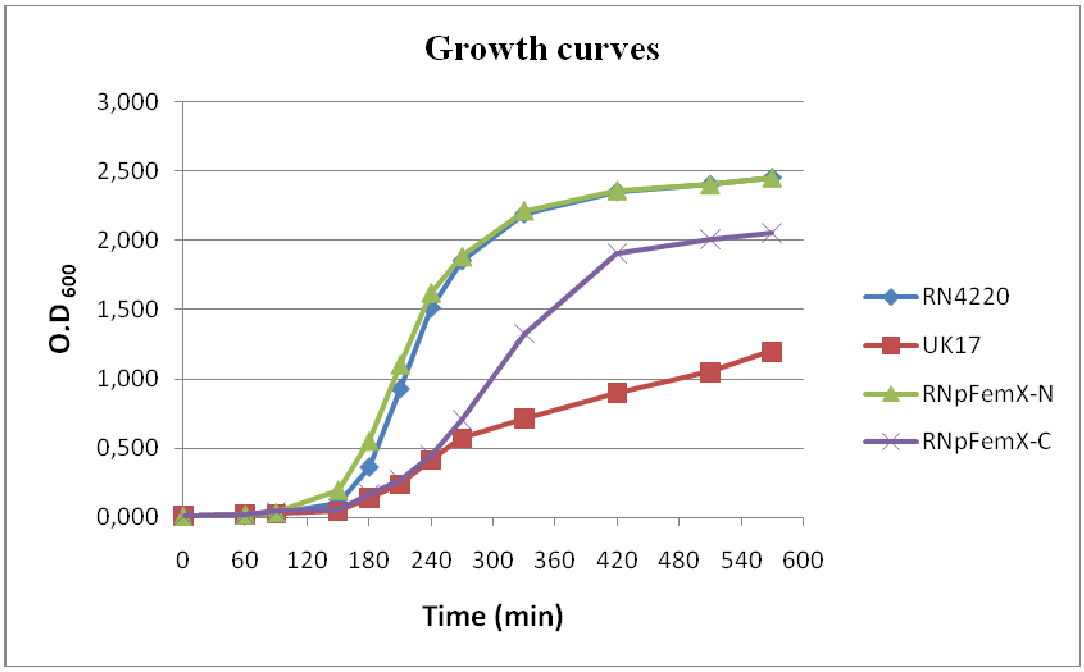

Figure 10 – Growth curves of MSSA strain RN4220, RN4220 expressing N-terminal (RNpFemX-N) and C-terminal (RNpFemX-C) GFP fusions to FemX and the *femA*-inactivated UK17 strain.

When the same GFP N- and C-terminal fusions to FemX were expressed in the background of MRSA strain COL, the two resulting strains had identical growth rates and doubling times (35 minutes), which were similar to the parental strain COL (doubling time 30 minutes) (Figure 11). Therefore, it seems that the presence in COL of a FemX fusion which is not fully functional, does not significantly affect growth.

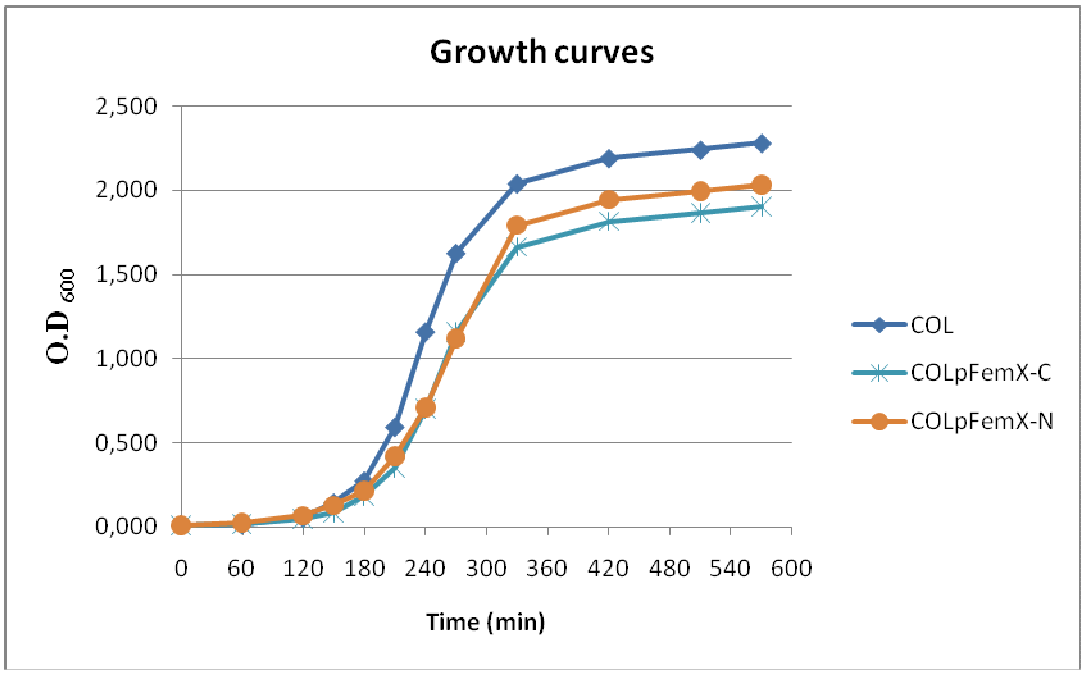

Figure 11 – Growth rates for parental MRSA strain COL and COL expressing N-terminal (COLpFemX-N) and C-terminal (COLpFemX-C) GFP fusions to FemX.

We have also determined the growth rates of strain COL expressing FemA-mCherry (doubling time 30 minutes) and FemB-GFP (doubling time 32 minutes) fusions (Figure 12), which we found to be identical to parental wild-type strain COL.

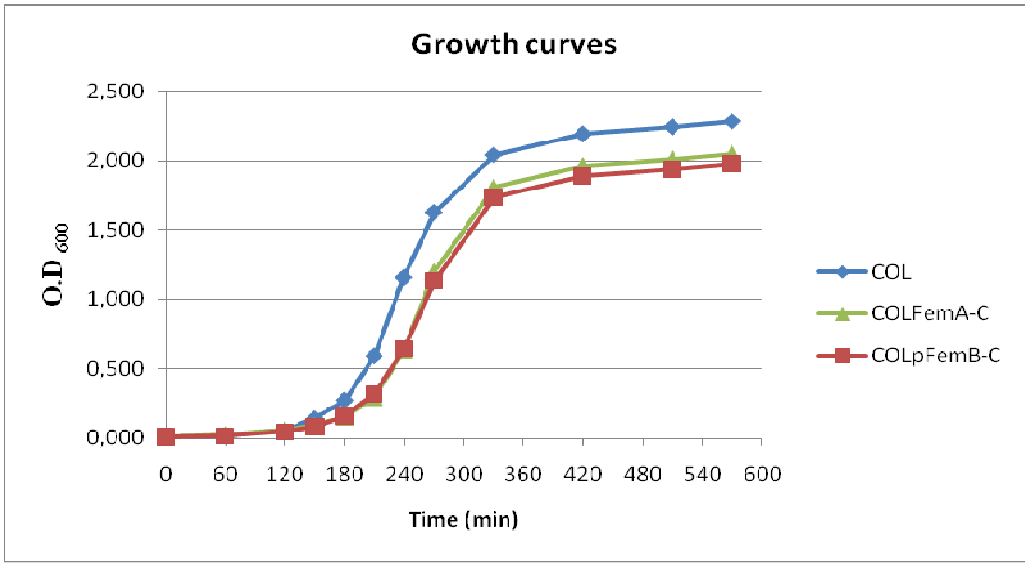

Figure 12 – Growth rates for parental MRSA strain COL and COL expressing a C-terminal mCherry fusion to FemA (COLFemA-C) and a C-terminal GFP fusion to FemB (COLpFemB-C).

The FemXAB proteins were initially identified as being essential for the expression of high level methicillin resistance (Berger-Bächi *et al.*, 1989; Henze *et al.*, 1993; Tschierske *et al.*, 1999). Therefore, if the fluorescent derivatives of the Fem proteins were not fully functional, we would expect that their expression in the COL background would cause a reduction in the oxacillin minimum inhibitory concentration (MIC). To further confirm the functionality of the fusion proteins, we proceeded to characterize the corresponding strains by testing resistance to four cell-wall active compounds (Table 3). Besides oxacillin, we also tested resistance to lysostaphin in mutants with fluorescent proteins fused to FemA, as the loss of activity of this protein leads to decreased amounts of muropeptides with pentaglycine crossbridges, thus depleting the targets of lysostaphin (*vide* p.10). As it was expected, both sensitivity to oxacillin and resistance to lysostaphin were observed in the *femA*-inactivated strain UK17. On the contrary, expression of GFP-FemX, FemA-mCherry or FemB-GFP did not cause a decrease in the oxacillin minimum inhibitory concentration of strain COL and COLFemA-C did not show increased resistance to lysostaphin, suggesting that the Fem proteins are functional in these strains. It is interesting to notice that the GFP C-terminal fusion to FemX, which resulted in a severe growth defect in the RN4220 background, caused a 8-fold reduction in the oxacillin MIC of COL, further confirming that this fusion is not fully functional. Tunicamycin and fosfomycin are cell-wall active antibiotics which were used in subsequent localization studies (see p.55). COLpFemX-C exhibited increased susceptibilities to both tunicamycin and fosfomycin, which constitutes another indication that the peptidoglycan structure might have been compromised in this strain. It seems that in the COL background, decrease of FemX activity does not affect cell growth as in the RN4220 background but it does have an impact in resistance to cell wall active antibiotics. The N-terminal GFP fusion to FemX, as well as FemA-mCherry and FemB-GFP caused no changes in the tunicamycin and fosfomycin MICs.

Table 3 –Minimum inhibitory concentrations of cell wall active compounds in relevant strains used in this study.

Strain	MIC (ug/ml)			
	Oxacillin	Lysostaphin	Tunicamycin	Fosfomycin
RN4220	0.125	-	12	19.5
RNpFemX-N	0.125	-	12	19.5
RNpFemX-C	0.125	-	1.5	4.8
COL	800	0.016	50	1250
COLpFemX-N	800	-	50	1250
COLpFemX-C	100	-	12.5	625
COLFemA-C	800	0.016	50	1250
COLpFemB-C	800	-	50	1250
COL-FemAB	400	0.016	-	-
COL-FemXA	800	-	-	-
UK17 (*femA*$^-$)	0.19	32	-	-

We also tested the activity/functionality of Fem proteins derivatives by analyzing the bacterial cell wall composition. To this end, cell wall extracts were prepared from bacterial cultures. Peptidoglycan was extracted, purified and digested with mutanolysin to yield a mixture of muropeptides, the building blocks of peptidoglycan. These muropeptides were resolved by high pressure liquid chromatography (HPLC). Analysis of the resulting chromatogram allows the identification of monomeric muropeptides, dimers, trimers, etc. This system does not have enough resolution to discern beyond hexamers and, as such, crosslinked muropeptide above this order of magnitude elute together. The amount of crosslinking can then be estimated by the area of the broad peak at the end of the chromatogram, above 100 minutes of retention time (Figure 13). To ascertain if the C-terminal GFP fusion to FemX on the COL background was causing loss of activity of this protein, the muropeptide composition of peptidoglycan of this mutant was compared to wild-type COL strain, as it is depicted in Figure 13, panel A and Figure 14. The FemX-GFP mutant exhibited striking changes in muropeptide composition.

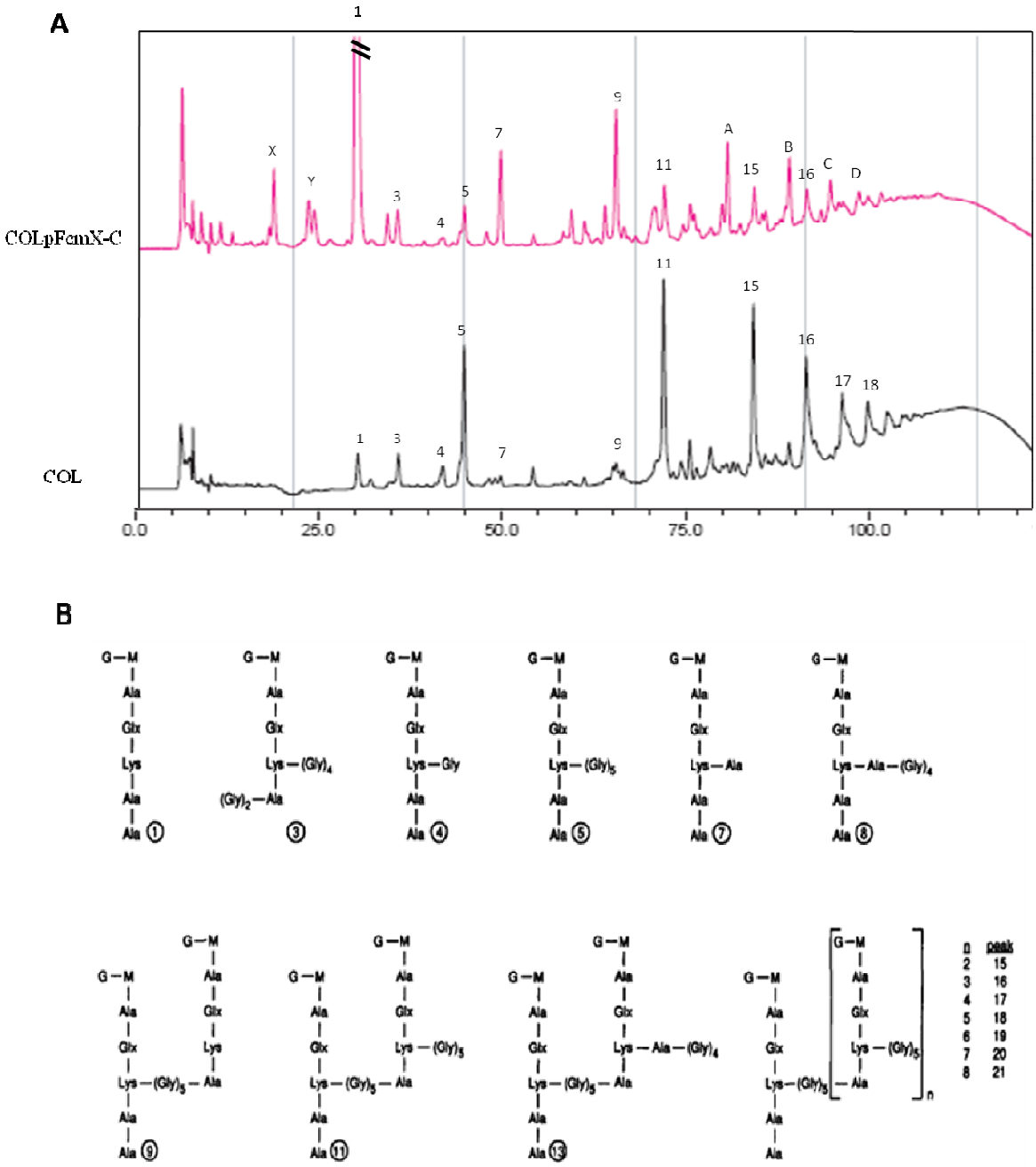

Figure 13 – **A** – muropeptide profiles of wild-type strain COL (in black) compared to the COL FemX-GFP (in red) derivative. The fusion of GFP to the C-terminus of FemX is shown to alter the cell wall composition significantly. Overall, a marked increase in the ratio of unsubstituted to pentaglycine-substituted muropeptides is visible in the profile of FemX-GFP. Peaks A, B, C and D are likely to be unsubstituted trimers, tetramers, pentamers and hexamers, respectively. Peaks X and Y are proposed to be alternative unsubstituted monomers (Rohrer *et al.*, 1999). A decrease in the amount of crosslinking is also observed. **B -** proposed chemical structures of the peak compositions in muropeptide chromatographic analysis, according to de Jonge and Tomasz, 1992. Muropeptides are numbered according to their specific retention times. In this way, for example, a NAG-NAM-pentapeptide molecule (1) elutes first, while an octamer (21) elutes last. G= *N*-acetylglucosamine; M = *N*-acetylmuramic acid.

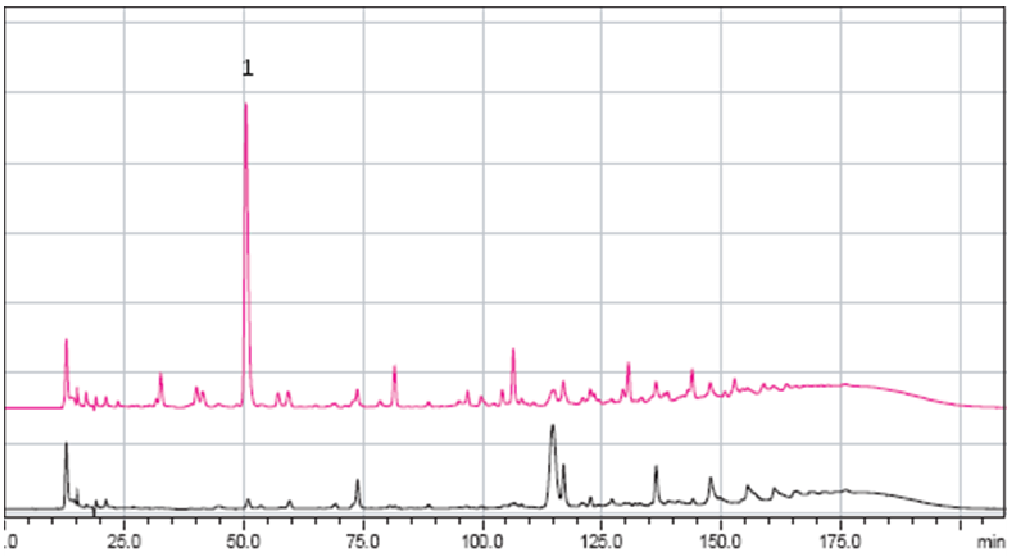

Figure 14 - Muropeptide profiles of wild-type strain COL (in black) compared to the COL FemX-GFP (in red) derivative, showing a massive increase of unsubstituted monomers (peak 1) in the cell wall composition of this mutant, relative to the parental strain. It is also shown that, unlike COL, unsubstituted muropeptides are the most prevalent species in the cell wall of COL FemX-GFP.

The same result was obtained for the FemX-GFP mutant constructed in the RN4220 background (data not shown). The most abundant peaks in the muropeptide profile of COL are 5, 11, 15, 16, 17 and 18. These correspond to monomers, dimers, trimers, etc. with at least one fully synthesized crossbridge that is not crosslinked to other muropeptide (see Figure 13, panel B). This indicates that there is a pool of muropeptides in the bacterial cell wall that are always readily available for crosslinking. In striking contrast, the muropeptide profile of the FemX-GFP mutant shows a massive accumulation of unsubstituted monomers (peak 1), with concomitant decrease of pentaglycine-containing ones (peak 5). Accordingly, there is also an increase in the ratio of unsubstituted (peak 9) to pentaglycil substituted (peak 11) dimers.

Peaks A, B, C and D, in Figure 13, panel A, are of unknown composition but could correspond to unsubstituted trimers, tetramers, pentamers and hexamers, respectively. Globally, this mutant displayed a diminished crosslinking, relative to wild-type. Peaks X and Y, only visible in the FemX-GFP profile, could be alternative unsubstituted monomers, with different amino acid compositions in the stem peptide. Interestingly, this mutant displays an unusual high peak 7, which may correspond to monomers substituted with one alanine. This could be attributed to a broader substrate specificity of FemX in this mutant.

Taken together, the decreased growth rate of RNpFemX-C; the decreased MICs to cell wall active antibiotics of COLpFemX-C and the altered muropeptide profile of this strain, indicate a decreased function of the FemX protein due to the C-terminal GFP fusion. However, the protein has to be partially functional otherwise the cell would not be viable. It is noteworthy that COLpFemX-C can maintain nominal growth rates with a partial functioning FemX protein, unlike RNpFemX-C.

The fluorescent derivatives COLpFemX-N, COLFemA-C and COLpFemB-C were found to have muropeptide profiles similar to wild-type COL strain, as shown in Figure 15. Strain COLFemA-C seemed to display a slight reduction in the amount of crosslinking, when compared to the control, which was likely due to less material being injected into the column. These results, together with the normal growth rates and antimicrobial resistance profiles, indicate that the fusion proteins expressed in these strains are functional and therefore can be used in localization studies.

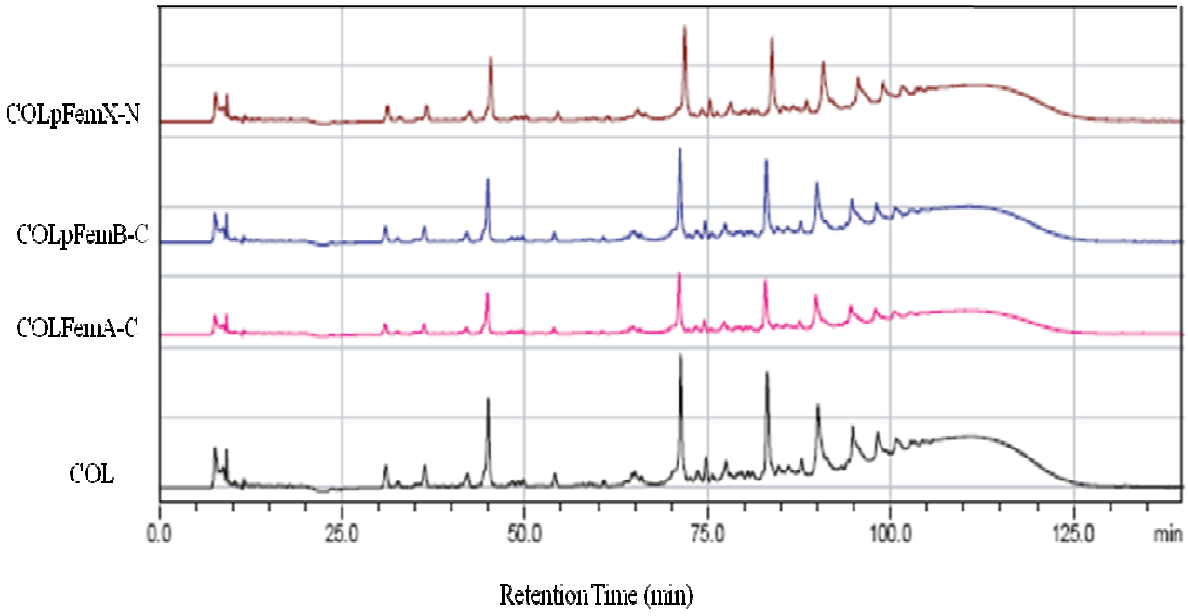

Figure 15 – Muropeptide profiles of parental strain COL (in black) and COL expressing an N-terminal GFP fusion to FemX (brown), C-terminal GFP fusion to FemB (blue) and C-terminal mCherry fusion to FemA (red). All strains expressing fluorescent derivatives of the Fem proteins display a muropeptide profile akin to the parental strain COL.

Localization of the FemXAB family of proteins

Staphylococcus aureus divides symmetrically by synthesizing a division septum midway through the cell. After the septum is complete, the daughter cells separate to undergo a second round of division, in which a new septum is synthesized perpendicularly to the first division plane (Tzagoloff and Novick, 1977). To characterize the localization of the Fem proteins during the cell cycle, live clonal populations derived from a single colony of the constructed strains expressing functional fluorescent derivatives of the Fem proteins were observed by fluorescence microscopy.

The localization studies of the FemX protein were done in COL and RN4220 backgrounds expressing the N-terminal GFP fusion to FemX. Figure 16 shows the localization of FemX in COL during the progression of the cell cycle. For that purpose, we assigned cells to four stages: the initial steps of septum synthesis, the formation of a complete septum, splitting of the septum and separation of the daughter cells. In order to aid the assignment of cells to each stage, bacterial cultures were often grown in the presence of membrane-binding and DNA-binding dyes. FemX was found to be present mostly at the membrane, including the septum, although some fluorescence at the cytoplasm was also observed. FemX seems to accumulate at the tips of the new division site and proceed to accompany septum formation during division. After, division, FemX is shown to be present along the membrane and accumulate randomly at new membrane sites, before localizing to the new division septum. As the fluorescent signal for this FemX fusion was very weak, the localization was confirmed on the RN4220 background. RN4220 cells are larger than COL cells, which also makes it easier to visualize the phenotype. The localization of FemX on RN4220, shown in Figure 17, was found to be consistent with COL.

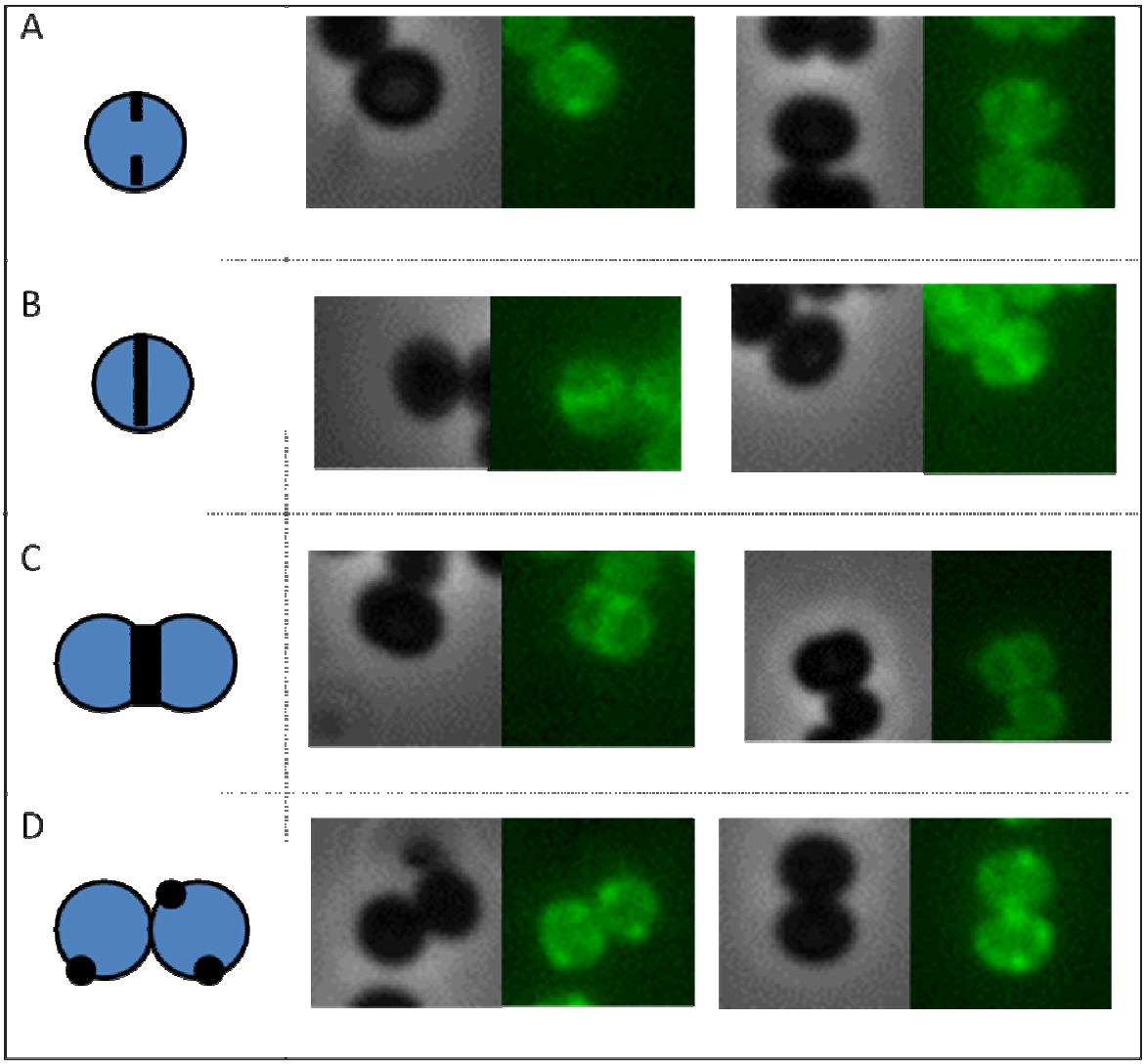

Figure 16 – Localization of the FemX protein with an N-terminal GFP fusion during the stages of the cell cycle in the COL background. Class A – initial steps of septum synthesis, B – formation of a complete septum, C – separation of the daughter cells, D – end of division. The FemX protein is shown to localize generally to the membrane, accumulate at the tips of the new division site and along the septum. After division, FemX accumulates randomly at new membrane sites. For each class (A-D), two examples are shown. For each example: left – phase contrast image; right – GFP image.

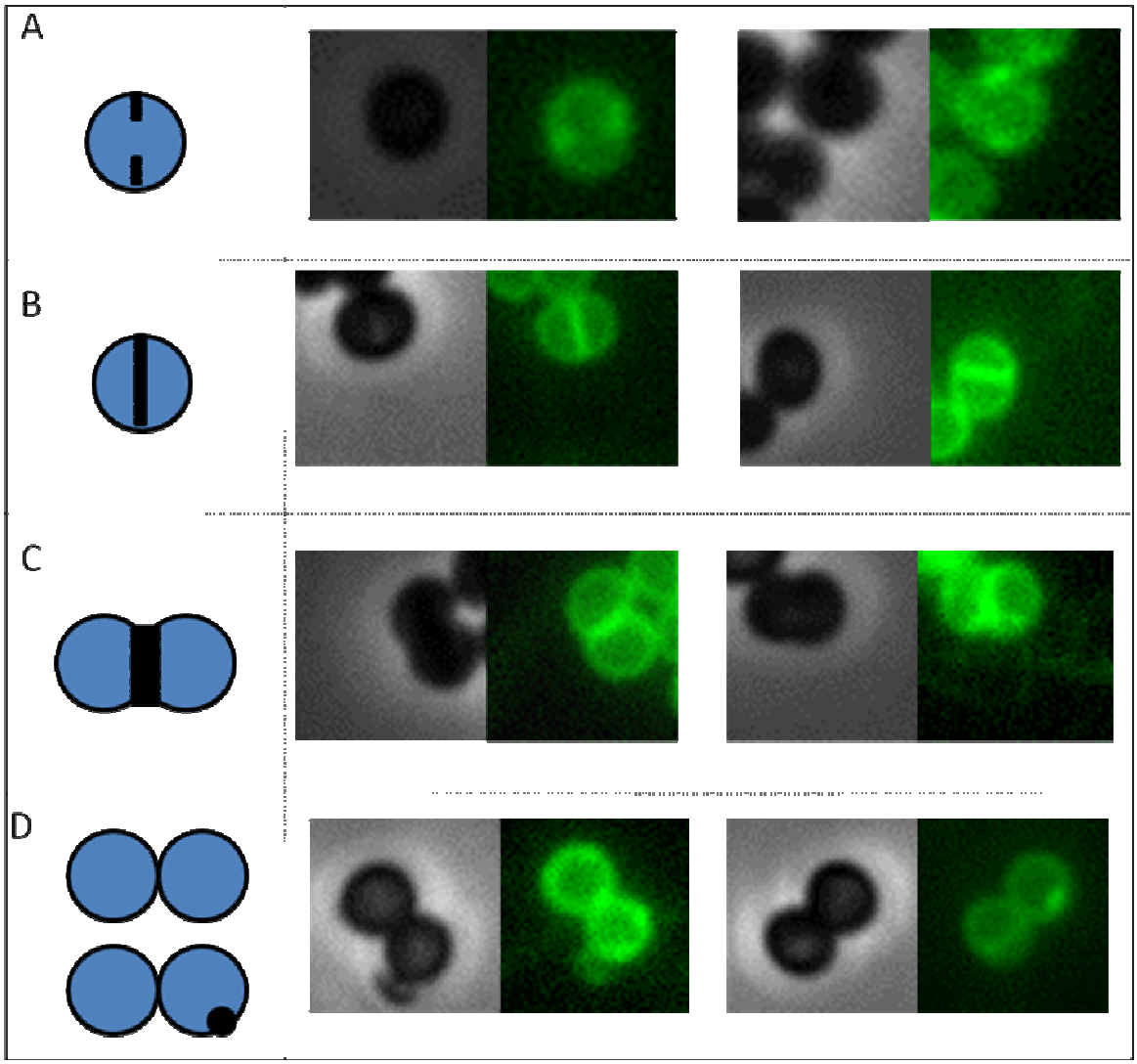

Figure 17 – Localization of the FemX protein with an N-terminal GFP fusion during the stages of the cell cycle in the RN4220 background. Class A –initial steps of septum synthesis, B – formation of a complete septum, C – separation of the daughter cells, D – end of division. The FemX protein is shown to localize generally to the membrane, accumulate at the tips of the new division site and along the septum. After division, FemX accumulates randomly at new membrane sites. For each class (A-D), two examples are shown. For each example: left – phase contrast image; right – GFP image.

As fusing GFP to the C-terminal region of the FemX protein resulted in mutants with partial loss of protein activity, we wondered whether this had affected proper localization as well. To this end, the FemX-GFP mutants constructed in the COL and RN4220 backgrounds were observed under the microscope, as it is shown in Figure 18.

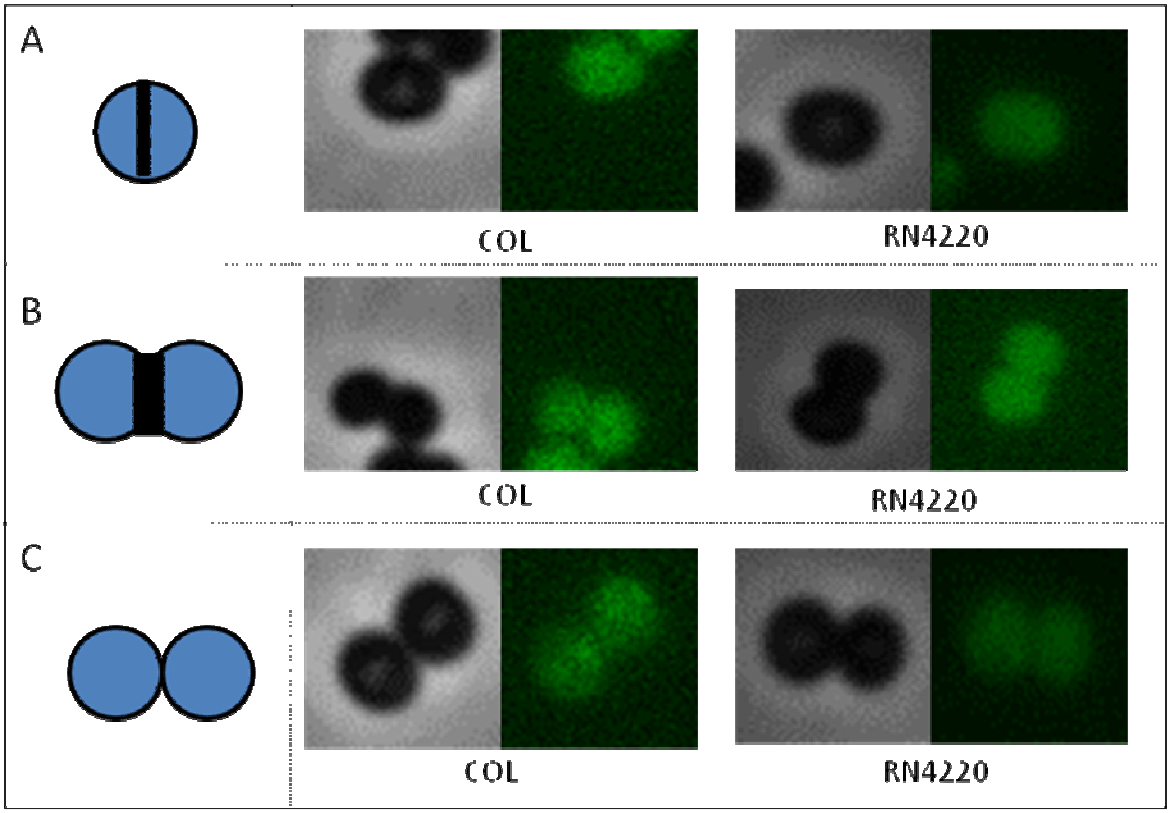

Figure 18 – Localization of the FemX protein with a C-terminal GFP fusion during the stages of the cell cycle in both COL and RN4220 backgrounds. Class A – septum formation; B – separation of the daughter cells; C –end of division. The FemX protein is shown to be localized to the cytoplasm during all stages of the cell cycle. For each class (A-C), one example for the COL and one for the RN4220 background is shown. For each example: left – phase contrast image; right – GFP image.

These mutants displayed a very low fluorescence signal. Nevertheless, the FemX protein localized homogeneously to the cytoplasm during all stages of the cell cycle. This could be due to cleavage of GFP from the FemX fusion protein by proteolytic activity. In order to test this hypothesis, total protein extracts from RNpFemX-C and COLpFemX-C were separated by SDS-PAGE and scanned with blue laser light at 395 nm, which enables the detection of GFP (Figure 19).

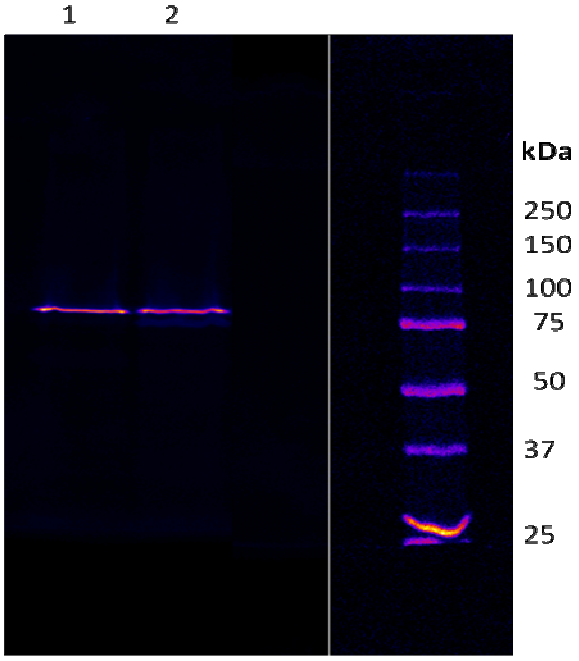

Figure 19 – Blue laser light scanning of the protein extracts from the FemX-GFP mutants after SDS-PAGE separation. Lane 1 – COL expressing a FemX-GFP fusion; lane 2 – RN4220 expressing FemX-GFP fusion.

A band between 75 kDa and 100 kDa was observed in both backgrounds. This is consistent with the expected size of a FemX (~50 KDa) and GFP (~27 KDa) fusion protein, implying that GFP was not being cleaved by proteolitic activity. These results led us to believe that the GFP fusion to the C-terminal region of FemX resulted in the protein failing to localize correctly to the membrane and septum. This explains the loss of FemX activity detected on the analysis of the muropeptide profiles of these mutants and suggests that the C-terminal region may be important for proper localization.

The localization of the FemA protein was also studied during the cell cycle, using COLFemA-mCherry. Figure 20 shows the localization pattern of FemA, which was found to be similar to FemX. However, in this case, the signal was stronger and less fluorescence was observed in the cytoplasm.

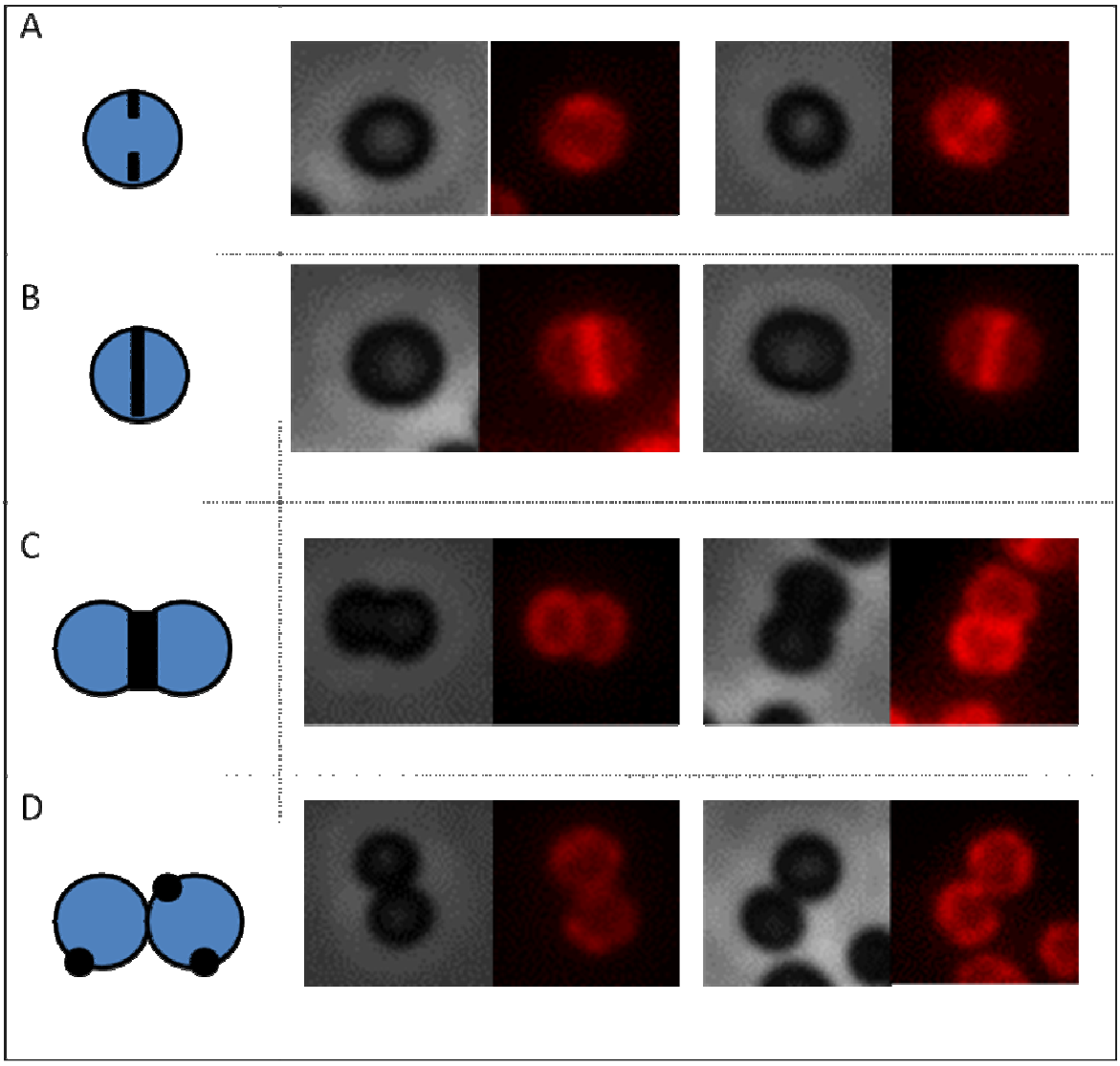

Figure 20 – Localization of the FemA protein with a C-terminal mCherry fusion in the COL background during the stages of the cell cycle. Class A –initial steps of septum synthesis, B – formation of a complete septum, C – separation of the daughter cells, D – end of division. The FemA protein is shown to localize generally to the membrane, accumulate at the tips of the new division site and along the septum. After division, FemA accumulates randomly at new membrane sites. For each class (A-D), two examples are shown. For each example: left – phase contrast image; right – TX red image.

The localization of the FemB protein was shown be similar to FemX and FemA during the entire cell cycle (Figure 21).

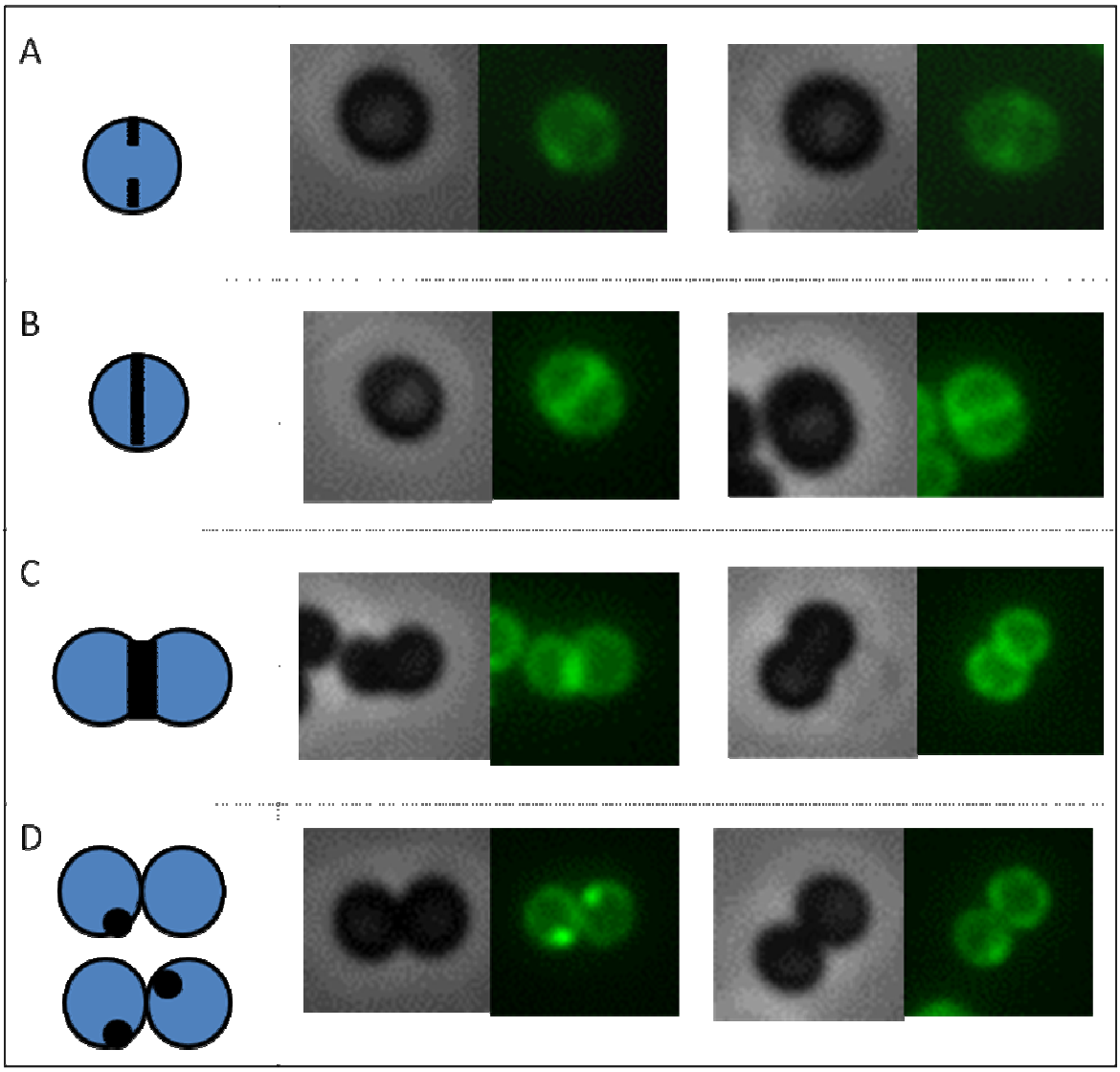

Figure 21 – Localization of the FemB protein with a C-terminal GFP fusion in the COL background during the stages of the cell cycle. Class A –initial steps of septum synthesis, B – formation of a complete septum, C – separation of the daughter cells, D – end of division. The FemB protein is shown to localize generally to the membrane, accumulate at the tips of the new division site and proceed along the septum. After division, FemB accumulates randomly at new membrane sites. For each class (A-D), two examples are shown. For each example: left – phase contrast image; right – GFP image.

The FemX, FemA and FemB proteins were found to localize around the entire membrane, including the septum, during the cell cycle. The localization at the division septum was expected, as that is the site of the cell where peptidoglycan synthesis occurs (Pinho and Errington, 2003), therefore where the Fem susbtrate (lipid II) should be localized. The observed permanent localization at the entire membrane was surprising. It seems that even

during septum formation and division there is always a pool of Fem proteins localized to the "lateral" membrane.

In order to determine if FemX, FemA and FemB are, in fact, localized over the entire membrane and not accumulating at the septum during division, we measured the fluorescence intensity signals at the lateral membrane and septum of COLpFemX-N, COLFemA-C and COLpFemB-C cells (n=100 for each). Wild-type COL cells (n=100) stained with lipophillic membrane dye Nile Red were also quantified, as a control. Only cells displaying a closed septum were considered. The fluorescence intensity values were normalized by subtracting the intensities of the background autofluorescence. The ratio of septal vs. lateral membrane intensity was calculated in each cell and plotted, as seen in Figure 22. Also shown are the values for a COL derived strain expressing an N-terminal GFP fusion to division protein PBP2. It has been demonstrated previously that PBP2 accumulates at the septum during division (Pinho and Errington, 2005). The septum is composed of two membranes, therefore if a fluorescent protein is equally distributed over the entire cell surface, the septal/lateral fluorescence ratio is expected to be close to 2. On the contrary, if a protein accumulates at the septum during cell division, the septal/lateral ratio is expected to be at above 2, as it was observed for PBP2 (average ratio - 3.97) (Figure 22). The calculated average ratios for FemX, FemA and FemB (1.93, 1.98 and 1.85, respectively) were found to be similar to the value obtained for membrane-stained cells (2.02). Therefore, it seems that Fem proteins are not specifically recruited to the division septum during bacterial division.

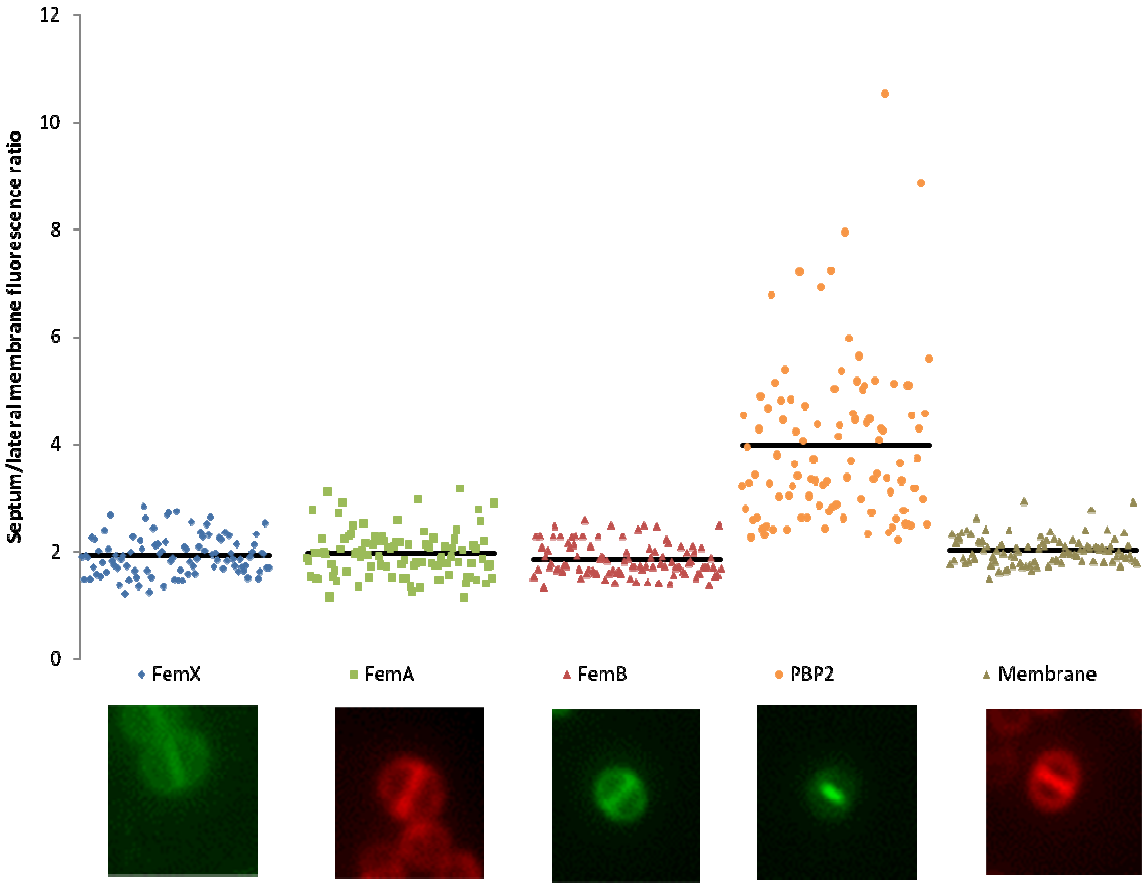

Figure 22 – Quantification of septum vs. lateral membrane fluorescence ratios for COLpFemX-N, COLFemA-C, COLpFemB-C, COLpPBP2-31 (expressing a GFP-PBP2 fusion) and COL stained with membrane dye Nile Red (n=100 for each strain). All cells displayed closed septa. The average ratios calculated for each fluorescent signal are depicted as straight lines: FemX – 1.91; FemA – 1.98; FemB – 1.85; PBP2 – 3.97; Membrane – 2.02. Fem proteins are shown to be evenly distributed along the membrane, unlike PBP2, which accumulates at the septum.

To further confirm that the Fem proteins were not accumulating in the septum, we visualized the COLpFemX-N, COLpFemA-C and COLpFemB-C mutants on the microscope after incubation with DNA labeling dye DAPI. We then selected cells (n=100 for each strain) in the latter stages of division, where two individualized nucleoids were already discernible and a fully-formed septum was present. These cells were quantified as described above and the average ratio of septum/lateral fluorescence was found to be approximately 2 for each protein, confirming the even distribution of the Fem proteins over the membrane.

Fem proteins co-localization

After having shown that Fem proteins did not accumulate at the septum before or during division, we wondered whether the apparently random membrane accumulations often observed during the cell cycle were coincident between proteins. Therefore, we decided to express pairs of two fluorescent proteins in the same cell. For this purpose, mutants COL-FemAB, expressing both FemA-mCherry and FemB-GFP fusions, and COL-FemXA, expressing both GFP-FemX and FemA-mCherry fusions were constructed. Table 4 summarizes the characterization of these mutants, which were found to have doubling times, MICs for oxacillin and lysostaphin, and muropeptide profiles similar to the parental strain COL.

Table 4 – Characterization of the parental MRSA strain COL and the derived COL-FemAB and COL-FemXA strains

Strain	Doubling time (min)	MIC (μg/ml)		Cell wall analysis
		Oxacillin	Lysostaphin	
COL	29	800	0.016	COL
COL-FemAB	36	400	0.016	= COL
COL-FemXA	35	800	0.016	= COL

When strain COL expressing FemA-mCherry and FemB-GFP was visualized by fluorescence microscopy, the FemA and FemB proteins appear to co-localize during all stages of the cell cycle and the random accumulations of FemA and FemB seem to be coincident in space and time. Three stages were chosen to depict this: the initial steps of septum synthesis, the formation of a complete septum and the separation of the daughter cells, as shown in Figure 23. In all cases, cells were exposed first to the mCherry channel and then to the GFP channel.

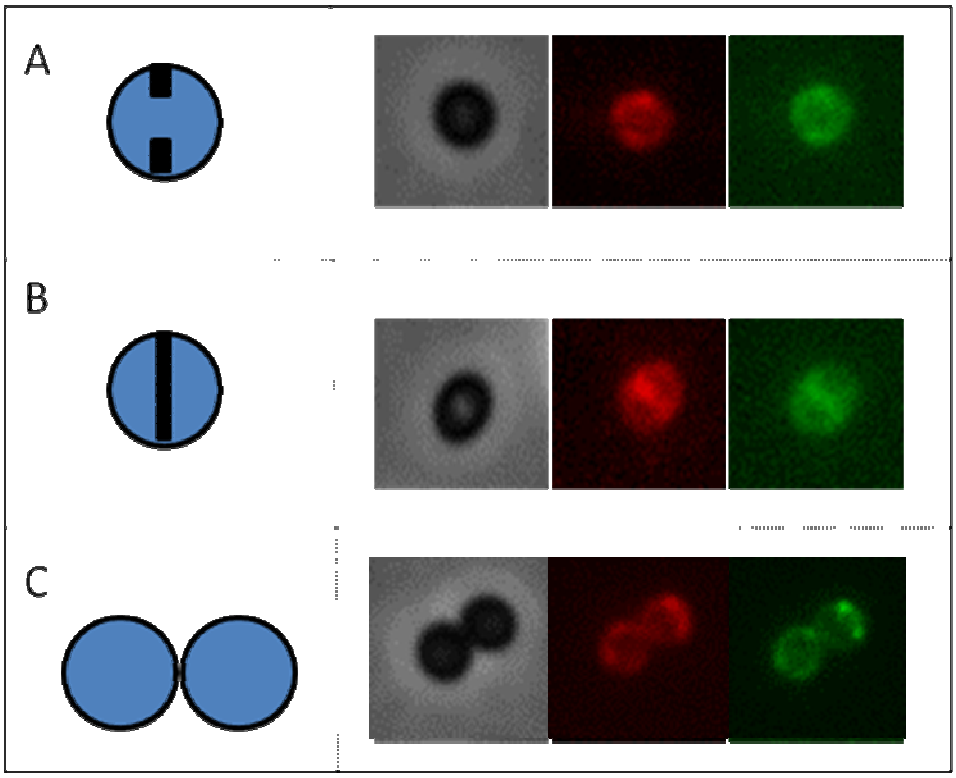

Figure 23 – Co-localization of FemA and FemB proteins during the cell cycle in COL-FemAB strain. Stage A – initial steps of septum synthesis; B – formation of a complete septum; C – separation of the daughter cells. Each stage: phase contrast image, TX red image, GFP image. Both proteins were found to be present in the same subcellular structures at the same time.

Figure 24 shows the co-localization study of GFP-FemX and FemA-mCherry proteins expressed in COL. Two stages of the cell cycle were chosen for this study: septum formation and end of division/separation. FemX and FemA were found to be co-localized during the end of division/separation in all cells observed and accumulating in the same distinct membrane spots (panel B). In contrast, during septum formation, most cells displayed protein co-localization (64%, n= 300), while in others, FemX was present at the septum while FemA was accumulated at the lateral membrane (36%, n= 300) (panel A).

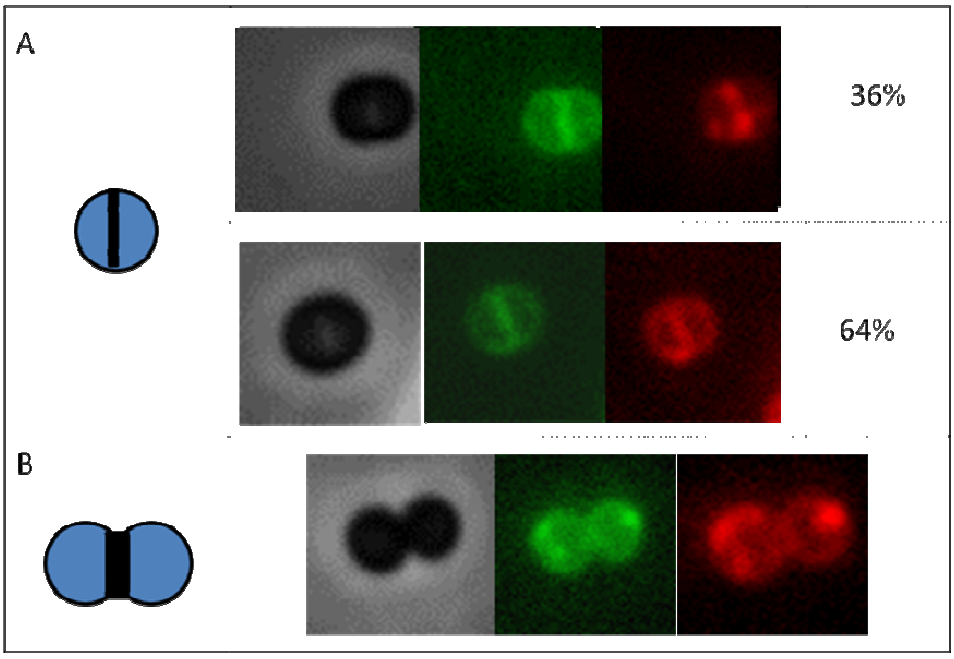

Figure 24 – Co-localization of FemX and FemA proteins during the cell cycle, as observed in the COL-FemXA strain. Stage A – septum formation; B – division/separation. Each stage – phase contrast image; TX Red contrast image; GFP contrast image. The proteins were found to co-localize during the end of division/separation in all cells observed. 36% of cells that displayed a division septum formed (n=300) were found to have FemX localized to it, while FemA was localized to distinct spots in the membrane. 64% of cells that displayed a division septum formed were found to have both proteins co-localized.

In order to test the possible earlier presence of FemX at the septum compared to FemA, 100 cells displaying defined green fluorescence at the septum and red fluorescence apparently absent from it were analyzed. The fluorescence intensity signals of GFP and mCherry were quantified at the membrane and septum of these cells and normalized by subtracting the intensities of the background autofluorescence. The ratio of septal vs. lateral membrane fluorescence intensity was calculated in each cell for each channel and plotted, as seen in Figure 25. In this way, an average ratio of 1.53 was determined for green fluorescence (FemX), while an average of 0.74 was determined for red fluorescence (FemA). This implies that, at the early steps of the synthesis of the division septum, FemA is not present at the septum, maybe because it was actively excluded.

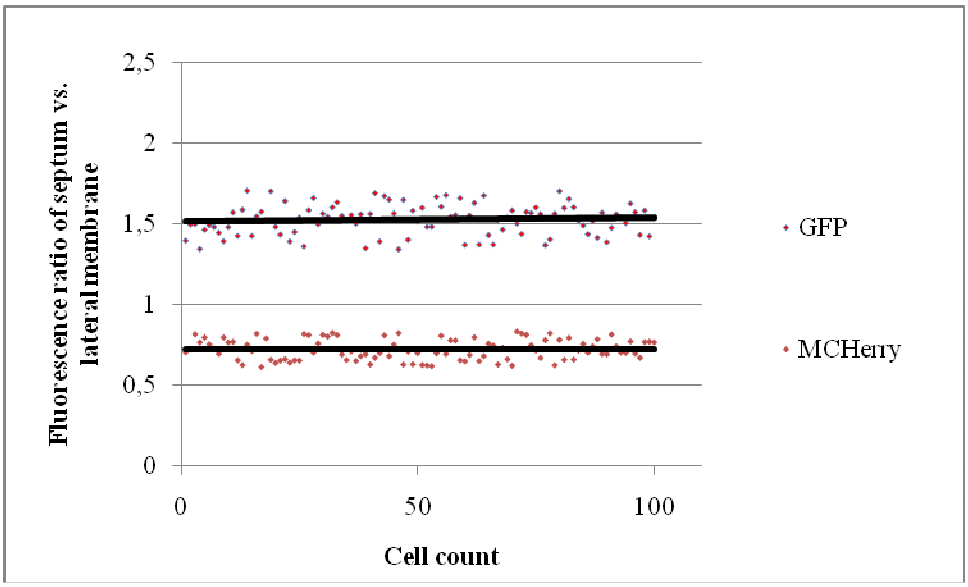

Figure 25 – Septum/membrane fluorescence ratios in 100 chosen cells of the COL strain expressing GFP-FemX and FemA-mCherry. These cells displayed green fluorescence at the septum and red fluorescence seemingly absent from it. An average 1.5 signal ratio was detected for the GFP signal, while an average 0.74 signal ratio was detected for mCherry. These results indicate that at this defined point in the cell cycle, there is localization of FemX at the septum while FemA is absent from it.

As FemA was shown to co-localize with FemB throughout the cell cycle, to further test if this pair was excluded from the initial steps of septum formation, we incubated the COL strain expressing a C-terminal GFP fusion to FemB with FM 1-43 red membrane dye. A subpopulation of 300 cells displaying early septum synthesis at the division site was inspected on both red and green channels and FemB was found to be localized to the division site in every cell, thus disproving the theory of septal exclusion. Wild-type COL strain was also incubated with the membrane dye and visualized on both channels, to discard the possibility of emission on the green channel by the FM-143 fluorophore (data not shown).

Inactivation of the *femA* gene

After having determined the localization of FemX, FemA and FemB, we wanted to assess if interactions between these proteins were important for localization. For this, we attempted to inactivate the *femA* gene, to see if the FemB protein would de-localize in the absence of FemA or in the presence of a FemA protein which had lost its activity (but not its correct folding). As *femA* is encoded in the policystronic *femAB* operon, we opted not to knockout the entire gene, to avoid interfering with the mRNA transcript. Instead, we attempted to promote the allelic replacement of *femA* using the thermosensitive plasmid pMAD (see Methods) by a copy of the *femA* gene from the UK17 strain, containing a premature stop codon. We have also tried to substitute putative key residues of FemA by alanines by site-directed mutagenesis. The selected residues had been proposed to have a role in substrate recognition (Lysine33 and Arginine220) or in tRNA-Gly stabilization (Tyr327) (Biarrotte-Sorin *et al.*, 2004; Maillard *et al.*, 2005).

Allellic replacement of wild-type copies of *S. aureus femA* by the desired mutant alleles proved to be unsuccessful in all attempts. The pMAD plasmid carrying the mutant *femA* allele could integrate into the chromosome by homologous recombination. However, this always happened through the region downstream of the mutation and therefore we never obtained a mutant allele under the control of the native promoter. Furthermore, excision of the plasmid from the chromosome always generated wild-type strains and never strains containing the desired mutations. Figure 26 shows the attempted replacement of wild-type *femA* by the UK17 allele, as an example.

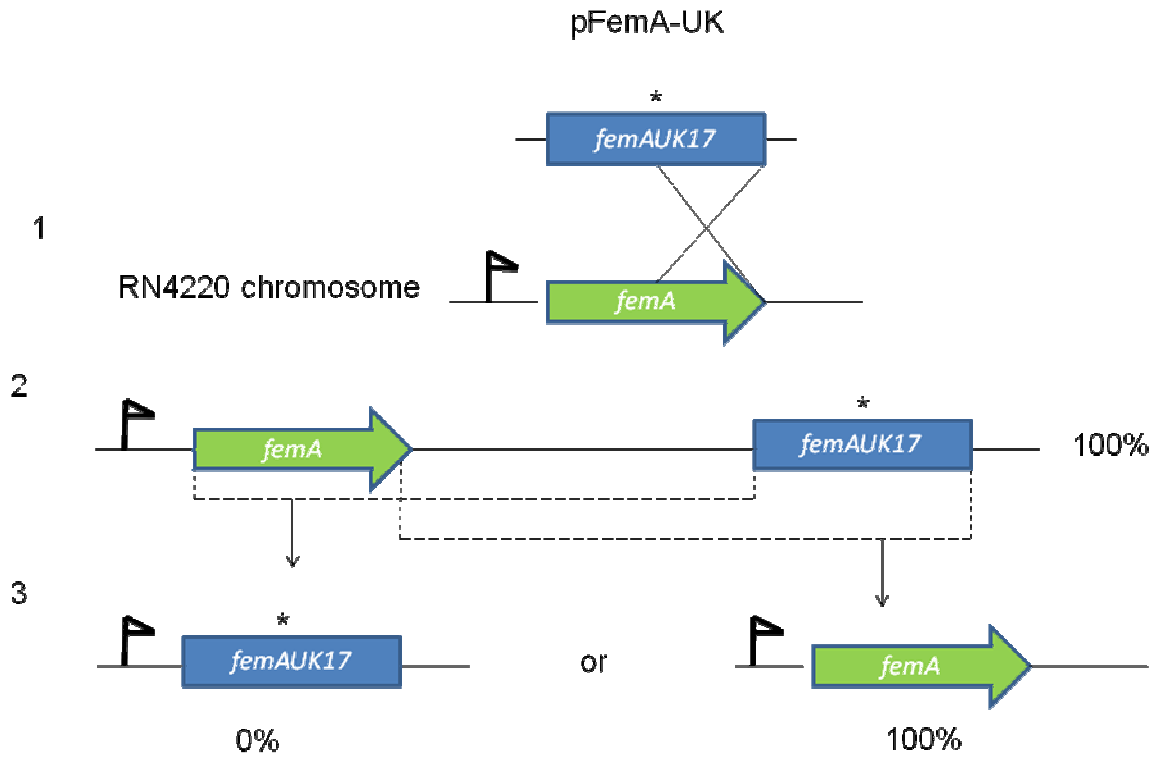

Figure 26 – Strategy for allellic replacement of the wild-type *femA* gene in RN4220 by the *femA* allele from the UK17 strain, cloned into the pMAD plasmid. This allele contains a point mutation (depicted by an asterisk) leading to a premature stop codon and subsequent expression of a truncated FemA protein. Integration through homologous recombination always occurred downstream of the point mutation, despite the upstream region having the same length. The second recombination event and loss of the plasmid always yielded wild-type colonies. Step 1 – homologous recombination between pFemA-UK and the bacterial chromosome; step 2 – integration (blue colonies); step 3 – second recombination event and loss of the plasmid (white colonies). Flag – native promoter of the *femAB* operon.

We modified the protocol for allelic replacement in several ways in order to maximize chances of isolating mutants:

i) *femA*-inactivated strains like UK17 were shown to be thermosensitive (Kusuma *et al.*, 2007). Therefore, during excision, we kept the final temperature at a maximum of 37ºC instead of 43ºC (see methods), to avoid losing the desired mutant. After the excision, we obtained the expected 1-5% of white colonies for double cross-over event. Screening PCR was performed on 20 clones for each of the four desired mutations and it was found that all carried wild-type copies of *femA*.

ii) As the doubling time of UK17 is twice as long as RN4220, it could be expected that growth of mutants carrying an inactivated *femA* locus would quickly be overtaken by wild-type cells. To try to avoid this, the excision protocol was modified. Colonies with integrated pMAD plasmid carrying the *femA* mutant alleles were allowed to grow for only 10 generations, instead of 30 (see Methods) at the permissive temperature before being plated. This process aimed to provide enough time to ensure that the second recombination event would likely occur, but trying to circumvent the expected fitness deficit of *femA* mutants, by plating earlier. With 10 generations only, the number of white colonies obtained was only 1%. Again, 20 excisates for each mutation were screened and none found to contain the desired replacements.

iii) As *femA* mutants are lysostaphin resistant, we also tried to introduce a final plating step in a lysostaphin 5 µg/ml plate, to select only the allelic replacement mutants and inhibit growth of wild-type cells. Colonies grew on lysostaphin plate but none of them carried the desired mutations in the *femA* gene and were proposed to be spontaneous mutants.

Despite the repeated attempts and different modifications of the protocol, inactivation of *femA* was always unsuccessful. These results suggest that *femA* may well be a lethal target and that the only reason that UK17 can cope with lack of FemA activity is by having compensatory mutations elsewhere in the chromosome.

Substrate dependency of the FemXAB family of proteins for localization

In order to assess if the localization of FemX, FemA and FemB proteins was dependent on interactions with the substrate, similarly to what happens for PBP2 (Pinho and Errington, 2005), we treated bacterial cultures of COL GFP-FemX, COL FemA-mCherry and COL FemB-GFP mutants with either tunicamycin or fosfomycin. Tunicamycin is a potent inhibitor of the MraY translocase (Lin *et al.*, 2002), thus preventing the peptidoglycan cytoplasmatic precursors from being attached to the lipid carrier bactoprenol. Fosfomycin inhibits the MurA enzyme, which catalyzes the first step commited to peptidoglycan

biosynthesis, therefore blocking peptidoglycan synthesis at the initial step in the cytoplasm (Kim *et al.*, 1996). Cells were incubated for 30 minutes with 10 times the determined MICs for each antibiotic and each strain, before being visualized under the microscope. Figures 27-29 depict the effect of these compounds on the localization of FemX, FemA and FemB, respectively. Cells appeared more aggregated and smaller/larger, when compared to untreated cells. These variations in cell size seem to be random in the studied populations. Localization of the three proteins on the lateral membrane and septa was lost. FemXAB proteins were shown to delocalize randomly across the cell, forming patches or dense accumulations. There was no observed difference between the treatment with fosfomycin and tunicamycin. These results suggest that the presence of the substrate is required, directly or indirectly, to keep FemX, FemA and FemB in place.

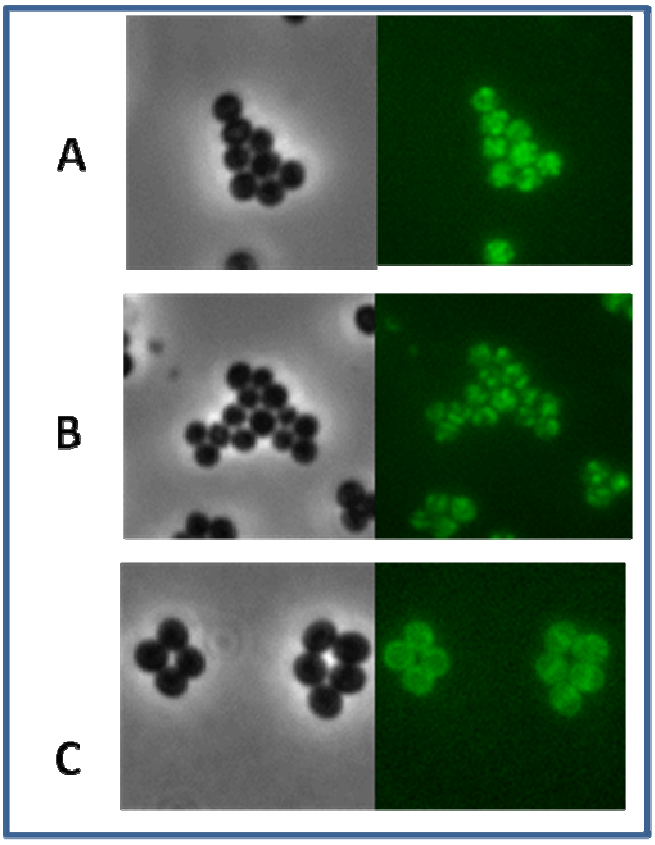

Figure 27 – Delocalization of FemX in COL GFP-FemX strain after treatment with cell-wall active compounds at 10X the corresponding MIC values for 30 minutes. Membrane and septum localization of FemX is lost, with the protein accumulating randomly throughout the cell. A – with fosfomycin; B- with tunicamycin; C – control, no compounds added. For each panel, left – phase contrast image; right – GFP image

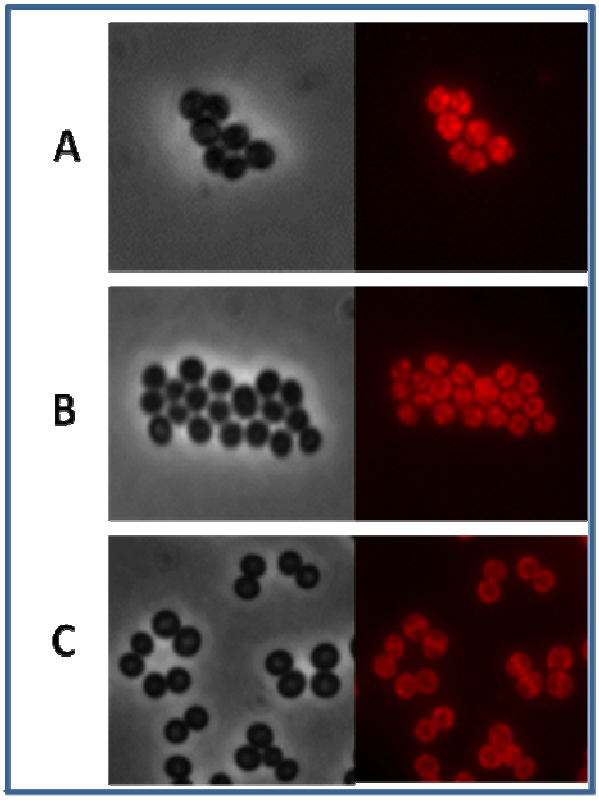

Figure 28 – Delocalization of FemA in COL FemA-mCherry strain after treatment with cell-wall active compounds at 10X the corresponding MIC values for 30 minutes. Membrane and septum localization of FemX is lost, with the protein accumulating randomly throughout the cell. A – with fosfomycin; B – with tunicamycin; C – control, no compounds added. For each panel, left – phase contrast image; right – TX red image.

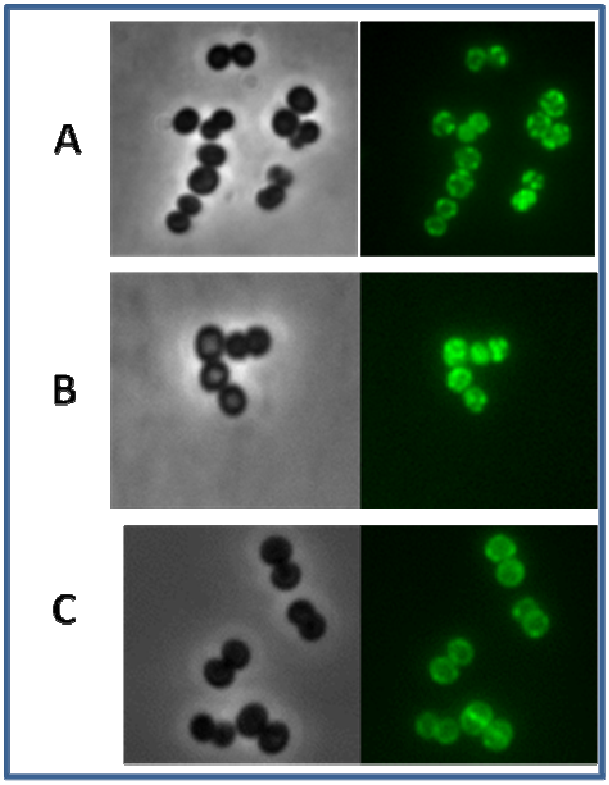

Figure 29 – Delocalization of FemB in COL FemB-GFP mutant after treatment with cell-wall active compounds at 10X the corresponding MIC values for 30 minutes. Membrane and septum localization of FemB is lost, with the protein accumulating randomly throughout the cell. A – with fosfomycin; B – with tunicamycin; C – control, no compounds added. For each panel, left – phase contrast image; right – GFP image.

Discussion

The unique FemXAB family of non-rybosomal peptidyl transferases catalyzes the stepwise addition of glycine residues to the stem peptides of the peptidoglycan precursors. FemX adds the first glycine, FemA adds the second and the third, FemB adds the fourth and the fifth. Our study of the localization of FemXAB proteins began by constructing a C-terminal GFP fusion to FemX on both MSSA and MRSA backgrounds. The protein appeared in the cytoplasm of the cell during growth and division, with no specific subcellular localization detected. Characterization of the cell wall composition and antibiotic resistance profile of these mutants revealed significant differences to the wild-type parental strains, leading us to conclude that FemX's function was partially hindered as a result of the GFP fusion to its C-terminus region. As FemX is an essential protein, it was interesting to analyze the consequences to the cell of having a partial loss of function of this protein. The most striking feature of FemX-GFP muropeptide profiles was the massive accumulation of muropeptide monomers with no glycine crossbridges, as opposed to muropeptides with a complete crossbridge present in wild-type strains. Similarly, there was accumulation of dimers with one pentaglycine crossbridge, trimers with two pentaglycine crossbridges, etc.

In wild-type strains, muropeptides with pentaglycine side chains, the substrates for the crosslinking reactions, are abundant in the peptidoglycan, suggesting that this pool of muropeptides is permanently available to the PBPs and, therefore, that the activity of the Fem proteins does not constitute a bottleneck in PG biosynthesis. The presence of the partially functional FemX results in a lower pool of crosslinkable muropeptides, as it is postulated that PBPs cannot crosslink unsubstituted muropeptides (de Jonge *et al.*, 1993). In these conditions, the FemX activity may be limiting for efficient PG biosynthesis. Another interesting feature of these FemX mutants is the accumulation of muropeptides with an alanine at the first position of the crossbridge, that are virtually absent from wild-type strain profiles. Muropeptides with serines or alanines in the crossbridge have been previously reported in *femA* mutant strains (de Jonge *et al.*, 1993; Strandén *et al.*, 1997) and in wild-type strains grown in a glycine poor medium (Swenson and Neuhaus, 1976). This suggests the presence of a FemX-like transferase protein present in *S. aureus* that is able to add alanine residues. Homologues of the MurM protein of *S. pneumoniae* are likely candidates for this function. This protein initiates the synthesis of the crossbridge in these species and it was shown to be

specific for either alanine or serine charged tRNA binding, depending on allele variability of the *murM* gene (Filipe *et al.*, 2001; Filipe and Tomasz, 2000). It is unlikely that this activity results from FemA or FemB, as their substrate specificities are thoroughly described (Schneider *et al.*, 2004). In wild-type strains, both FemX and the alanyl transferase could compete for the muropeptide substrate, with the former being able to bind it more efficiently. This would explain why, in the presence of a partially functional FemX protein, alanine containing muropeptides would accumulate in the cell wall. Alternatively, it is possible that the C-terminal fusion of GFP to FemX would decrease its specificity to glycine charged tRNAs by some extent. In the aforementioned MurM, a 30 amino acid segment contained in the coiled-coil helical arms of the protein was determined to be critical for the selectivity of tRNA recognition (Filipe *et al.*, 2001). This segment seems to be, however, structurally distant from the C-terminal domain of MurM (Fiser *et al.*, 2003). The muropeptide binding domain of Fem and Fem-like proteins is at the vicinity of the C-terminus of the protein, however C-terminal fluorescent protein fusions to FemA and FemB constructed in this work did not affect these proteins' activities or localization. It is therefore unlikely that the fusion disrupted the specificity of FemX to glycil-tRNA or its proper muropeptide recognition.

Muropeptides containing an alanine seem to be poor substrates for FemA as they accumulate massively in the FemX mutant. On the contrary, monoglycil substituted muropeptides are never accumulated. Muropeptides containing one alanine and 2-4 glycines in the crossbridge are also not present in the peptidoglycan composition of the FemX mutant, further confirming the substrate specificity of FemA for monoglycil substituted precursors. Given the changes in PG precursors' availability and, by extension, the amount of PG crosslinking, it could be expected that expression of a not fully functional copy would cause severe growth defects in the bacteria. This was found to be true in the MSSA strain RN4220, but not in MRSA strain COL. Strain RNpFemX-C had a 2,5-fold increase in doubling time and a longer lag phase, comparatively to wild-type. The growth rate of COLpFemX-C, on the other hand, is only slightly reduced, compared to wt COL. This suggests that in the COL background, despite the reduced FemX activity, there is a sufficient muropepeptide precursor pool to maintain normal growth. The COL strain takes on average 10 minutes more than RN4220 to divide, therefore different metabolic flux, namely for PG biosynthesis, may be characteristic of this strain. This would explain the ability of COL to maintain growth rate without a fully functional FemX protein. However, it is important to notice that, despite the normal growth, a reduction in FemX activity caused an increased susceptibility to cell wall

active compounds in strain COL, similarly to what was observed for RN4220. This is in accordance to previous data that implicate FemXAB proteins in oxacillin resistance (Strandén *et al.*, 1997). As the localization of FemX with a C-terminal GFP fusion was shown to be mainly cytoplasmic, we believe that the C-terminus of FemX may be a critical region for protein-protein or protein/substrate interactions responsible for keeping this protein at the membrane, where it is active.

N-terminal GFP fusion to FemX in COL and RN4220, as well as C-terminal GFP or mCherry fusions to FemA and FemB, yielded mutants with wild-type cell wall muropeptide composition and similar growth rates to the parental strains. The oxacillin MIC of COL expressing fluorescent derivatives of the FemXAB proteins was also identical to the one of parental strain COL. As functional FemXAB proteins are essential for the expression of β-lactam resistance in COL, this result is a further indication that the fusions are functional and can be used for localization studies.

When the localization of FemX was studied in live *S. aureus* cells, the protein was found to be at the membrane and to accumulate around the future division site, corresponding to spots on the microscopy images. FemX then accompanied the closing of the septum, although it did not localize exclusively at the septum, but rather over the entire cell membrane. At the end of division, when the daughter cells are ready to separate, FemX localized over the entire membrane of both daughter cells, accumulating randomly in spots during separation and before the next round of division. FemA and FemB proteins were found to have a pattern of localization akin to FemX during the cell cycle.

The membrane localization of the FemXAB family was unexpected because these proteins lack a transmembranar domain or membrane anchors. As protein-protein interactions between FemA and FemB proteins have been described previously (Rohrer and Berger-Bächi, 2003), we wondered whether proper localization and activity of the FemA protein was vital for FemB also to localize and, therefore, we sought to express FemA proteins either truncated or with loss of activity in *S. aureus*. Our attempts at inactivating *femA* during this work proved to be fruitless. Despite successive attempts to replace the wild-type allele by a mutated *femA,* it was never possible to obtain the desired mutants, even when using lysostaphin, to which *femA* mutants are resistant, as a selection. Therefore, we were not yet able to study if FemB is dependent of FemA for proper localization. Since the discovery of the *femAB* operon, there have been numerous attempts to inactivate the *femA* gene, using a variety of

methods. In one experiment to address this issue, a *femAB* null mutant (AS145) was constructed by replacing the operon with a tetracycline resistance cassette (Tet), followed by screening of positives in lysostaphin plates (Strandén *et al.*, 1997). This mutant was shown to have exclusively monoglycine crossbridges in its peptidoglycan, severe growth defects and hypersusceptibility to β-lactams. Complementation with either intact *femA* or *femAB* copies resulted in the extension of the crossbridges to triglycines and pentaglycines, respectively. Surprisingly, complementation in these mutants did not restore normal growth rate nor β-lactam resistance as was expected. Furthermore, transduction of the Tet resistance marker to other strains was always unsuccessful, except when lysostaphin was added as a second selective agent. In another experiment, by means of chemical mutagenesis with ethyl methanesulfate upon MRSA strain BB270 and subsequent selection on lysostaphin plates, mutants UK14-20 were isolated. Sequencing of the *femA* gene in these mutants revealed point mutations expected by the treatment with the mutagenic agent, along with spontaneous mutations selected for by growth on lysostaphin, both leading to the expression of truncated FemA proteins (Ehlert *et al.*, 1997). Spontaneous mutants obtained after selective pressure on lysostaphin have also been reported recently, both *in vitro* and during preclinical trials of lysostaphin therapy for *S. aureus* infections. These isolates, like the UK strains, were shown to have mutations in the *femA* genes, a *femA*-like phenotype and also decreased virulence (Kusuma *et al.*, 2007). Taken together, these results indicate that *femAB* deletion by itself may be lethal unless some compensatory mutation occurs to allow survival. The existing *femAB* null mutant (AS145) and the *femA* point mutants (UK) probably have metabolic changes that allow them to grow with such drastically reduced side-chains (Ling and Berger-Bächi, 1998). It is interesting to mention that three of the four *femA* mutant alleles that we were trying to introduce in the *S. aureus* chromosome contained mutations in residues which are only postulated to be important for the activity of FemA (Lys33, Arg220, Tyr327). The fact that these mutations were never found during the allelic replacement PCR screenings, suggested a determining role in the activity of FemA. The successful replacement of the wild-type *femA* allele by a *femA-mCherry* allele that was performed for the localization studies validates the methodology employed in cloning mutated *femA* constructs.

The observed pattern of localization of FemXAB proteins is in contrast to the pattern of the cell wall synthethic enzymes that have been previously studied in *S. aureus*, namely PBP1 and PBP2. These proteins were shown to localize specifically at the septum (Pereira *et*

al., 2007; Pinho and Errington, 2005). Fem proteins, on the other hand, were shown here not to accumulate in the division septum, which suggests that this protein family does not necessarily function exclusively at the septum. PBP2, like all high molecular weight PBPs, contains an N-terminal non-cleavable signal peptide that is anchored to the cytoplasmic membrane and accumulates at the septum, the main place where cell wall synthesis occurs. Substrate recognition is crucial for the protein's localization, as PBP2 was shown to become dispersed over the entire cell surface after being acylated by oxacillin (Pinho and Errington, 2005). All three Fem proteins were shown here to accumulate randomly in patches throughout the cell when it was challenged with cell-wall active antibiotics tunicamycin and fosfomycin, which resulted in the inhibition of the synthesis of the substrate of FemX. This suggests that Fem proteins are dependent on their membrane-bound substrates for proper localization and, as they do not possess an anchor that would hold them at the membrane after substrate depletion, they are released into the cytoplasm. Alternatively, as the tested compounds are likely to affect all reactions downstream of the reactions they inhibit, their addition could result in loss of protein-protein interactions, which could be responsible for keeping the Fem proteins at the membrane.

Fem A and FemB proteins were found to co-localize during all stages of the cell cycle, which is in agreement with the hypothesis, although not proving it, that these proteins function together, maybe as heterodimers or even tetramers of two subunits of each (Rohrer and Berger-Bächi, 2003). FemX was shown to co-localize with FemA in most of the cells displaying septa, but a subpopulation in which FemX localized to the division site before FemA was also observed. This is in accordance with the biochemical activity of each protein: FemX is essential and adds the first glycine and therefore its activity drives the whole crossbridge formation event and it is reasonable to assume that it localizes first to the substrate. However, it still is curious that there was a time gap between the FemX and the FemA reactions so perceptible that it actually could be detected in nearly 40% of the cells preparing to divide. It was shown by Schneider and colleagues (Schneider *et al.*, 2004), that FemA and FemB interfered with the FemX reaction *in vitro*, probably because both these proteins recognize the phosphate moieties of lipid II and compete for them. FemX was shown to add the first glycine to lipid II *in vitro* within 5 minutes, when incubated in the absence of FemA and FemB. When FemA or FemAB were added to the reaction, the incorporation of the first glycine was delayed to 15 minutes and 30 minutes, respectively. It is, therefore,

reasonable to assume that the cell could have mechanisms to prevent FemA (and FemB) to localize to the division septum when FemX is adding the first glycine residue. Although this preposition is theoretically logical, it was not validated by membrane staining of bacteria expressing FemB-GFP, as septal exclusion of FemB was not verified in any cells.

We propose a model for FemXAB localization in which molecules of the lipid II precursor of peptidoglycan are present over the entire membrane during the cell cycle. This implies that the first membrane-bound stages of the peptidoglycan biosynthesis also occur outside of the septum. The FemXAB proteins would localize to the membrane either by substrate interactions via recognition of the sugar moieties of lipid II, by protein-protein interactions or by both, and synthesize the pentaglycin-substituted lipid II, which becomes evenly distributed along the membrane, including the septum, where it is presumably translocated to the outer membrane. The transpeptidation/transglycosilation machinery of the bacterium is also accumulated specifically in the septum, ensuring that lateral growth is kept to a minimum.

Alternatively, the Fem proteins could localize to the membrane via structural motifs. *S. aureus* FemA possesses a coiled-coil domain. By analogy of sequence similarity, FemB and FemX, whose structures are still unresolved, should also comprise this domain. Coiled-coil motifs have been found to be essential for proteins localized to membranes, or interacting with membrane proteins, such as *Caulobacter Crescentus* Crescentin (Margolin, 2004) or *Bacillus subtillis* DivIVA (Lenarcic *et al.*, 2009). Interestingly, the FemX protein of *W. veridescens* does not possess this coiled-coil domain and its activity has been thoroughly described to lie in the cytoplasm (Biarrotte-Sorin *et al.*, 2004; Maillard *et al.*, 2005). The FemXAB family in *S. aureus* could be present at the membrane and recognize the lipid II substrate. However, the FemA and FemB proteins may compete with FemX for the substrate, inhibiting the FemX reaction at the lateral membrane and therefore preventing theaddition of any glycines to lipid II. During the early stages of the septum formation, FemX would interact weakly with an initial division protein, such as FtsZ, for example, possibly via its C-terminal region. FemA and FemB may not be able to interact with these complexes and would not be recruited to the septum. FemX would start adding the first glycine to the lipid II present at the septum, generating the substrate of FemAB. Finally, FemA and FemB would then also accumulate to the tips of the division septum, perhaps by interactions with the substrate or with the hypothethical flippase. As this machinery moves on, FemA and FemB add the 4

glycines to lipid II-Gly1 successively as a putative tetramer that could then be translocated, transglycosilated and transpeptidated into the growing glycan chain, thickening the septum.

Further studies into possible interactions between Fem proteins among themselves and with other division proteins will hopefully allow us to shed further knowledge into the complexities of bacterial peptidoglycan synthesis.

References

Alborn, W. J., J. Hoskins, S. Unal, J. Flokowitsch, C. Hayes, J. Dotzlaf, W. Yeh, and P. Skatrud, 1996, Cloning and characterization of *femA* and *femB* from *Staphylococcus epidermidis*.: Gene, v. 180, p. 177-81.

Arnaud, M., A. Chastanet, and M. Débarbouillé, 2004, New vector for efficient allelic replacement in naturally nontransformable, low-GC-content, gram-positive bacteria.: Appl Environ Microbiol, v. 70, p. 6887-91.

Barber, M., and M. Rozwadowska-Dowzenko, 1948, Infection by penicillin-resistant staphylococci.: Lancet, v. 2, p. 641-4.

Benson, T., D. Prince, V. Mutchler, K. Curry, A. Ho, R. Sarver, J. Hagadorn, G. Choi, and R. Garlick, 2002, X-ray crystal structure of *Staphylococcus aureus* FemA.: Structure, v. 10, p. 1107-15.

Berger-Bächi, B., 1983, Insertional inactivation of staphylococcal methicillin resistance by *Tn551*.: J Bacteriol, v. 154, p. 479-87.

Berger-Bächi, B., L. Barberis-Maino, A. Strässle, and F. Kayser, 1989, FemA, a host-mediated factor essential for methicillin resistance in *Staphylococcus aureus*: molecular cloning and characterization.: Mol Gen Genet, v. 219, p. 263-9.

Berger-Bächi, B., and S. Rohrer, 2002, Factors influencing methicillin resistance in staphylococci.: Arch Microbiol, v. 178, p. 165-71.

Berger-Bächi, B., A. Strässle, J. Gustafson, and F. Kayser, 1992, Mapping and characterization of multiple chromosomal factors involved in methicillin resistance in *Staphylococcus aureus*.: Antimicrob Agents Chemother, v. 36, p. 1367-73.

Berger-Bächi, B., and M. Tschierske, 1998, Role of fem factors in methicillin resistance.: Drug Resist Updat, v. 1, p. 325-35.

Biarrotte-Sorin, S., A. Maillard, J. Delettré, W. Sougakoff, M. Arthur, and C. Mayer, 2004, Crystal structures of *Weissella viridescens* FemX and its complex with UDP-MurNAc-pentapeptide: insights into FemABX family substrates recognition.: Structure, v. 12, p. 257-67.

Biou, V., A. Yaremchuk, M. Tukalo, and S. Cusack, 1994, The 2.9 A crystal structure of *T. thermophilus* seryl-tRNA synthetase complexed with tRNA(Ser). Science, v. 263, p. 1404-10.

Bishburg, E., and K. Bishburg, 2009, Minocycline--an old drug for a new century: emphasis on methicillin-resistant *Staphylococcus aureus* (MRSA) and *Acinetobacter baumannii*.: Int J Antimicrob Agents, v. 34, p. 395-401.

Boyce, J., M. Jackson, G. Pugliese, M. Batt, D. Fleming, J. Garner, A. Hartstein, C. Kauffman, M. Simmons, and R. Weinstein, 1994, Methicillin-resistant *Staphylococcus aureus* (MRSA): a briefing for acute care hospitals and nursing facilities. The AHA Technical Panel on Infections Within Hospitals.: Infect Control Hosp Epidemiol, v. 15, p. 105-15.

Casewell, M., and R. Hill, 1986, The carrier state: methicillin-resistant *Staphylococcus aureus*.: J Antimicrob Chemother, v. 18 Suppl A, p. 1-12.

CDC, 2002, *Staphylococcus aureus* resistant to vancomycin--United States, 2002.: MMWR Morb Mortal Wkly Rep, v. 51, p. 565-7.

Chambers, H., 2005, Community-associated MRSA--resistance and virulence converge.: N Engl J Med, v. 352, p. 1485-7.

Chambers, H., and F. Deleo, 2009, Waves of resistance: *Staphylococcus aureus* in the antibiotic era: Nature Reviews Microbiology, v. 7, p. 629-641.

Couto, I., S. Wu, A. Tomasz, and H. de Lencastre, 2003, Development of methicillin resistance in clinical isolates of *Staphylococcus sciuri* by transcriptional activation of the *mecA* homologue.: J Bacteriol, v. 185, p. 645-53.

Cusack, S., A. Yaremchuk, and M. Tukalo, 1996, The crystal structure of the ternary complex of *T.thermophilus* seryl-tRNA synthetase with tRNA(Ser) and a seryl-adenylate analogue reveals a conformational switch in the active site.: EMBO J, v. 15, p. 2834-42.

de Jonge, B., T. Sidow, Y. Chang, H. Labischinski, B. Berger-Bachi, D. Gage, and A. Tomasz, 1993, Altered muropeptide composition in *Staphylococcus aureus* strains with an inactivated *femA* locus.: J Bacteriol, v. 175, p. 2779-82.

de Jonge, B., and A. Tomasz, 1992, Abnormal peptidoglycan produced in a methicillin-resistant strain of *Staphylococcus aureus* grown in the presence of methicillin: functional role for penicillin-binding protein 2A in cell wall synthesis.: Antimicrob Agents Chemother, v. 37, p. 342-6.

de Jonge, B., and A. Tomasz, 1993, Abnormal peptidoglycan produced in a methicillin-resistant strain of *Staphylococcus aureus* grown in the presence of methicillin: functional role for penicillin-binding protein 2A in cell wall synthesis.: Antimicrob Agents Chemother, v. 37, p. 342-6.

de Lencastre, H., and A. Tomasz, 1994, Reassessment of the number of auxiliary genes essential for expression of high-level methicillin resistance in *Staphylococcus aureus*.: Antimicrob Agents Chemother, v. 38, p. 2590-8.

De Lencastre, H., S. Wu, M. Pinho, A. Ludovice, S. Filipe, S. Gardete, R. Sobral, S. Gill, M. Chung, and A. Tomasz, 1999, Antibiotic resistance as a stress response: complete sequencing of a large number of chromosomal loci in *Staphylococcus aureus* strain COL that impact on the expression of resistance to methicillin.: Microb Drug Resist, v. 5, p. 163-75.

Dmitriev, B., F. Toukach, O. Holst, E. Rietschel, and S. Ehlers, 2004, Tertiary structure of *Staphylococcus aureus* cell wall murein.: J Bacteriol, v. 186, p. 7141-8.

Dmitriev, B., F. Toukach, K. Schaper, O. Holst, E. Rietschel, and S. Ehlers, 2003, Tertiary structure of bacterial murein: the scaffold model.: J Bacteriol, v. 185, p. 3458-68.

Dutnall, R., S. Tafrov, R. Sternglanz, and V. Ramakrishnan, 1998, Structure of the yeast histone acetyltransferase Hat1: insights into substrate specificity and implications for the Gcn5-related N-acetyltransferase superfamily.: Cold Spring Harb Symp Quant Biol, v. 63, p. 501-7.

Ehlert, K., W. Schröder, and H. Labischinski, 1997, Specificities of FemA and FemB for different glycine residues: FemB cannot substitute for FemA in staphylococcal peptidoglycan pentaglycine side chain formation.: J Bacteriol, v. 179, p. 7573-6.

Eschenburg, S., W. Kabsch, M. Healy, and E. Schonbrunn, 2003, A new view of the mechanisms of UDP-N-acetylglucosamine enolpyruvyl transferase (MurA) and 5-enolpyruvylshikimate-3-phosphate synthase (AroA) derived from X-ray structures of their tetrahedral reaction intermediate states.: J Biol Chem, v. 278, p. 49215-22.

Fay, A., and J. Dworkin, 2009, *Bacillus subtilis* homologs of MviN (MurJ), the putative *Escherichia coli* lipid II flippase, are not essential for growth.: J Bacteriol, v. 191, p. 6020-8.

Filipe, S., E. Severina, and A. Tomasz, 2001, The role of murMN operon in penicillin resistance and antibiotic tolerance of *Streptococcus pneumoniae*.: Microb Drug Resist, v. 7, p. 303-16.

Filipe, S., and A. Tomasz, 2000, Inhibition of the expression of penicillin resistance in *Streptococcus pneumoniae* by inactivation of cell wall muropeptide branching genes.: Proc Natl Acad Sci U S A, v. 97, p. 4891-6.

Fiser, A., S. Filipe, and A. Tomasz, 2003, Cell wall branches, penicillin resistance and the secrets of the MurM protein.: Trends Microbiol, v. 11, p. 547-53.

Francius, G., O. Domenech, M. Mingeot-Leclercq, and Y. Dufrêne, 2008, Direct observation of *Staphylococcus aureus* cell wall digestion by lysostaphin.: J Bacteriol, v. 190, p. 7904-9.

Fuda, C., J. Fisher, and S. Mobashery, 2005, Beta-lactam resistance in *Staphylococcus aureus*: the adaptive resistance of a plastic genome.: Cell Mol Life Sci, v. 62, p. 2617-33.

Gales, A., H. Sader, S. Andrade, L. Lutz, A. Machado, and A. Barth, 2006, Emergence of linezolid-resistant *Staphylococcus aureus* during treatment of pulmonary infection in a patient with cystic fibrosis.: Int J Antimicrob Agents, v. 27, p. 300-2.

Gan, L., S. Chen, and G. Jensen, 2008, Molecular organization of Gram-negative peptidoglycan.: Proc Natl Acad Sci U S A, v. 105, p. 18953-7.

Glauner, B., J. Höltje, and U. Schwarz, 1988, The composition of the murein of *Escherichia coli*.: J Biol Chem, v. 263, p. 10088-95.

Goffin, C., and J. Ghuysen, 2002, Biochemistry and comparative genomics of SxxK superfamily acyltransferases offer a clue to the mycobacterial paradox: presence of penicillin-susceptible target proteins versus lack of efficiency of penicillin as therapeutic agent.: Microbiol Mol Biol Rev, v. 66, p. 702-38, table of contents.

Gorwitz, R., D. Kruszon-Moran, S. McAllister, G. McQuillan, L. McDougal, G. Fosheim, B. Jensen, G. Killgore, F. Tenover, and M. Kuehnert, 2008, Changes in the prevalence of nasal colonization with *Staphylococcus aureus* in the United States, 2001-2004.: J Infect Dis, v. 197, p. 1226-34.

Grundmann, H., M. Aires-De-Sousa, J. Boyce, and E. Tiemersma, 2006, Emergence and resurgence of meticillin-resistant *Staphylococcus aureus* as a public-health threat: LANCET, v. 368, p. 874-885.

Hall, L., K. A. Doerr, S. L. Wohlfiel, and G. D. Roberts, 2003, Evaluation of the MicroSeq system for identification of mycobacteria by 16S ribosomal DNA sequencing and its integration into a routine clinical mycobacteriology laboratory: J Clin Microbiol, v. 41, p. 1447-53.

Hartman, B., and A. Tomasz, 1984, Low-affinity penicillin-binding protein associated with beta-lactam resistance in *Staphylococcus aureus*.: J Bacteriol, v. 158, p. 513-6.

Hegde, S., and T. Shrader, 2001, FemABX family members are novel nonribosomal peptidyltransferases and important pathogen-specific drug targets.: J Biol Chem, v. 276, p. 6998-7003.

Henze, U., T. Sidow, J. Wecke, H. Labischinski, and B. Berger-Bächi, 1993, Influence of femB on methicillin resistance and peptidoglycan metabolism in *Staphylococcus aureus*.: J Bacteriol, v. 175, p. 1612-20.

Hiramatsu, K., H. Hanaki, T. Ino, K. Yabuta, T. Oguri, and F. Tenover, 1997, Methicillin-resistant *Staphylococcus aureus* clinical strain with reduced vancomycin susceptibility.: J Antimicrob Chemother, v. 40, p. 135-6.

Hirschwerk, D., C. Ginocchio, M. Bythrow, and S. Condon, 2006, Diminished susceptibility to daptomycin accompanied by clinical failure in a patient with methicillin-resistant *Staphylococcus aureus* bacteremia.: Infect Control Hosp Epidemiol, v. 27, p. 315-7.

Holden, M., E. Feil, J. Lindsay, S. Peacock, N. Day, M. Enright, T. Foster, C. Moore, L. Hurst, R. Atkin, A. Barron, N. Bason, S. Bentley, C. Chillingworth, T. Chillingworth,

C. Churcher, L. Clark, C. Corton, A. Cronin, J. Doggett, L. Dowd, T. Feltwell, Z. Hance, B. Harris, H. Hauser, S. Holroyd, K. Jagels, K. James, N. Lennard, A. Line, R. Mayes, S. Moule, K. Mungall, D. Ormond, M. Quail, E. Rabbinowitsch, K. Rutherford, M. Sanders, S. Sharp, M. Simmonds, K. Stevens, S. Whitehead, B. Barrell, B. Spratt, and J. Parkhill, 2004, Complete genomes of two clinical *Staphylococcus aureus* strains: evidence for the rapid evolution of virulence and drug resistance.: Proc Natl Acad Sci U S A, v. 101, p. 9786-91.

Howden, B., P. Johnson, P. Charles, and M. Grayson, 2004, Failure of vancomycin for treatment of methicillin-resistant *Staphylococcus aureus* infections.: Clin Infect Dis, v. 39, p. 1544; author reply 1544-5.

Höltje, J., and C. Heidrich, 2001, Enzymology of elongation and constriction of the murein sacculus of *Escherichia coli*.: Biochimie, v. 83, p. 103-8.

Ikeda, M., M. Wachi, H. Jung, F. Ishino, and M. Matsuhashi, 1991, The *Escherichia coli* mraY gene encoding UDP-N-acetylmuramoyl-pentapeptide: undecaprenyl-phosphate phospho-N-acetylmuramoyl-pentapeptide transferase.: J Bacteriol, v. 173, p. 1021-6.

Ito, T., Y. Katayama, K. Asada, N. Mori, K. Tsutsumimoto, C. Tiensasitorn, and K. Hiramatsu, 2001, Structural comparison of three types of staphylococcal cassette chromosome *mec* integrated in the chromosome in methicillin-resistant *Staphylococcus aureus*.: Antimicrob Agents Chemother, v. 45, p. 1323-36.

Jevons, M., A. Coe, and M. Parker, 1963, Methicillin resistance in staphylococci.: Lancet, v. 1, p. 904-7.

Kamiryo, T., and M. Matsuhashi, 1972, The biosynthesis of the cross-linking peptides in the cell wall peptidoglycan of *Staphylococcus aureus*.: J Biol Chem, v. 247, p. 6306-11.

Katayama, Y., F. Takeuchi, T. Ito, X. Ma, Y. Ui-Mizutani, I. Kobayashi, and K. Hiramatsu, 2003, Identification in methicillin-susceptible *Staphylococcus hominis* of an active primordial mobile genetic element for the staphylococcal cassette chromosome mec of methicillin-resistant *Staphylococcus aureus*.: J Bacteriol, v. 185, p. 2711-22.

Kazakova, S., J. Hageman, M. Matava, A. Srinivasan, L. Phelan, B. Garfinkel, T. Boo, S. McAllister, J. Anderson, B. Jensen, D. Dodson, D. Lonsway, L. McDougal, M. Arduino, V. Fraser, G. Killgore, F. Tenover, S. Cody, and D. Jernigan, 2005, A clone of methicillin-resistant *Staphylococcus aureus* among professional football players.: N Engl J Med, v. 352, p. 468-75.

Kennedy, A., M. Otto, K. Braughton, A. Whitney, L. Chen, B. Mathema, J. Mediavilla, K. Byrne, L. Parkins, F. Tenover, B. Kreiswirth, J. Musser, and F. DeLeo, 2008, Epidemic community-associated methicillin-resistant *Staphylococcus aureus*: recent clonal expansion and diversification.: Proc Natl Acad Sci U S A, v. 105, p. 1327-32.

Kim, D., W. Lees, K. Kempsell, W. Lane, K. Duncan, and C. Walsh, 1996, Characterization of a Cys115 to Asp substitution in the *Escherichia coli* cell wall biosynthetic enzyme UDP-GlcNAc enolpyruvyl transferase (MurA) that confers resistance to inactivation by the antibiotic fosfomycin.: Biochemistry, v. 35, p. 4923-8.

Kirby, W., 1944, Extraction of a highly potent penicillin inactivator from penicillin resistant staphylococci.: Science, v. 99, p. 452-453.

Klevens MR, M. M., Nadle J, Petit S, Gershman K, Ray S, 2007, Active Bacterial Core Surveillance (ABCs) MRSA Investigators. Invasive methicillin, JAMA, p. 71.

Kluytmans, J., A. van Belkum, and H. Verbrugh, 1997, Nasal carriage of *Staphylococcus aureus*: epidemiology, underlying mechanisms, and associated risks.: Clin Microbiol Rev, v. 10, p. 505-20.

Kobayashi, N., K. Taniguchi, and S. Urasawa, 1998, Analysis of diversity of mutations in the *mecI* gene and *mecA* promoter/operator region of methicillin-resistant *Staphylococcus*

aureus and *Staphylococcus epidermidis*.: Antimicrob Agents Chemother, v. 42, p. 717-20.

Kopp, U., M. Roos, J. Wecke, and H. Labischinski, 1996, Staphylococcal peptidoglycan interpeptide bridge biosynthesis: a novel antistaphylococcal target?: Microb Drug Resist, v. 2, p. 29-41.

Kraemer, G. R. I., J.J., 1990, High Frequency transformation of *Staphylococcus aureus*: Curr Microb, v. 21, p. 373-376.

Kuroda, M., T. Ohta, I. Uchiyama, T. Baba, H. Yuzawa, I. Kobayashi, L. Cui, A. Oguchi, K. Aoki, Y. Nagai, J. Lian, T. Ito, M. Kanamori, H. Matsumaru, A. Maruyama, H. Murakami, A. Hosoyama, Y. Mizutani-Ui, N. Takahashi, T. Sawano, R. Inoue, C. Kaito, K. Sekimizu, H. Hirakawa, S. Kuhara, S. Goto, J. Yabuzaki, M. Kanehisa, A. Yamashita, K. Oshima, K. Furuya, C. Yoshino, T. Shiba, M. Hattori, N. Ogasawara, H. Hayashi, and K. Hiramatsu, 2001, Whole genome sequencing of meticillin-resistant *Staphylococcus aureus*.: Lancet, v. 357, p. 1225-40.

Kusuma, C., A. Jadanova, T. Chanturiya, and J. Kokai-Kun, 2007, Lysostaphin-resistant variants of *Staphylococcus aureus* demonstrate reduced fitness in vitro and in vivo.: Antimicrob Agents Chemother, v. 51, p. 475-82.

Lapidot, A., and C. Irving, 1977, Dynamic structure of whole cells probed by nuclear Overhauser enhanced nitrogen-15 nuclear magnetic resonance spectroscopy.: Proc Natl Acad Sci U S A, v. 74, p. 1988-92.

Lapidot, A., and C. Irving, 1979, Comparative in vivo nitrogen-15 nuclear magnetic resonance study of the cell wall components of five Gram-positive bacteria.: Biochemistry, v. 18, p. 704-14.

Laupland, K., T. Ross, and D. Gregson, 2008, *Staphylococcus aureus* bloodstream infections: risk factors, outcomes, and the influence of methicillin resistance in Calgary, Canada, 2000-2006.: J Infect Dis, v. 198, p. 336-43.

Lenarcic, R., S. Halbedel, L. Visser, M. Shaw, L. Wu, J. Errington, D. Marenduzzo, and L. Hamoen, 2009, Localisation of DivIVA by targeting to negatively curved membranes.: EMBO J, v. 28, p. 2272-2282.

Li, M., B. Diep, A. Villaruz, K. Braughton, X. Jiang, F. DeLeo, H. Chambers, Y. Lu, and M. Otto, 2009, Evolution of virulence in epidemic community-associated methicillin-resistant *Staphylococcus aureus*.: Proc Natl Acad Sci U S A, v. 106, p. 5883-8.

Li, X., Y. Xiong, X. Fan, Z. Zhong, P. Feng, H. Tang, and T. Zhou, 2008, A study of the regulating gene of *femA* from methicillin-resistant *Staphylococcus aureus* clinical isolates.: J Int Med Res, v. 36, p. 420-33.

Lin, Y., Z. Li, G. Francisco, L. McDonald, R. Davis, G. Singh, Y. Yang, and T. Mansour, 2002, Muraymycins, novel peptidoglycan biosynthesis inhibitors: semisynthesis and SAR of their derivatives.: Bioorg Med Chem Lett, v. 12, p. 2341-4.

Ling, B., and B. Berger-Bächi, 1998, Increased overall antibiotic susceptibility in *Staphylococcus aureus femAB* null mutants.: Antimicrob Agents Chemother, v. 42, p. 936-8.

Llarrull, L., J. Fisher, and S. Mobashery, 2009, Molecular basis and phenotype of methicillin resistance in *Staphylococcus aureus* and insights into new beta-lactams that meet the challenge.: Antimicrob Agents Chemother, v. 53, p. 4051-63.

Lowy, F., 1998, *Staphylococcus aureus* infections.: N Engl J Med, v. 339, p. 520-32.

Luong, T., S. Ouyang, K. Bush, and C. Lee, 2002, Type 1 capsule genes of *Staphylococcus aureus* are carried in a staphylococcal cassette chromosome genetic element.: J Bacteriol, v. 184, p. 3623-9.

Maidhof, H., B. Reinicke, P. Blümel, B. Berger-Bächi, and H. Labischinski, 1991, *femA*, which encodes a factor essential for expression of methicillin resistance, affects glycine content of peptidoglycan in methicillin-resistant and methicillin-susceptible *Staphylococcus aureus* strains.: J Bacteriol, v. 173, p. 3507-13.

Maillard, A., S. Biarrotte-Sorin, R. Villet, S. Mesnage, A. Bouhss, W. Sougakoff, C. Mayer, and M. Arthur, 2005, Structure-based site-directed mutagenesis of the UDP-MurNAc-pentapeptide-binding cavity of the FemX alanyl transferase from *Weissella viridescens*.: J Bacteriol, v. 187, p. 3833-8.

Margolin, W., 2004, Bacterial shape: concave coiled coils curve caulobacter.: Curr Biol, v. 14, p. R242-4.

Massova, I., and S. Mobashery, 1998, Kinship and diversification of bacterial penicillin-binding proteins and beta-lactamases.: Antimicrob Agents Chemother, v. 42, p. 1-17.

Matsuhashi, Y., T. Sawa, T. Takeuchi, H. Umezawa, and I. Nagatsu, 1976, Localization of aminoglycoside 3'-phosphotransferase II on a cellular surface of R factor resistant *Escherichia coli*.: J Antibiot (Tokyo), v. 29, p. 1129-30.

McKinney, T., V. Sharma, W. Craig, and G. Archer, 2001, Transcription of the gene mediating methicillin resistance in *Staphylococcus aureus* (*mecA*) is corepressed but not coinduced by cognate *mecA* and beta-lactamase regulators.: J Bacteriol, v. 183, p. 6862-8.

Mengin-Lecreulx, D., L. Texier, M. Rousseau, and J. van Heijenoort, 1991, The *murG* gene of *Escherichia coli* codes for the UDP-N-acetylglucosamine: N-acetylmuramyl-(pentapeptide) pyrophosphoryl-undecaprenol N-acetylglucosamine transferase involved in the membrane steps of peptidoglycan synthesis.: J Bacteriol, v. 173, p. 4625-36.

Meroueh, S., K. Bencze, D. Hesek, M. Lee, J. Fisher, T. Stemmler, and S. Mobashery, 2006, Three-dimensional structure of the bacterial cell wall peptidoglycan.: Proc Natl Acad Sci U S A, v. 103, p. 4404-9.

Miller, L., and B. Diep, 2008, Clinical practice: colonization, fomites, and virulence: rethinking the pathogenesis of community-associated methicillin-resistant *Staphylococcus aureus* infection.: Clin Infect Dis, v. 46, p. 752-60.

Mongkolrattanothai, K., S. Boyle, T. Murphy, and R. Daum, 2004, Novel non-*mecA*-containing staphylococcal chromosomal cassette composite island containing *pbp4* and *tagF* genes in a commensal staphylococcal species: a possible reservoir for antibiotic resistance islands in *Staphylococcus aureus*.: Antimicrob Agents Chemother, v. 48, p. 1823-36.

Moran, G., A. Krishnadasan, R. Gorwitz, G. Fosheim, L. McDougal, R. Carey, and D. Talan, 2006, Methicillin-resistant *S. aureus* infections among patients in the emergency department.: N Engl J Med, v. 355, p. 666-74.

Munoz, E., J. Ghuysen, and H. Heymann, 1967, Cell walls of *Streptococcus pyogenes*, type 14. C polysaccharide-peptidoglycan and G polysaccharide-peptidoglycan complexes.: Biochemistry, v. 6, p. 3659-70.

Muto, C., J. Jernigan, B. Ostrowsky, H. Richet, W. Jarvis, J. Boyce, and B. Farr, 2003, SHEA guideline for preventing nosocomial transmission of multidrug-resistant strains of *Staphylococcus aureus* and enterococcus.: Infect Control Hosp Epidemiol, v. 24, p. 362-86.

Navarre, W., and O. Schneewind, 1999, Surface proteins of gram-positive bacteria and mechanisms of their targeting to the cell wall envelope.: Microbiol Mol Biol Rev, v. 63, p. 174-229.

Noble, W., H. Valkenburg, and C. Wolters, 1967, Carriage of *Staphylococcus aureus* in random samples of a normal population.: J Hyg (Lond), v. 65, p. 567-73.

Noto, M., B. Kreiswirth, A. Monk, and G. Archer, 2008, Gene acquisition at the insertion site for *SCCmec*, the genomic island conferring methicillin resistance in *Staphylococcus aureus*.: J Bacteriol, v. 190, p. 1276-83.

Oliveira, D., S. Wu, and H. de Lencastre, 2000, Genetic organization of the downstream region of the *mecA* element in methicillin-resistant *Staphylococcus aureus* isolates carrying different polymorphisms of this region.: Antimicrob Agents Chemother, v. 44, p. 1906-10.

Oshida, T., and A. Tomasz, 1992, Isolation and characterization of a *Tn551*-autolysis mutant of *Staphylococcus aureus*.: J Bacteriol, v. 174, p. 4952-9.

Pereira, S., A. Henriques, M. Pinho, H. de Lencastre, and A. Tomasz, 2007, Role of PBP1 in cell division of *Staphylococcus aureus*.: J Bacteriol, v. 189, p. 3525-31.

Pinho, M., H. de Lencastre, and A. Tomasz, 2001, An acquired and a native penicillin-binding protein cooperate in building the cell wall of drug-resistant staphylococci.: Proc Natl Acad Sci U S A, v. 98, p. 10886-91.

Pinho, M., and J. Errington, 2003, Dispersed mode of *Staphylococcus aureus* cell wall synthesis in the absence of the division machinery.: Mol Microbiol, v. 50, p. 871-81.

Pinho, M., and J. Errington, 2004, A *divIVA* null mutant of *Staphylococcus aureus* undergoes normal cell division.: FEMS Microbiol Lett, v. 240, p. 145-9.

Pinho, M., and J. Errington, 2005, Recruitment of penicillin-binding protein PBP2 to the division site of *Staphylococcus aureus* is dependent on its transpeptidation substrates.: Mol Microbiol, v. 55, p. 799-807.

Pootoolal, J., J. Neu, and G. Wright, 2002, Glycopeptide antibiotic resistance.: Annu Rev Pharmacol Toxicol, v. 42, p. 381-408.

Rogers, H. J., H. R. Perkins, and J. B. Ward, 1980, Microbial cell walls and membranes: London, Chapman and Hall, x, 564 p. p.

Rohrer, S., and B. Berger-Bächi, 2003, Application of a bacterial two-hybrid system for the analysis of protein-protein interactions between FemABX family proteins.: Microbiology, v. 149, p. 2733-8.

Rohrer, S., K. Ehlert, M. Tschierske, H. Labischinski, and B. Berger-Bächi, 1999, The essential *Staphylococcus aureus* gene *fmhB* is involved in the first step of peptidoglycan pentaglycine interpeptide formation.: Proc Natl Acad Sci U S A, v. 96, p. 9351-6.

Ruiz, N., 2008, Bioinformatics identification of MurJ (MviN) as the peptidoglycan lipid II flippase in Escherichia coli.: Proc Natl Acad Sci U S A, v. 105, p. 15553-7.

Sambrook, J., E. Fritsch, and T. Maniatis, 1989, Molecular cloning: a laboratory manual, Cold Spring Harbor Laboratory, Cold Spring Harbor, New York.

Schleifer, K., and O. Kandler, 1972, Peptidoglycan types of bacterial cell walls and their taxonomic implications.: Bacteriol Rev, v. 36, p. 407-77.

Schneewind, O., A. Fowler, and K. Faull, 1995, Structure of the cell wall anchor of surface proteins in *Staphylococcus aureus*.: Science, v. 268, p. 103-6.

Schneider, T., M. Senn, B. Berger-Bächi, A. Tossi, H. Sahl, and I. Wiedemann, 2004, In vitro assembly of a complete, pentaglycine interpeptide bridge containing cell wall precursor (lipid II-Gly5) of *Staphylococcus aureus*.: Mol Microbiol, v. 53, p. 675-85.

Sharif, S., S. Kim, H. Labischinski, and J. Schaefer, 2009, Characterization of peptidoglycan in *fem*-deletion mutants of methicillin-resistant *Staphylococcus aureus* by solid-state NMR.: Biochemistry, v. 48, p. 3100-8.

Sharma, V., C. Hackbarth, T. Dickinson, and G. Archer, 1998, Interaction of native and mutant MecI repressors with sequences that regulate *mecA*, the gene encoding penicillin binding protein 2a in methicillin-resistant staphylococci.: J Bacteriol, v. 180, p. 2160-6.

Shockman, G., L. Daneo-Moore, R. Kariyama, and O. Massidda, 1996, Bacterial walls, peptidoglycan hydrolases, autolysins, and autolysis.: Microb Drug Resist, v. 2, p. 95-8.

Skarzynski, T., A. Mistry, A. Wonacott, S. Hutchinson, V. Kelly, and K. Duncan, 1996, Structure of UDP-N-acetylglucosamine enolpyruvyl transferase, an enzyme essential for the synthesis of bacterial peptidoglycan, complexed with substrate UDP-N-acetylglucosamine and the drug fosfomycin.: Structure, v. 4, p. 1465-74.

Smith, T., S. Blackman, and S. Foster, 2000, Autolysins of *Bacillus subtilis*: multiple enzymes with multiple functions.: Microbiology, v. 146 (Pt 2), p. 249-62.

Strandén, A., K. Ehlert, H. Labischinski, and B. Berger-Bächi, 1997, Cell wall monoglycine cross-bridges and methicillin hypersusceptibility in a *femAB* null mutant of methicillin-resistant *Staphylococcus aureus*.: J Bacteriol, v. 179, p. 9-16.

Sugai, M., T. Fujiwara, K. Ohta, H. Komatsuzawa, M. Ohara, and H. Suginaka, 1997, *epr*, which encodes glycylglycine endopeptidase resistance, is homologous to *femAB* and affects serine content of peptidoglycan cross bridges in *Staphylococcus capitis* and *Staphylococcus aureus*.: J Bacteriol, v. 179, p. 4311-8.

Swenson, J., and F. Neuhaus, 1976, Biosynthesis of peptidoglycan in *Staphylococcus aureus*: incorporation of the Nepsilon-Ala-Lys moiety into the peptide subunit of nascent peptidoglycan.: J Bacteriol, v. 125, p. 626-34.

Tipper, D., W. Katz, J. Strominger, and J. Ghuysen, 1967a, Substituents on the alpha-carboxyl group of D-glutamic acid in the peptidoglycan of several bacterial cell walls.: Biochemistry, v. 6, p. 921-9.

Tipper, D., J. Strominger, and J. Ensign, 1967b, Structure of the cell wall of *Staphylococcus aureus*, strain Copenhagen. VII. Mode of action of the bacteriolytic peptidase from Myxobacter and the isolation of intact cell wall polysaccharides.: Biochemistry, v. 6, p. 906-20.

Touhami, A., M. Jericho, and T. Beveridge, 2004, Atomic force microscopy of cell growth and division in *Staphylococcus aureus*.: J Bacteriol, v. 186, p. 3286-95.

Tschierske, M., K. Ehlert, A. Strandén, and B. Berger-Bächi, 1997, Lif, the lysostaphin immunity factor, complements FemB in staphylococcal peptidoglycan interpeptide bridge formation.: FEMS Microbiol Lett, v. 153, p. 261-4.

Tschierske, M., C. Mori, S. Rohrer, K. Ehlert, K. Shaw, and B. Berger-Bächi, 1999, Identification of three additional femAB-like open reading frames in *Staphylococcus aureus*.: FEMS Microbiol Lett, v. 171, p. 97-102.

Tzagoloff, H., and R. Novick, 1977, Geometry of cell division in *Staphylococcus aureus*.: J Bacteriol, v. 129, p. 343-50.

Ubukata, K., R. Nonoguchi, M. Matsuhashi, and M. Konno, 1989, Expression and inducibility in *Staphylococcus aureus* of the *mecA* gene, which encodes a methicillin-resistant *S. aureus*-specific penicillin-binding protein.: J Bacteriol, v. 171, p. 2882-5.

van Heijenoort, J., 1998, Assembly of the monomer unit of bacterial peptidoglycan.: Cell Mol Life Sci, v. 54, p. 300-4.

van Heijenoort , J., 2001, Formation of the glycan chains in the synthesis of bacterial peptidoglycan.: Glycobiology, v. 11, p. 25R-36R.

Vandenesch, F., T. Naimi, M. Enright, G. Lina, G. Nimmo, H. Heffernan, N. Liassine, M. Bes, T. Greenland, M. Reverdy, and J. Etienne, 2003, Community-acquired

methicillin-resistant *Staphylococcus aureus* carrying Panton-Valentine leukocidin genes: worldwide emergence.: Emerg Infect Dis, v. 9, p. 978-84.

Vollmer, W., D. Blanot, and M. de Pedro, 2008, Peptidoglycan structure and architecture.: FEMS Microbiol Rev, v. 32, p. 149-67.

Vollmer, W., and J. Höltje, 2004, The architecture of the murein (peptidoglycan) in gram-negative bacteria: vertical scaffold or horizontal layer(s)?: J Bacteriol, v. 186, p. 5978-87.

Waxman, D., and J. Strominger, 1983, Penicillin-binding proteins and the mechanism of action of beta-lactam antibiotics.: Annu Rev Biochem, v. 52, p. 825-69.

Wenzel, R., and T. Perl, 1995, The significance of nasal carriage of *Staphylococcus aureus* and the incidence of postoperative wound infection.: J Hosp Infect, v. 31, p. 13-24.

Wu, S., H. de Lencastre, and A. Tomasz, 2001, Recruitment of the *mecA* gene homologue of *Staphylococcus sciuri* into a resistance determinant and expression of the resistant phenotype in *Staphylococcus aureus*.: J Bacteriol, v. 183, p. 2417-24.

Wurch, T., F. Lestienne, and P. Pauwels, 1998, A modified overlap extension PCR method to create chimeric genes in the absence of restriction enzymes, Biotechnology Techniques, p. 653-657.